THE UNIVERSITY OF QUEENSLAND

AUSTRALIA

Analysing visual behaviour in *Drosophila Dscam2* mutants using optimised optomotor and operant control assays

Danny Stefan Bosch

MSc

A thesis submitted for the degree of Doctor of Philosophy at

The University of Queensland in 2016

School of Biomedical Sciences

Abstract

The patterns of synaptic connections between neurons in the brain are key determinants of behaviour, but how specific neural circuits lead to distinct behaviours is largely unknown. Cell recognition molecules that mediate interactions between neurons play a crucial role in establishing synaptic connections. Down Syndrome Cell Adhesion Molecule 2 (Dscam2) is required for establishing modularity in the visual system. *Dscam2*^{null} flies have a disorganized visual system, lack boundaries between neighbouring modules in the optic lobe and exhibit changes in the postsynaptic composition of photoreceptor synapses. The behavioural consequences of these wiring defects have not been explored previously. In this thesis, I begin to dissect how these changes in neural circuitry affect visual system behaviours such as the optomotor response, object-orientation preference, and attention-like object-tracking. In order to do so, a population and single tethered-fly assay have been optimized and used to explore motion perception by assessing the visual response to a wide range of psychophysical parameters of black/green moving gratings. In addition, a single tethered-fly virtual reality assay has been set-up and used to explore orientation preference and attention-like tracking. Through the population and single tethered-fly optomotor assays, it is shown that *Dscam2*^{null} flies can track motion but that their response is opposite to control flies under defined experimental conditions. Through the single tethered-fly virtual reality assay, it is shown that *Dscam2*^{null} flies anti-fixate on a dark bar, again the opposite behaviour to control flies. Responses to a light bar are in contrast, the same as controls. It is shown that this anti-fixation is bar width dependent. Together these results demonstrate that the disrupted visual system of the *Dscam2*^{null} flies can dramatically change the perception of specific visual cues and modify behaviour. Lastly, other perturbations of *Dscam2* were studied such as *Dscam2* single isoform and *Dscam2* trisomic flies. Dscam2B single isoform flies displayed some motion detection phenotypes. In addition, they were not responding to either a dark or light bar in the tethered virtual reality assay. *Dscam2* trisomic flies were able to detect gratings with different spatial and temporal frequencies but had a change in orientation behaviour as they displayed fixation behaviour to both a dark and a light bar. The results provide a foundation for understanding how brain miswiring can lead to changes in behaviour.

In chapter 1, I outline the background information to provide context for the experiments and overall research aim. In chapter 2, I contrast a population and single fly assay to explore motion detection in *Drosophila*. In chapter 3, I present a new single fly virtual reality assay which goes beyond simple visual reflexes by measuring object-orientation preferences and attention-like tracking. In chapter 4, I test motion detection in *Dscam2*^{null} flies. In chapter 5, I test object-orientation preference and attention-like tracking in *Dscam2*^{null} flies. In chapter 6, I test motion detection and object-orientation preference in other *Dscam2* related mutants. Lastly, in chapter 7, I present a general discussion to explore how the combined experimental results further our knowledge of the research topic.

Declaration by author

This thesis is composed of my original work, and contains no material previously published or written by another person except where due reference has been made in the text. I have clearly stated the contribution by others to jointly-authored works that I have included in my thesis.

I have clearly stated the contribution of others to my thesis as a whole, including statistical assistance, survey design, data analysis, significant technical procedures, professional editorial advice, and any other original research work used or reported in my thesis. The content of my thesis is the result of work I have carried out since the commencement of my research higher degree candidature and does not include a substantial part of work that has been submitted to qualify for the award of any other degree or diploma in any university or other tertiary institution. I have clearly stated which parts of my thesis, if any, have been submitted to qualify for another award.

I acknowledge that an electronic copy of my thesis must be lodged with the University Library and, subject to the policy and procedures of The University of Queensland, the thesis be made available for research and study in accordance with the Copyright Act 1968 unless a period of embargo has been approved by the Dean of the Graduate School.

I acknowledge that copyright of all material contained in my thesis resides with the copyright holder(s) of that material. Where appropriate I have obtained copyright permission from the copyright holder to reproduce material in this thesis.

Publications during candidature

Peer-reviewed papers

Bosch, D. S., van Swinderen, B., & Millard, S. S. (2015). Dscam2 affects visual perception in *Drosophila melanogaster*. Frontiers in Behavioral Neuroscience 9.

Conference abstracts:

Bosch, D. S., van Swinderen, B. & Millard, S. S. (2012). Analysing visual system behaviours in *Drosophila Dscam2* mutants. Poster presentation, Annual conference 2012, Genetic Society of AustralAsia, Melbourne, Australia.

Bosch, D. S., van Swinderen, B. & Millard, S. S. (2012). Analysing visual system behaviours in *Drosophila Dscam2* mutants. Oral presentation, 4th Brain Plasticity Symposium: Circuits, Synapses and Behaviour, Queensland Brain Institute, University of Queensland, Australia.

Bosch, D. S., van Swinderen, B. & Millard, S. S. (2012). Analysing visual system behaviours in *Drosophila Dscam2* mutants. Oral presentation, International Postgraduate Symposium, School of Biomedical Sciences, Brisbane, University of Queensland, Australia.

Bosch, D. S., van Swinderen, B. & Millard, S. S. (2013). *Drosophila Dscam2* mutants have an inverted visual response. Oral presentation, Postgraduate Symposium, School of Medical Sciences, University of Otago, New Zealand.

Bosch, D. S., van Swinderen, B. & Millard, S. S. (2013). *Drosophila Dscam2* mutants have an inverted visual response. Oral presentation, International Postgraduate Symposium, School of Biomedical Sciences, Brisbane, University of Queensland, Australia.

Bosch, D. S., van Swinderen, B. & Millard, S. S. (2014). *Drosophila Dscam2* mutants have an inverted visual response. Poster presentation, 11th International Neuroethology Conference, Sapporo, Japan.

Bosch, D.S., van Swinderen, B. & Millard, S. S. (2014). *Drosophila Dscam2* mutants have an inverted visual response. Poster presentation, International Postgraduate Symposium, School of Biomedical Sciences, Brisbane, University of Queensland, Australia.

Publications included in this thesis

No publications included.

Contributions by others to the thesis

The majority of work completed throughout this thesis was undertaken by D.S. Bosch (candidate).

Dr. S. Millard was significantly involved in the conception and design of the project, and helped with critical revision and interpretations of all chapters.

A/P B. van Swinderen assisted with the experimental equipment and provided feedback and revisions for chapter 1 to 6.

Dr. I. Schiffner, Dr. G. Taylor, Dr. A. Paulk, Dr. L. Kirszenblat, Dr. Y. Zhou and M. van der Pol assisted with parts of the VisionEgg code and MATLAB scripts for the visual stimuli and analysis of the behavioural data.

Dr. A. Paulk, Dr. L. Kirszenblat, Dr. Y. Zhou assisted with the set-up of the single fly assay used in chapter 2,3,4,5 and 6.

Dr. G. Lah and J. Li provided the *w*- Dscam2 single isoform and BAC lines respectively.

Statement of parts of the thesis submitted to qualify for the award of another degree

None

Acknowledgements

Science requires passion, curiosity, and imagination, things that made me decide to do a Ph.D., and I am grateful to the many colleagues, friends, and family who shared these traits with me.

First and foremost, I wish to thank my principal advisor, Sean Millard, for his assistance and guidance with all aspects of my project, sharing his enthusiasm and knowledge throughout my Ph.D. Your teaching, encouragement, and experimental guidance made the completion of this project possible. I would also like to thank my co-supervisor, Bruno van Swinderen for the fruitful discussions about the project, sharing of his knowledge and providing the assistance with experimental equipment. I am very grateful for the help and assistance of Millard and van Swinderen lab members be it past or present: Sarah Kerwin, Lorenzo Odierna, Joshua Li, Kevin Mutemi, Wei Tan, Katie Scott, Alex Quirk, Grace Lah, Sorenta De Gasperi, Aoife Larkin, Oressia Zalucki, Kathy Asmussen, Leonie Kirszenblat, Melvyn Yap, Michael Troup, Yanqiong Zhou, Angelique Paulk and Bart van Alphen. Regardless of which project you worked on, the cooperation between lab members was instrumental to the success of both labs as a whole and the individual projects involved. I also would like to thank Ingo Schiffner from Srinivasan's lab for his input with statistics and ideas for this Ph.D. project.

I would like to thank the funding bodies that have supported my research, travel and professional development. I am grateful for the School of Biomedical Sciences at the University of Queensland for awarding me a Student Travel Award to attend a conference organized by the International Society for Neuroethology. This was a wonderful opportunity to learn about neuroscience and meet other researchers in the amazing field of neural systems and behaviour. Also at the School of Biomedical Sciences, I want to thank Fiona Gilloway for providing assistance with all the admin work involved in my Ph.D.

I like to thank my Ph.D. committee of Ethan Scott and Massimo Hilliard for their feedback and encouragement during my candidature.

A special thank you to the friends I made during the last four years, most notably members of the SBMS Postgraduate Student Association and fellow Ph.D. students. Thank you for the wonderful

discussions about science and life. It is amazing how sometimes a campfire and a glass of whisky with friends can brings up new ideas for experiments or even solutions to a problem.

I would like to thank all of my family at the other end of the globe for their love and support to pursue my passion, curiosity, and imagination.

Finally, I am grateful to all the flies which produced valuable behavioural data and without whom this thesis would not have been possible.

Keywords

Drosophila melanogaster, synapse, vision, behaviour, Dscam2, visual system, optomotor response, object orientation, object tracking, motion detection

Australian and New Zealand Standard Research Classifications (ANZSRC)

ANZSRC code: 060801: Animal Behaviour, 40%

ANZSRC code: 060805: Animal Neurobiology, 30%

ANZSRC code: 110902: Cellular Nervous System, 30%

Fields of Research (FoR) Classification

FoR code: 1109: Neurosciences (100%)

Table of Contents

Abstract ii
Declaration by author iv
Publications during candidature v
Publications included in this thesis vi
Contributions by others to the thesis vii
Statement of parts of the thesis submitted to qualify for the award of another degree vii
Acknowledgements viii
Keywords x
Australian and New Zealand Standard Research Classifications (ANZSRC) x
Fields of Research (FoR) Classification x
Table of Contents xi
List of Figures xvi
List of Tables xvii
List of Abbreviations xviii
Chapter 1 General introduction 1
1.1 Brain development and behaviour 1
1.2 A general introduction to the Drosophila visual system 3
1.3 Motion detection 5
1.3.1 Optomotor response 5
1.3.2 A theoretical model for motion detection computation 6
1.3.3 Eye geometry and aliasing 7
1.3.4 Circuits involved in motion detection 8
1.4 Object orientation and attention-like behaviour 14
1.4.1 Fixation and anti-fixation 14
1.4.2 Computation of object-orientation behaviour 16
1.4.3 Neurons involved in object-orientation behaviour 16
1.5 Cell adhesion molecule requirements in fly visual system development 18
1.5.1 Efficient wiring in the fly brain 18
1.5.2 *Dscam2* in the fly visual system 19

1.6 Thesis outline 21
Chapter 2 Optomotor assays: population and single fly paradigms 22
2.1 Chapter overview 22
2.2 Methods and results 22
2.2.1 A population assay for monitoring optomotor responses 22
2.2.1.1 Fly preparation 22
2.2.1.2 Experimental setup 23
2.2.1.3 Data analysis and statistics 25
2.2.1.4 Wild-type flies follow the direction of motion 25
2.2.2 A single tethered-fly assay for monitoring optomotor responses 27
2.2.2.1 Fly preparation 27
2.2.2.2 Experimental setup 27
2.2.2.3 Data analysis and statistics 29
2.2.2.4 Wild-type flies turn with the direction of motion in a tethered-fly assay 30
2.3 Discussion 31
2.3.1 A population assay to assess motion detection 31
2.3.2 A single tethered-fly motion detection assay 31
2.3.3 Comparison between a population and single fly assay 32
Chapter 3 Operant behaviour and attention-like mechanisms 33
3.1 Chapter overview 33
3.2 Methods and results 33
3.2.1 Control flies display contrasting orientation preferences 33
3.2.1.1 Fly preparation and experimental setup 33
3.2.1.2 Data analysis and statistics 34
3.2.1.3 A single fly virtual reality assay for monitoring orientation preferences 36
3.2.2 Wild-type flies correct automated bar perturbations 38
3.2.3 Wild-type object-orientation preferences depends on bar width 40
3.3 Discussion 42
3.3.1 Different responses to dark and light bars 42
3.3.2 Wild-type flies correct perturbations 43

3.3.3 Fixation and anti-fixation response is bar width dependent 43
Chapter 4 Motion detection phenotypes of Dscam2^{null} flies 45
4.1 Chapter overview 45
4.2 Materials and methods 45
4.2.1 Fly husbandry 45
4.2.2 General behaviours 46
4.2.2.1 Response to gravity: geotaxis 46
Fly preparation 46
General procedure 46
Data analysis 46
4.2.2.2 Response to non-volatile attractants: chemotaxis 46
Fly preparation 46
General procedure 46
Data analysis 47
4.2.2.3 Response to light: fast phototaxis assay 47
Fly preparation 47
General procedure 47
Data analysis 48
4.2.3 Population visual response assay 48
4.2.4 Single tethered-fly assay 48
4.3 Results 49
4.3.1 General behaviours 49
4.3.1.1 *Dscam2* mutant flies have an impaired geotactic response 49
4.3.1.2 *Dscam2* mutant flies can detect odours 50
4.3.1.3 *Dscam2* mutant flies exhibit reduced phototaxis 51
4.3.2 *Dscam2* mutant flies in a population assay 52
4.3.2.1 *Dscam2^{null}* flies turn against the direction of motion in a population assay 53
4.3.2.2 *Dscam2* gene dosage affects the optomotor response 56
4.3.2.3 The *Dscam2^{null-2}* line carries an assay-specific modifier 57
4.3.3 *Dscam2* mutant flies in a single fly assay 59

4.3.3.1 *Dscam2* mutants are able to detect motion but perceive it in the opposite direction at a specific visual parameter 59
4.3.3.2 *Dscam2* mutants respond to clockwise but not counter-clockwise translational stimuli 62
4.4 Discussion 63
4.4.1 The geotactic response is impaired in *Dscam2* mutant flies 65
4.4.2 *Dscam2* mutant flies can detect odours 65
4.4.3 Phototaxis is impaired in *Dscam2* mutant flies 65
4.4.4 *Dscam2* mutant flies move against the direction of the motion in the population visual response assay 66
4.4.5 One copy of *Dscam2* is sufficient to rescue most optomotor phenotypes in the population visual response assay 67
4.4.6 An unidentified modifier in the *Dscam2*$^{null-2}$ line affects the magnitude of the visual responses 67
4.4.7 *Dscam2* mutant flies are able to track motion but respond opposite from control flies at specific conditions 67
4.4.8 *Dscam2* flies respond to clockwise stimuli only 68
Chapter 5 Operant behaviour and attention-like mechanisms of Dscam2^{null} flies 70
5.1 Chapter overview 70
5.2 Results 70
5.2.1 *Dscam2* mutant flies anti-fixate on a dark bar 70
5.2.2 *Dscam2* mutant flies correct automated bar perturbations 73
5.2.3 Object-orientation in *Dscam2* mutants depends on bar width 77
5.3 Discussion 83
5.3.1 *Dscam2* mutant flies anti-fixate on a dark bar 83
5.3.2 The anti-fixation response to a dark bar is bar width dependent 84
Chapter 6 Visual behaviour of other Dscam2 mutants 85
6.1 Chapter overview 85
6.2 Methods and results 85
6.2.1 Visual behaviour of *Dscam2* single isoform flies 85
6.2.1.1 Phototactic behaviour of *Dscam2* single isoform flies 86

Fly husbandry and experimental setup ... 86
Dscam2 single isoform flies respond to light ... 86
6.2.1.2 *Dscam2* single isoform flies have a change in acuity ... 87
6.2.1.3 *Dscam2* single isoform flies do not display object-orientation behaviour ... 89
6.3 Visual behaviour of *Dscam2* trisomic flies ... 92
6.3.1 *Dscam2* trisomic flies respond to light ... 92
6.3.2 *Dscam2* trisomy does not alter optomotor behaviour ... 93
6.3.3 *Dscam2* trisomic flies display only fixation behaviour ... 94
6.4 Discussion ... 96
6.4.1 *Dscam2* single isoform flies demonstrate a change in motion detection sensitivity ... 97
6.4.2 *Dscam2* trisomy leads to visual defects ... 98
Chapter 7 General Discussion ... 99
7.1 Behavioural readout of motion detection ... 99
7.2 Behavioural readout of object orientation ... 101
7.3 *Dscam2* is required for visual behaviours ... 102
7.4 Differences between $Dscam2^{null}$ strains ... 106
7.5 Other *Dscam2* related mutants ... 107
7.6 Concluding remarks ... 107
References ... 109

List of Figures

Figure 1.1 The fly visual system. 4
Figure 1.2 Optomotor assay to study motion detection in *Drosophila*. 6
Figure 1.3 The Hassenstein-Reichardt model of the Elementary Motion Detector. 7
Figure 1.4 Motion detection in the fly visual system. 9
Figure 1.5 Motion detection circuitry in the fly visual system. 13
Figure 1.6 Object-orientation assays. 15
Figure 1.7. Wiring diagram of the optic lobes of wild type and the *Dscam2* mutant. 20
Figure 2.1. The maze visual response assay. 24
Figure 2.2. Wild-type flies respond to motion in the population visual response assay. 26
Figure 2.3. Single tethered-fly assay for assessment of motion tracking in flies. 28
Figure 2.4. Wild-type flies respond to motion in the single fly assay. 30
Figure 3.1. Data analysis in the single fly virtual reality assay. 35
Figure 3.2. Wild-type flies display distinct object-orientation preferences. 37
Figure 3.3. Wild-type flies correct bar perturbations 39
Figure 3.4. Object-orientation preference of wild-type flies depends on bar width. 41
Figure 4.1. *Dscam2* mutants have an impaired geotactic response. 49
Figure 4.2. *Dscam2* mutants have normal odour detection. 50
Figure 4.3. *Dscam2* mutants exhibit reduced phototaxis. 52
Figure 4.4. *Dscam2* mutants have a weakened and inverted response to motion in the population visual response assay. 54
Figure 4.5. Differences between *Dscam2* mutants in the population visual response assay 55
Figure 4.6. *Dscam2* heterozygotes respond similarly to control flies under most conditions. 57
Figure 4.7. *Dscam2* transhomozygotes respond similarly to $Dscam2^{null}$ flies under most conditions. 58
Figure 4.8. *Dscam2* mutant flies have conditional responses to motion in the single fly assay. 61
Figure 4.9 *Dscam2* mutants do not respond to counter-clockwise translational motion. 63
Figure 4.10 *Dscam2* mutant visual behaviour is conditionally perturbed. 64
Figure 5.1. *Dscam2* mutant flies anti-fixate to a dark bar. 71
Figure 5.2. *Dscam2* mutant flies anti-fixate to a light bar. 72
Figure 5.3. *Dscam2* mutant flies follow a single rotating bar similarly to control flies. 73
Figure 5.4. $Dscam2^{null}$ flies correct perturbations only partially. 75
Figure 5.5. Object-orientation preference of control and *Dscam2* mutant flies depends on dark bar width. 78
Figure 5.6. Object-orientation preference of control and *Dscam2* mutant flies depends on light bar width. 81
Figure 6.1. Dscam2B single isoform flies have a normal phototaxis response. 87
Figure 6.2. Dscam2B single isoform flies have conditional responses to motion in the single fly assay. 89
Figure 6.3. *Dscam2* single isoform flies have defects in object-orientation behaviour. 91
Figure 6.4. *Dscam2* trisomic flies have a normal phototaxis response. 93
Figure 6.5. *Dscam2* trisomic flies respond to motion in the tethered single fly assay. 94
Figure 6.6. *Dscam2* trisomic flies fixate on dark and light bars. 95
Figure 6.7. *Dscam2*-related manipulations lead to perturbed behavioural responses. 96

List of Tables

Table 6.1. Visual stimuli used to access visual responses. 88

List of Abbreviations

CRT	cathode-ray tube
Dscam1	Down Syndrome Cell Adhesion Molecule 1 - gene
Dscam2	Down Syndrome Cell Adhesion Molecule 2 - gene
Dscam2	Down Syndrome Cell Adhesion Molecule 2 – protein
EMD	Elementary Motion Detection
FAS II	Fasciclin II
GABA	γ-aminobutyric acid
LED	light-emitting diode
RNA	ribonucleic acid
SD	standard deviation
SEM	standard error of the mean
UAS	upstream activating sequence

Chapter 1

General introduction

1.1 Brain development and behaviour

The brain is the most complex organ in the human body as it utilizes an organized network of billions of neurons. These neurons relay sensory information into actions and are the foundation of unique behaviours. Neuronal wiring in the brain is a complex process. It is estimated that in the human brain 10^{12} neurons make 10^{15} synaptic connections. The accuracy of the wiring process is fundamental for brain function, and abnormal connectivity leads to nervous system disorders that modify behaviour. The molecular mechanisms required for patterning of connections during development are still largely unknown (Li & Sheng, 2003), but likely mediated by interactions between cell surface proteins expressed on axons and dendrites (Huberman *et al.*, 2010, Tessier-Lavigne & Goodman, 1996). In order to establish a functionally connected network, neurons need to be able to discriminate and identify not only their own neurites but also those of their neighbouring cells. This discrimination is typically achieved through cell recognition molecules expressed on the plasma membrane. Protein-protein interactions between different neurons play crucial roles in generating distinct boundaries in the brain, in guiding neurons to their targets, and in promoting the formation of synapses between pre- and postsynaptic cells (Tessier-Lavigne & Goodman, 1996).

Miswiring in the human brain is suggested to be the underlying cause of numerous developmental disorders including Down syndrome, autism and fragile X syndrome (Becker *et al.*, 1991, Lightbody & Reiss, 2009, Mitchell, 2011). However, it is still unclear how the formation of erroneous connections in the brain leads to behavioural problems. Understanding brain development and the behaviours that result when miswiring occurs will allow us to gain a better understanding of neurodevelopmental disorders. Using *Drosophila* behavioural paradigms, we can ask questions about how wiring changes in the brain affect behaviour. Flies' natural attraction to food and light, as well as their reflexive responses to gravity and motion, can be utilized to measure behavioural output. By combining these behavioural paradigms with genetic tools, more insight into the relationship between neural connectivity and behaviour can be obtained.

The *Drosophila* visual system has been used to understand the molecular requirements of neural connectivity. The fly visual system is a topographically arranged system and it is this modular organisation that makes it ideal for studying the connections between neurons. The *Drosophila* eye faces a problem similar to the eyes of all other organisms; the view of the outside world needs to be coded by a finite array of neurons. Each of these neurons has a limited signalling capacity defined by their fundamental cellular properties, and as a result, an efficient computational way of extracting specific information such as contrast, shape, motion, colour, and polarisation. These principles of visual information extraction are very similar across different species, resulting in the *Drosophila* eye being widely used to study general principles of visual coding and processing.

Vision is an important sensory resource for many animals including *Drosophila*. Objects and their movement need to be detected and this requires a complex computation that is carried out by numerous neurons that integrate information from different parts of the eye. Visual computation has been of interest for many decades, beginning with motion detection models developed in the early 1950's and 1960's. Even with over 50 years of intensive investigation, there is still a lot to be learned about how visual coding and processing takes place. Today, technological advances, and the development of visual behavioural assays can be used to unravel the computational function of each neuron and how miswiring in the visual system changes visual behaviour. In this thesis, three assays have been set-up to study visual behaviour in *Drosophila*, including a mutant with miswiring in the brain.

This thesis contributes to the field by providing new assays that can be used to study the relationship between brain wiring and behaviour. This is demonstrated by studying visual behaviours in *Dscam2* mutant flies and uncovering unexpected phenotypes based on the known wiring defects in these animals.

1.2 A general introduction to the Drosophila visual system

Flies can detect and process colour, motion, polarized light and geometric pattern information from visual stimuli (Giurfa & Menzel, 1997) and use a complex neuronal network to do so. Dipterans such as the housefly (*Musca domestica*), blowfly (*Calliphoridae erythtroccephala*), and fruit fly (*Drosophila melanogaster*) share a very similar visual system structure. The housefly and blowfly have classically been used for electrophysiology because their neurons are large whereas *Drosophila* has been used more for molecular genetic explorations of the visual system due to the wide range of genetic tools available (Eichner *et al.*, 2011, Meinertzhagen & Hanson Thomas, 1993, Sato *et al.*, 2013, Takemura *et al.*, 2013, Tayler & Garrity, 2003, Vogt & Desplan, 2007, Zhu, 2013). Studying how neurons establish connections in the mammalian brain is challenging due to the sheer number and complexity of connections. The *Drosophila* brain abides by similar rules in terms of neural connectivity and development, but only contains about 100,000 neurons (Clandinin & Zipursky, 2002, Meinertzhagen & Hanson, 1993).

The *Drosophila* visual system consists of the retina and four morphologically separated ganglia, called the lamina, the medulla, the lobula and the lobula plate, as shown in figure 1.1 (Hadjieconomou *et al.*, 2011). In the retina, photoreceptors (R-cells) are organized into ~750 modular units called ommatidia (Clandinin & Zipursky, 2002; figure 1.1). Each ommatidium contains one of each type of photoreceptor (R1-8). The motion-detecting R1-6 cells extend axons to the lamina, where they form ~750 synaptic units called lamina cartridges. Within each cartridge, R1-6 axons form a cage around two postsynaptic cells, namely lamina neurons L1 and L2. Each photoreceptor terminal consists of 50 output synapses (Meinertzhagen & Sorra, 2001), each containing four postsynaptic elements, two of which are invariantly lamina neurons L1 and L2 (Meinertzhagen & O'neil, 1991; figure 1.1, inset). L1 and L2 axons project to the medulla where they form connections within a single medulla module called a column. The neurons bundled in lamina cartridges and medulla columns receive information from photoreceptors which see the same points of space (Kirschfeld, 1967). This means that photoreceptors from several ommatidia, which receive information from the same point in space, will give input to a single lamina cartridge. This modular organisation is important for its function in motion detection.

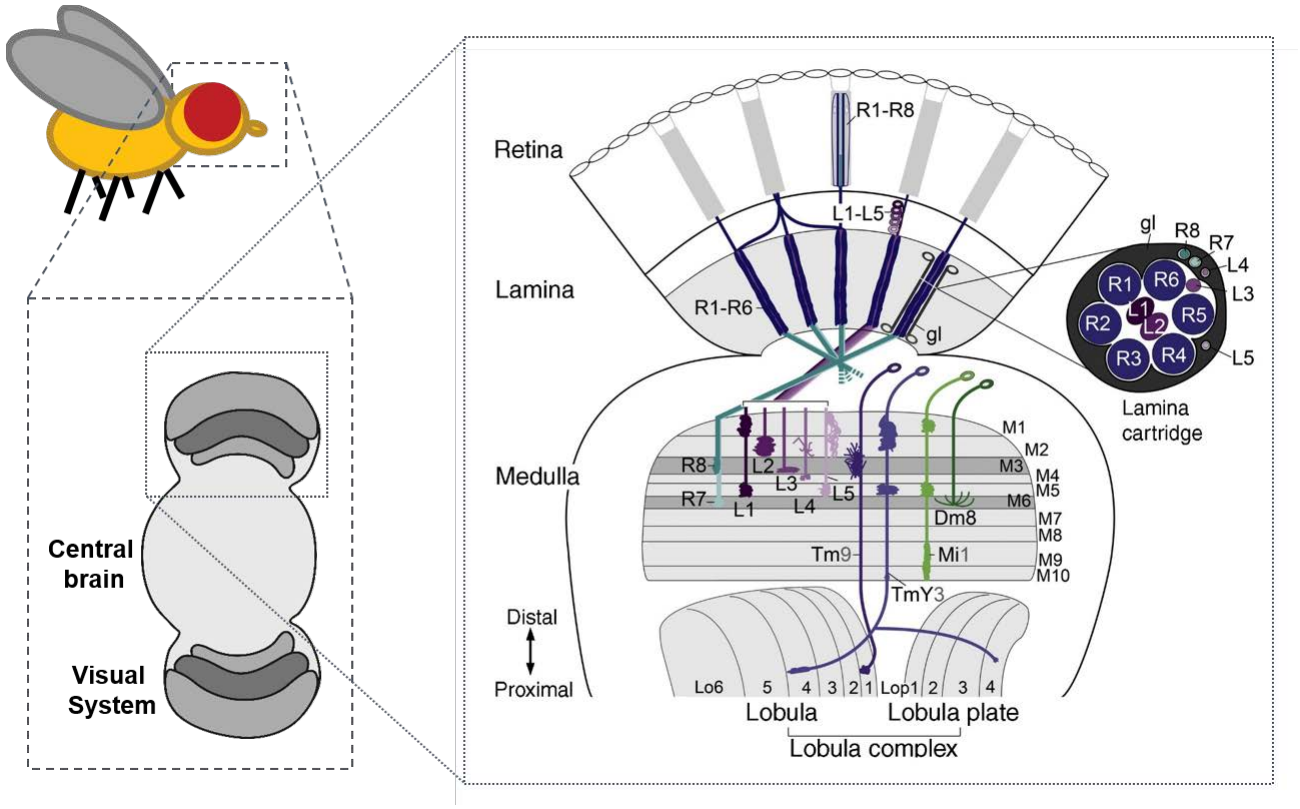

Figure 1.1 The fly visual system.
The adult fly visual system consists of the retina and four optic ganglia. Directly under the retina, the lamina is found, which overlays the medulla. Under the medulla, the lobula complex is found which consists of the lobula and the lobula plate. In the retina there are eight photoreceptor cells, R1-8 of which R1-6 target to the lamina and R7 and R8 target directly to the medulla. The lamina consists of synaptic modules called cartridges which contain R1-6 and 12 other lamina processes of which lamina neurons L1-5 are indicated here. They are surrounded by glia cells (gl). L1-L5, along with R7 and R8, project axons to specific layers of the medulla. Transmedullary neurons (Tm) connect the medulla with the lobula complex. Modified from Current Opinion in Neurobiology, 21/1, Hadjieconomou, D., A step-by-step guide to visual circuit assembly in Drosophila, 1, 2011, with permission from Elsevier.

1.3 Motion detection

1.3.1 Optomotor response

The optomotor response is an animal response to involuntarily course deviations. It is found in all sight-reliant animals where it plays a role in course stabilization during free locomotion (Mccann, 1965). When an animal involuntarily deviates from a straight course, it has the tendency to turn with the surroundings to regain its course. Due to its highly reflexive origin, the optomotor response has been used to study motion detection and vision limitations in mice (Kretschmer *et al.*, 2013), zebrafish (Neuhauss, 2003) and flies (Mccann & Macginitie, 1965). For this, optomotor assays often use a moving repetitive stimulus pattern of vertical stripes, i.e. a grating, which elicits a strong behavioural response.

Assays that assess the optomotor response can be divided into free-walking and tethered assays. Free-walking assays can be performed either on populations or on single flies, whereas the tethered assays are limited to single fly experiments. The behavioural response to a moving grating differs depending on the assay. When a group of flies is placed in a tube and subjected to a moving grating perpendicular to the tube, the flies move against the direction of motion (Lee *et al.*, 2001, Zhu & Frye, 2009; figure 1.2A/B). In contrast, populations of flies walking through an 8-tiered maze (figure 1.2C), single free walking flies in a paper/plastic striped drum (figure 1.2D) or tethered flies (figure 1.2E-F) move in the direction of the moving grating (Blondeau & Heisenberg, 1982, Bosch *et al.*, 2015, Buchner, 1976, Evans *et al.*, 2011, Götz, 1968, Götz & Wenking, 1973, Mccann & Macginitie, 1965, Van Swinderen & Flores, 2007). Why the optomotor response is assay-dependent is not known, and this thesis will provide new insight into this problem using both population and single fly assays.

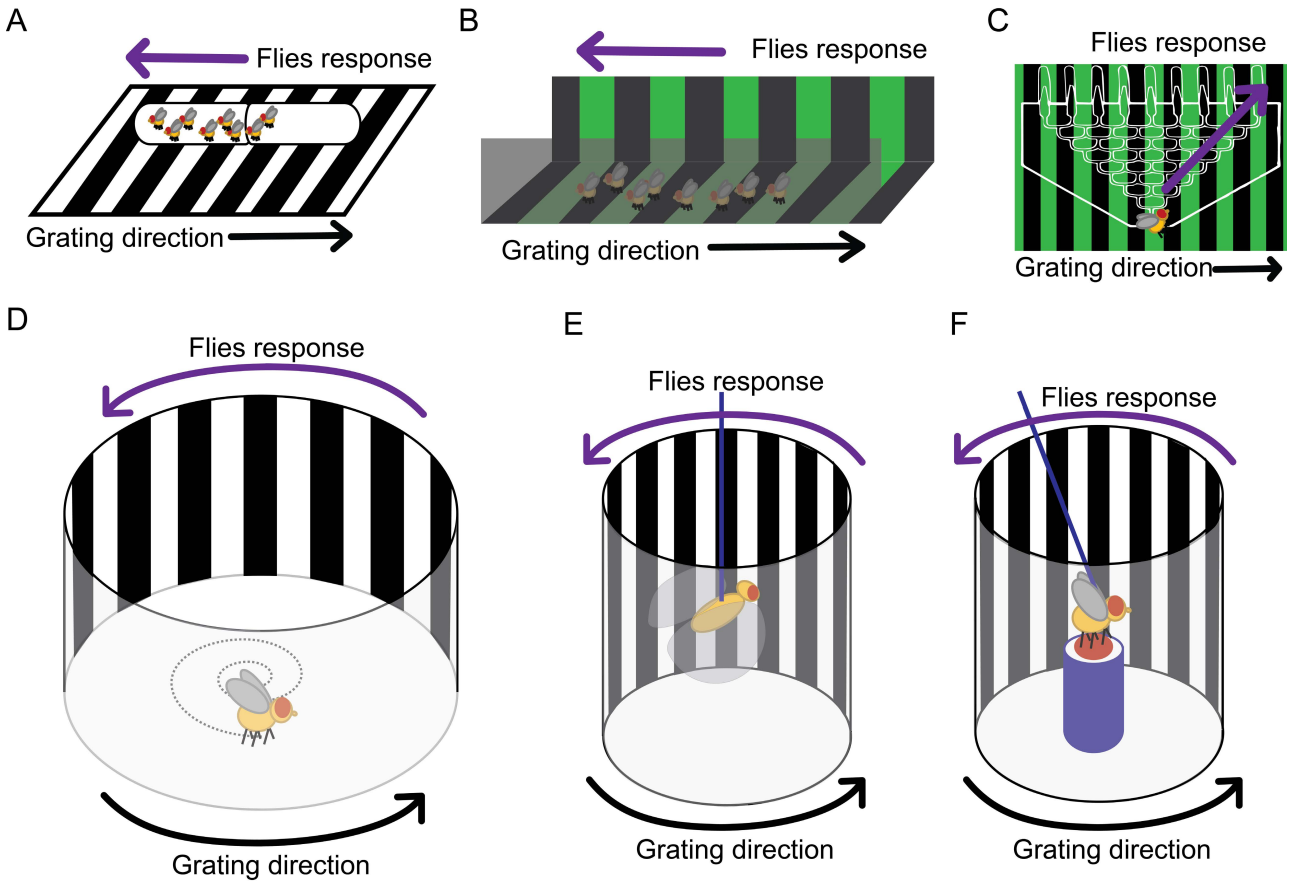

Figure 1.2 Optomotor assay to study motion detection in *Drosophila*.
Schematic of free-walking and tethered optomotor assays. **(A-B)** Free-walking assays which use a population of flies located in a tube **(A)** or "fly-stampede" **(B)** are found to move against the direction of a displayed moving grating (Lee *et al.*, 2001, Zhu & Frye, 2009). **(C)** A population of flies walking through an 8-tiered maze follows the direction of the moving grating (Van Swinderen & Flores, 2007). **(D)** In a single fly free-walking assay in which the fly is located within a rotating paper/plastic striped drum, the fly moves with the direction of the moving grating (Mccann & Macginitie, 1965). **(E-F)** The perception of the visual stimulus can be controlled in a tethered fly set-up. The tethered flying **(E)** or walking **(F)** fly is exposed to a moving grating. In the flying fly setup **(E)**, steering reactions are measured where in the walking fly setup **(F)** the ball is used as a joystick. In both cases, the reactions of the tethered fly do not interact with the visual input. Here, the fly's perception of the visual stimulus can be rigorously tested by manipulating different aspects of the moving grating. This approach has led to mechanistic models on visual course control in walking (Buchner, 1976, Götz & Wenking, 1973) and flying *Drosophila* (Blondeau & Heisenberg, 1982, Götz, 1968).

1.3.2 A theoretical model for motion detection computation

Hassenstein and Reichardt proposed a theoretical model of motion detection in 1956 (Hassenstein & Reichardt, 1956b) which has withstood a wide number of experimental tests. They conceptualised this model after careful analysis of the turning tendency of the snout beetle (*Chlorophanus viridis*)

walking on a spherical Y-maze (figure 1.3D). The beetle had an tendency to follow the movement of the visual surrounding to compensate for its false perception of self-motion in the opposite direction, a response termed the optomotor response (Hassenstein & Reichardt, 1956b).

Hassenstein and Reichardt (1956b) proposed that detecting the direction of motion must involve a comparison between two sampling points in the eye. Each pair of sampling points would have a preferred direction that elicits a positive response (figure 1.3A-C). They hypothesised that this could be achieved by delaying the signal from one sampling point so that it was in phase with the second one only when the motion is in the preferred direction; this provides the basis of their EMD model (Hassenstein & Reichardt, 1956b, Reichardt & Rosenblith, 1961). The directionality of this system is such that if the same sampling points experience motion in the opposite direction, they will be out of phase and therefore not elicit a response. It is proposed that the visual system consists of hundreds of elementary units, covering collectively the whole visual field and each elementary unit extracts locally the direction of motion (Hassenstein & Reichardt, 1956b).

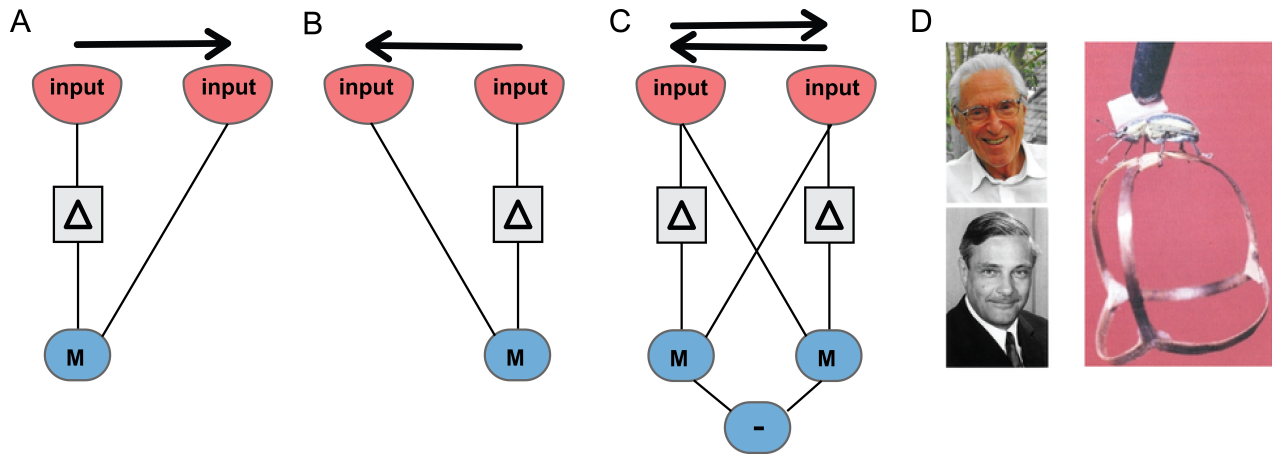

Figure 1.3 The Hassenstein-Reichardt model of the Elementary Motion Detector.
(A-C) Theoretical model of motion detection, also known as the Hassenstein-Reichardt detector. It relies on brightness changes between two brightness sensitive inputs. One input is delayed (Δ) compared to the other input. Both inputs are multiplied (M) which allows the calculation of the direction to the right **(A)**, left **(B)** or both directions **(C)**. This is done in two mirror-symmetrical subunits of which the outputs are subtracted from each other (-). The two inventors Bernhardt Hassenstein (top) and Werner Reichardt (bottom) came up with this model based on data derived with their behavioural setup of a beetle walking on a Y-maze (right). Panel D reprinted from European Journal of Neuroscience, 40/9, Borst, A., In search of the holy grail of fly motion vision, 9, 2014, with permission from John Wiley and Sons.

1.3.3 Eye geometry and aliasing

Classically, psychophysical parameters like contrast, luminance, and spatial and temporal frequencies have been manipulated to test the efficiency and limits of motion detection (Duistermars *et al.*, 2012, Duistermars *et al.*, 2007, Götz, 1965, Götz, 1972). Although all of these parameters are dependent on

the sensitivity and acuity of the visual system, each one provides unique information about visual system processing. For example, an animal that can distinguish an object from its background at low speeds, but not at high speeds, would have an impairment in the circuitry that controls temporal frequency, but not contrast. Similarly, when the spatial frequency, i.e. the distance between repetitive objects such as bars in a grating, is decreased, more information will be gained on the acuity of the visual system. This parameter can be used to identify impairments in the circuitry that determines visual system acuity as it depends on the spatial separation of input elements. Motion detection in *Drosophila* is based on processing brightness changes between motion detection units in the eye and its limitation in spatial resolution is dependent on the distance between the inputs, called the sampling base or inter-ommatidial angle $\Delta\Phi$. *Drosophila* has approximately 750 ommatidia per eye, i.e. 750 sampling points distributed over almost 180 degrees of visual space. By reducing the spatial period, i.e. distance between the bars, and measuring the optomotor response it has been found that *Drosophila* has an inter-ommatidial angle of 4.6 degrees (Götz, 1964). Interestingly, it was found that a decrease in spatial frequency to between 2 $\Delta\Phi$ and 1 $\Delta\Phi$, results in an optomotor response against the direction of motion, also referred to as (spatial) aliasing (Götz, 1964, Götz, 1972). In aliasing, the motion is perceived in opposite direction from the actual direction due to the geometrical interference between the moving grating and the sampling array, i.e. ommatidia. The temporal frequency of the grating, e.g. speed at which the grating is moving, is correlated with the optomotor response in a Gaussian fashion with a pronounced optimum peak of which the magnitude but not the temporal frequency is dependent on the spatial frequency (Duistermars *et al.*, 2007)). Together, the strength and direction of the optomotor response have been found to depend on specific spatial and temporal frequencies of the stimulus pattern and provided a basic understanding of visual system sensitivity (Duistermars *et al.*, 2007, Götz, 1964, Götz, 1972).

1.3.4 Circuits involved in motion detection

Two different types of motion exist: (1) object and (2) self-motion. Both types of motion start with the detection a movement through neurons in the visual system. To ascertain how different neurons in the optic lobe respond to motion, researchers have recorded from different cell types, such as photoreceptors and lobula plate cells, while presenting a moving bar to a fly. Photoreceptors elicit a nondirectional response to motion; they fire in response to changes in light intensity independent of direction (Borst, 2014; figure 1.4A-B). Interestingly, recordings from lobula plate tangential cells, which are large cells located in the lobula complex (figure 1.4A-B), demonstrated directionality in which some cells would depolarize when the bar moves to the right (their “preferred direction”) and hyperpolarise when the bar moves to the left (their “null direction”) and others do the opposite

(Douglass & Strausfeld, 1995). Considering the very different responses, the direction computation must take place somewhere between the photon-capturing photoreceptor cells, and directionally-selective lobula plate tangential cells and it is this part of the circuitry that is the main focus in this thesis.

Although motion detection has been well described in a theoretical EMD model (Hassenstein & Reichardt, 1956b), limited and conflicting information on the neuronal representation of this model is available. This demonstrates that even in the relatively simple compound eye of the fruit fly, rather complex computation takes place. Although the cells that perform the delay computation still remain controversial, much of the circuitry that forms the input and output of the motion detection network has been identified (Borst, 2014, Takemura *et al.*, 2013).

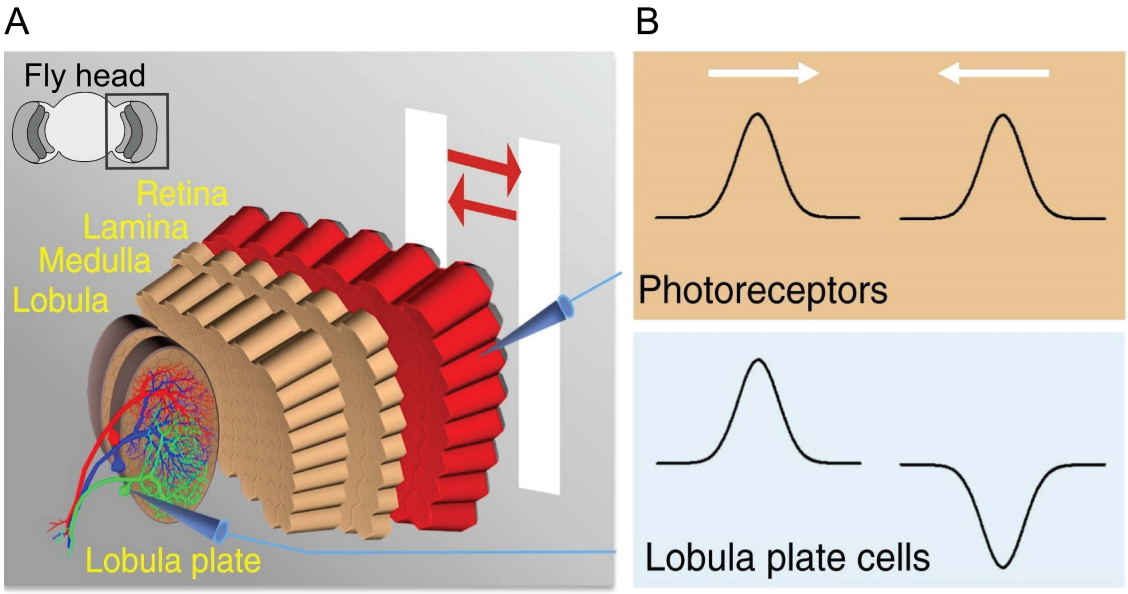

Figure 1.4 Motion detection in the fly visual system.
(A) Schematic of the fly visual system. The retina (red) overlays the lamina and medulla in a retinotopical manner, creating a modular structure. The neuronal response (displayed in **B**) can be measured from photoreceptors and lobula plate cells using electrodes to a white bar moving either to the left or right. **(B)** The response from the photoreceptors to right- and leftward motion is identical. Tangential cells depolarize for motion to the right and hyperpolarize during motion to the left, making them directionally selective (Hausen, 1982). Modified from Current Biology, 21/24, Borst, A., Fly Vision: Moving Into the Motion Detection Circuit, 1, 2011, with permission from Elsevier.

One way to explore how the motion circuitry is connected is to analyse the neuroanatomy. These types of studies were originally performed using rather crude Golgi impregnation (Ramón Y Cajal, 1913), but have advanced to include ultrastructural (Meinertzhagen & Hanson, 1993) and morphological descriptions using advanced microscopy (Takemura *et al.*, 2013). However, because an anatomical connection does not provide evidence for a behavioural function, molecular genetic techniques such as the GAL4/UAS system have been used to transiently inactivate or activate specific

neurons, to assess their necessity during optomotor behavioural tests. Examples of such transgenes are the temperature sensitive *shibire*^{ts}, which inhibits synaptic vesicle recycling and by doing so prevents neurotransmitter release (Kitamoto, 2001), the inwardly rectifying K^+ channel activator Kir2.1 which suppresses synaptic activity in neurons by hyperpolarizing the resting potential (Baines *et al.*, 2001) and the temperature-gated cation channel dTrpA1 (Hamada *et al.*, 2008) which depolarizes neurons (Hodge, 2009, Pulver *et al.*, 2009). Another approach is to measure activity of individual neurons using either electrophysiology or calcium imaging. Electrophysiology can be used to measure the behaviour of individual neurons and identify specific visual system circuits. Much of the initial work in this area has been performed on flies such as the housefly and blowfly because of their larger neurons (Hardie, 1979). Electrophysiology is invasive is limited in some parts of the *Drosophila* visual system, such as the lamina, where neurons are much smaller. In addition, it can be questioned if the fly is able to behave 'normally' when electrodes are insert into the brain. This has resulted in the development of alternative techniques such as two-photon calcium imaging which measures the activity of specific neurons in live animals (Seelig *et al.*, 2010).

Using a combination of these techniques, information has been gathered on the function and roles of specific neurons in the fly visual system. Presented here is a brief overview of the neuronal circuits involved in motion detection. The information presented is based on experimental data from the housefly, blowfly and fruit fly, which have been found to share similar visual pathways (Buschbeck & Strausfeld, 1996). An emphasis will be placed on lamina neurons L1 and L2, which are postsynaptic to R1-6 photoreceptors and have been shown to play an essential role in motion detection. A large part of this thesis is dedicated to the assessment of visual behaviours in a mutant which has a change in the postsynaptic composition of photoreceptor synapses.

Vision starts at the retina with photoreceptors R1-8 located in individual ommatidia. Motion detection has been found to be independent from colour vision (Yamaguchi *et al.*, 2008) but R7 and R8 improve motion perception (Wardill *et al.*, 2012). Photoreceptors R1-6 form the first synapse in the motion detection circuit with lamina neuron L1 and L2 cells (Strausfeld & Campos-Ortega, 1977), and it has therefore been hypothesized that the early stages of motion computation may occur in the lamina (Coombe *et al.*, 1989, Douglass & Strausfeld, 1995). L1 and L2 are found in every lamina cartridge, representing the modularity required for motion detection and could therefore represent the two offset inputs into the EMD (Braitenberg & Hauser-Holschuh, 1972). They both hyperpolarize in response to depolarizing photoreceptors (Strausfeld & Campos-Ortega, 1977) and express different neurotransmitter phenotypes, with L1 being glutamatergic and L2 cholinergic (Gao *et al.*, 2008).

Simultaneous blocking of L1 and L2 completely abolishes the ability to detect motion demonstrating that these neurons are essential for motion detection (Rister *et al.*, 2007). Multiple studies observed that L1 and L2 represent different channels of visual information, responding to increments (OFF-ON, also termed ON-edge) and decrements (ON-OFF, also termed OFF-edge) in light, respectively (Joesch *et al.*, 2010, Reiff *et al.*, 2010). However, there is some controversy about how independent these channels are as work from Clark *et al.* (2011) and Eichner *et al.* (2011) revealed that L1 and L2 have similar responses to both moving ON- and OFF-edges, indicating that L1 and L2 both process information about light and dark. In contrast, Joesch *et al.* (2013) found that L1 specially transmits information about ON-ON (sequence of light-light) and L2 about OFF-OFF (sequence of dark-dark). The differences in results from these groups can potentially be attributed to differences between behavioural assays and/or activation of multiple, parallel motion circuits as well as gap junctions on L1 and L2 neurons. To summarize, L1 has been found to be involved in the detection of light increments and L2 with contributions of L1, is involved in the detection of light decrements (Clark *et al.*, 2011, Joesch *et al.*, 2010). In addition to a behavioural specialisation of increments and decrements of light, also a specialization of L1 and L2 for translational stimuli such as back-to-front and front-to-back motion respectively has been suggested (Rister *et al.*, 2007) and confirmed for L2 (Tuthill *et al.*, 2013).

L1 and L2 are not the only lamina neurons receiving input from photoreceptors R1-6; L3 receives input from these as well. L3 is found in only a third of the lamina cartridges and was originally thought to be primarily involved in landmark orientation and spectral preference (Gao *et al.*, 2013, Rister *et al.*, 2007). Recent evidence provided by behavioural assays combined with calcium imaging and neuronal silencing experiments, suggest a role for L3 in motion detection by contributing to L2 in the detection of moving OFF-edges (Silies *et al.*, 2013). This suggests that L2, with contributions from L1 and L3, is involved in the detection of moving OFF-edges (Clark *et al.*, 2011, Joesch *et al.*, 2010, Silies *et al.*, 2013). L4 receives input from three L2's, one located in the same cartridge, as well as L2 neurons in the adjacent postero-dorsal and postero-ventral cartridges (Meinertzhagen & O'neil, 1991). This morphological structure of L4 suggested it could play a role in motion detection (Braitenberg, 1970, Meinertzhagen & O'neil, 1991, Rister *et al.*, 2007, Strausfeld & Campos-Ortega, 1973, Strausfeld & Campos-Ortega, 1977, Takemura *et al.*, 2011). Recent evidence acquired through neuronal silencing techniques suggest however, that L4 does not play a role in translational or rotational motion, but may provide input to motion detection circuits under other stimulus conditions (Silies *et al.*, 2013). L5 receives few synaptic connections in the lamina and its function is unknown.

Together these results demonstrate the importance of L1 and L2 for motion detection, along with their role in providing input to motion circuits. However, it appears that L1 and L2 are not directly involved in elementary motion computation suggesting that the directional computation happens downstream from these neurons.

L1 provides input to Mi1 and Tm3 and L2 provides input to Tm1 and Tm2 in the medulla (Bausenwein *et al.*, 1992, Takemura *et al.*, 2013; figure 1.5). Consistent with this anatomical arrangement, Mi1 and Tm3 respond selectively to brightness increments and the Mi1 response is delayed relative to Tm3 (Behnia *et al.*, 2014). It has also been shown that Tm1 and Tm2 respond selectively to brightness decrements and the Tm1 response is delayed relative to Tm2 (Behnia *et al.*, 2014). These pathways are potentially critical for the processing of delayed and non-delayed input channels of the EMD. Mi1 and Tm3 provide input to T4 (Takemura *et al.*, 2013) and Tm1 and Tm2 provide input to T5 (Shinomiya *et al.*, 2014). T4 and T5 are found in the lobula complex and through neuronal silencing and electrophysiological experiments in *Drosophila* it has been found that they respond selectively to moving light edges and dark edges respectively (Maisak *et al.*, 2013) and provide input to the LPTCs in a directionally selective manner (Douglass & Strausfeld, 1995, Douglass & Strausfeld, 1996, Schnell *et al.*, 2012, Strausfeld & Lee, 1991). T4 and T5 come in four different variants and project to four different layers in the LPTCs, each of which is dedicated to motion processing of a direction (Buchner *et al.*, 1984, Schnell *et al.*, 2012). These layers contain horizontal and vertical sensitive cells that respond to horizontal or vertical motion in a specific direction and provide input to central brain structures (Hausen, 1984, Strausfeld & Bassemir, 1985). These cells are direction sensitive and therefore suggested to be the output of the EMD (reviewed in Borst and Haag (2002)).

In conclusion, the pathways proposed by Bausenwein and Fischbach (1992) and Strausfeld (1984) in which a signal from R1-6 transmits information from L1 through Mi1 and T4 to LPTC and L2 through Tm1 and T5 to LPTC (figure 1.5), is supported by experimental evidence. To date, the role of L1, L2 and LPTCs in motion detection are well established (Rister *et al.*, 2007, Seelig *et al.*, 2010, Sen *et al.*, 2014), with recent evidence that Mi1 with Tm3, and Tm1 with Tm2 provide the critical processing of the delayed and non-delayed input channels of the EMD (Behnia *et al.*, 2014). However, there are more than one hundred different classes of neurons found in the fly visual system, meaning that it is unlikely that these pathways provide the complete picture of the neuronal correlates of motion detection. Therefore, more research is required to understand the role of other neurons such as L4 in motion detection.

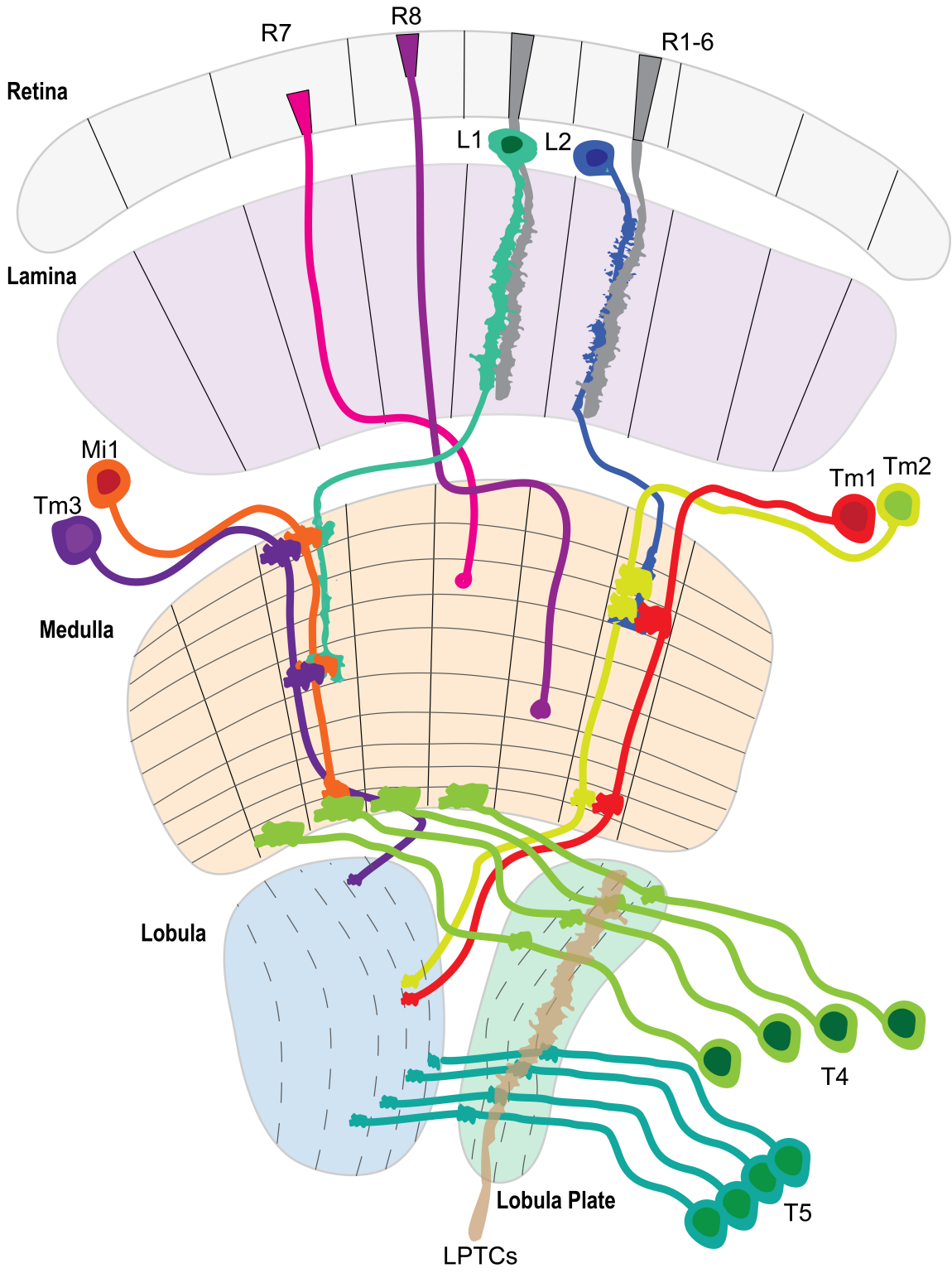

Figure 1.5 Motion detection circuitry in the fly visual system.
Photoreceptors R1-6 (grey) in the retina transmit visual information to L1 (green) and L2 (blue) lamina neurons which respond to increments and decrements in light, respectively (Clark et al., 2011; Joesch et al., 2010). Photoreceptors R7 (pink) and R8 (light purple) project directly to the medulla. The information from L1 is transmitted to Mi1 (orange) and Tm3 (dark purple) in the medulla, and both provide the critical processing of the delayed and non-delayed input channels of the EMD (Behnia *et al.*, 2014). Similarly, Tm1 (red) and Tm2 (dark yellow) receive their information in the medulla from L2 lamina neurons (Behnia *et al.*, 2014). T4 (light green), arborizing in the medulla and lobula plate, and T5 (turquoise) arborizing in the lobula and lobula plate, provide input to the LPTCs in the lobula plate in a directionally selective manner (Douglass & Strausfeld, 1995, Douglass & Strausfeld, 1996, Schnell *et al.*, 2012, Strausfeld & Lee, 1991).

1.4 Object orientation and attention-like behaviour

Another simple visual behaviour that flies can perform is object orientation. It has been found that certain objects can elicit fixation behaviour, in which a fly will walk towards the object, or anti-fixation behaviour, in which a fly will walk away from the object (Reichardt & Wenking, 1969). Fixation and anti-fixation are important for landing, tracking and chasing behaviour (Bülthoff, 1980, Collett & Land, 1975). The decision to fixate or anti-fixate to an object such as a bar has been shown to be dependent on bar length (Maimon *et al.*, 2008) and the assay. For example, a light bar on a dark background elicits an anti-fixation response in some assays (Bülthoff, 1980, Collett & Land, 1975) but not in others (Maimon *et al.*, 2008, Reiser & Dickinson, 2008). These behaviours also provide a means for studying attention-like mechanisms in flies. Random displacement of the object elicits attention-like tracking processes. Attention involves an awareness of a stimulus (Posner, 1980) and is a major area of investigation in neuropsychology. Object orientation can involve both self- and object motion so it is no surprise that part of the neuronal circuitry involved in motion detection contributes to orientation behaviour. However, there does not appear to be a strict requirement given that motion-blind flies can still fixate (Bahl *et al.*, 2013, Bülthoff *et al.*, 1982). Orientation and attention-like behaviour in *Drosophila* are based on an elementary position detector model.

1.4.1 Fixation and anti-fixation

Fixation and anti-fixation behaviours have been well studied in freely walking (Coombe, 1984, Horn & Wehner, 1975, Morton & Cosens, 1978, Osorio *et al.*, 1990, Wehner, 1972) and tethered flies (Bahl *et al.*, 2013, Heisenberg, 1984, Heisenberg & Wolf, 1979, Wolf & Heisenberg, 1980). In the free walking setup, a fly is placed in a visual arena where it can walk around while being exposed to visual stimuli such as single bars (figure 1.6A). The movement of the fly is tracked and its orientation preference is recorded. Flies have been found to orientate towards and fixate on edges in a freely walking setup (Wehner, 1972). When a fly is presented with two dark bars 180 degrees from each other in the arena (Buridan's paradigm), it will walk back and forth from bar to bar, unable to choose one of the two bars (Gotz, 1980). In a tethered flying fly set-up, the fly is held in place, eliminating head movement but allowing the animal to otherwise move its legs and wings freely (figure 1.6B). In a tethered walking fly set-up, the fly is also held in place but is able to walk on an air-supported ball (figure 1.6C). In both setups, a fly is located in a visual arena and controls the position of the object is electronically, a so-called closed-loop condition. This is different from the optomotor assay, an open-loop condition, where the fly is unable to interact with the visual input.

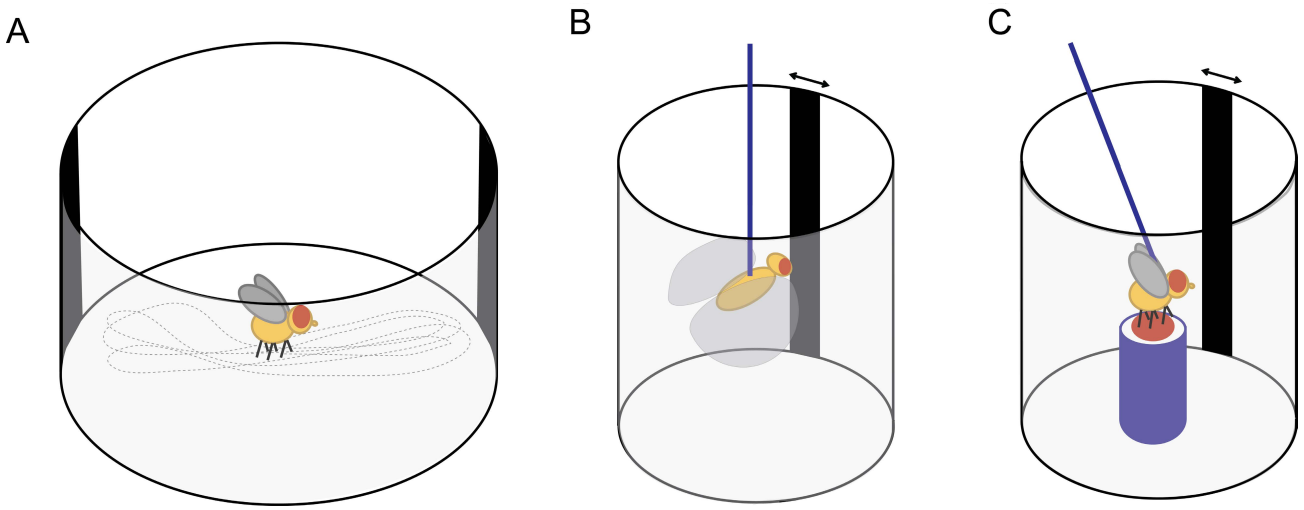

Figure 1.6 Object-orientation assays.
Schematic of free-walking and tethered object-orientation assays. **(A)** A free-walking assay using a single fly in a visual arena where it can walk around while being exposed to visual stimuli such as two single bars placed 180 degrees from each other (Buridan's paradigm). Here, the fly will walk back and forth from bar to bar, unable to choose one of the two bars (Gotz, 1980). **(B)** In a flying tethered-fly set-up, the fly is held in place in a visual arena. The fly controls the position of the object electronically by its wing behaviour, in a closed-loop manner (Heisenberg & Wolf, 1979). Similarly, in a walking tethered-fly set-up, the fly is able to control the position of the object electronically by using an air-supported ball as a joystick (Bülthoff, 1980).

Flies have been found to orientate towards and fixate on dark bars in both walking (Bülthoff, 1980) and flying assays (Heisenberg, 1984, Heisenberg & Wolf, 1979, Maimon *et al.*, 2008, Wolf & Heisenberg, 1980). Similar to the fixation observed in Buridan's paradigm, this is a very robust response under optimal conditions, with sustained object fixation measured in a nearly continuous 32-hour period (Götz, 1987). Though it is not uncommon that flies exhibit fixation for a very short time or do not fixate. The introduction of random bar displacements in this assay improves fixation behaviour, likely because the displacement triggers the attention of the fly (Heisenberg & Wolf, 1979). The strength of the fixation and anti-fixation response has been found to be dependent on bar length (Maimon *et al.*, 2008). When the bar length becomes smaller, anti-fixation behaviour will become the dominant choice (Maimon *et al.*, 2008). Anti-fixation has been observed by some groups as the response to a light bar on a dark background in a tethered fly setup (Bülthoff, 1980, Heisenberg & Wolf, 1979, Wolf & Heisenberg, 1980) while others more recently reported fixation behaviour for the same stimulus (Maimon *et al.*, 2008, Reiser & Dickinson, 2008). Fixation and anti-fixation are a decision-making processes: a fly can choose to non-fixate, fixate or anti-fixate to an object. There is limited literature on the neuronal components of this decision making process, but neurochemical factors have been reported. For example, it has been shown that injection of a GABA antagonist can change fixation to an anti-fixation response (Bulthoff & Bulthoff, 1987), suggesting that this decision process relies on inhibition of specific neurons. There is also limited literature on anti-fixation

behaviour, possibly due to a number of assay- or visual stimulus-related differences. Consequently, anti-fixation is not well understood and it is unclear what makes an object unattractive for a fly. This is why a more detailed analysis of these behaviours is required. It is however important to point that anti-fixation is distinct from non-fixation. The former involves attention, whereas the latter is defined as disinterest in an object. In conclusion, studying the underlying mechanisms of fixation and anti-fixation as well as the use of these behaviours to study attention-like mechanisms offers a deeper understanding of computational processing in the fly.

1.4.2 Computation of object-orientation behaviour

In contrast to the optomotor response which compares activation of two sampling points, the fixation response works through individual elementary position detectors (EPDs) which are summed and lead to a response (Bahl *et al.*, 2013, Poggio & Reichardt, 1973). Initial work suggested that object position is based primarily on motion detection (Bulthoff & Bulthoff, 1987) but more recent evidence with flies which are not able to detect motion but are able to track objects suggest a separation of these pathways (Bahl *et al.*, 2013). Orientation behaviour and the optomotor response have been found to work in independent, parallel processing streams in the fly visual system (Aptekar *et al.*, 2012, Bahl *et al.*, 2013, Fox *et al.*, 2014) but it is unclear where in the fly eye the information captured by photoreceptors gets separated into these different processing streams.

1.4.3 Neurons involved in object-orientation behaviour

Object-induced orientation behaviour involves some neurons that are part of the motion-detection circuitry, but is also thought to involve other pathways (Aptekar *et al.*, 2012, Bahl *et al.*, 2013, Bausenwein *et al.*, 1986, Heisenberg *et al.*, 1978, Strauss *et al.*, 2001, Tuthill *et al.*, 2013). Photoreceptors consist of two sections, mainly a cell body and a rhabdomere of which the latter absorbs light. To investigate the role of the R1-6 photoreceptors play in fixation, two photoreceptor mutants, ort^{1} (former designation: ora^{JK84} *, outer rhabdomeres absent*) which lack R1-6 rhabdomeres except for a small vestigial tip (Stark & Carlson, 1983) and *rdgB* (*retinal degeneration B*) in which R1-6 rhabdomeres degenerate with age and exposure to light (Coombe, 1984), were used. Coombe (1984) found that flies without intact R1-6 do not fixate on narrow stripes but are able to fixate on broad stripes in a free walking, circular arena, demonstrating the importance of R1-6 in fixation. A role for lamina neurons in the fixation response was investigated initially using Vacuolar medulla mutant (Vam) which results in degeneration of the lamina and the medulla. The Vam mutant reportedly lacks functional L1 and L2 neurons in adult stages (Coombe & Heisenberg, 1986,

Heisenberg & Bohl, 1979). These mutants did not exhibit an optomotor response in a tethered flying setup but were able to fixate to dark stripes of at least 20 degrees in width, suggesting that L1 and L2 are not required for fixation (Coombe & Heisenberg, 1986). Different results were obtained by Rister *et al.* (2007) using a free walking illuminated circular arena. Blocking the synaptic output of R1-6 abolished orientation to a 10-degree dark bar and blocking of L1 and L2 led only to a significant reduction in orientation (Rister *et al.*, 2007). Output from L1 and L2 was also required for narrower dark bars (5°) or 10° dark bars of a low contrast (Rister *et al.*, 2007). Considering orientation behaviour was still functional when L1, L2, and T1 were blocked, the authors speculated about the possibility that the L3 pathway, possibly interacting with R7 + 8 may mediate orientation behaviour (Rister *et al.*, 2007). The difference in results between Coombe and Heisenberg (1986) and Rister *et al.* (2007) could possibly be explained by the difference between orientation in a free walking and tethered flying setup. In a more recent experiment, neuronal silencing of L1 and L2 independently and together both significantly decreased the fixation response to a dark bar in a tethered fly setup (Tuthill *et al.*, 2013). Silencing L1 and L2 affects fixation behaviour while silencing T4 and T5 only affects the optomotor response and reduces but does not eliminates fixation (Bahl *et al.*, 2013). This suggests that the information captured by photoreceptors is separated into a different orientation and optomotor processing streams downstream from L1 and L2 but upstream from T4 and T5. Where this separation happens and which neuronal network it involves is unknown and therefore requires a more detailed experimental analysis.

1.5 Cell adhesion molecule requirements in fly visual system development

1.5.1 Efficient wiring in the fly brain

The functionality of sensory systems such as the fly visual system is dependent on precise synaptic connections between neurons. The specificity of synaptic connections unfolds in three major steps: pathway selection, target selection, and remodelling. During development, neurons travel long distances whilst searching for their targets (Harrison, 1910). Growth cones at the end of these neurons are guided by proteins on their cell surface to find their way to the correct target location where they will form synapses.

Ramón y Cajal performed extensive studies on the structure and organization of the developing and mature nervous system in a wide variety of species. These studies led to the idea that neurons find their way by selective chemical or electrical forces and introduced the term chemotaxis (Ramón Y Cajal, 1890). In the 1930's and 40's, experiments were performed that favoured a pure mechanical interpretation of how pattering of nerve tracts and fibre systems are established during development. Roger Sperry believed in a form of chemical selectivity and postulated in 1939 that patterning of synaptic connections must be regulated by *"highly specific cytochemical affinities that arise systematically among the different types of neurons involved via self-differentiation, induction through terminal contacts, and embryonic gradient effects."* (Sperry, 1963). Today, it is known that cell surface proteins, often referred to as cell recognition molecules, represent the cytochemical affinities about which Sperry hypothesised. Recognition mechanisms can either be contact-independent whereby cell surface molecules on the growth cone are able to interact with secreted ligands, or contact-dependent in which the receptor and ligand are both membrane bound and therefore require cell-cell contact. Both mechanisms serve to direct neurons to their appropriate synaptic targets in the brain.

An example of such an adhesive contact-dependent interaction in *Drosophila* is demonstrated at the *Drosophila* larval neuromuscular junction. Here, Fasciclin II (Fas II) assists in the adherence, i.e. fasciculation, of growing axons to each other during the process of growth cone guidance (Grenningloh *et al.*, 1991, Lin *et al.*, 1994). Lack of Fas II on these axons results in partial loss of this adherence, i.e. defasciculation, and consequently morphological changes to the neuronal network (Lin *et al.*, 1994). In this example, adhesion is used for fasciculation of specific axons.

In other cases neurons need to be repelled from each other to prevent inappropriate connections or to maximize population density. This can be established with cell surface proteins that activate repulsive mechanisms such as Eph/Ephrins and Down Syndrome Cell Adhesion Molecules 1 and 2 (*Dscam1* and *Dscam2*). Neurons expressing these cell surface proteins are able to bind and recognize each other which activates cell repulsive mechanisms. During *Drosophila* development, these repulsive cell surface proteins can promote neural connectivity through several mechanisms. Eph receptors and Ephrin ligands are membrane bound molecules expressed in many developing tissues such as in the *Drosophila* mushroom bodies which is the olfactory learning and memory centre (Heisenberg, 2003). During mushroom body development, neurons bifurcate and extend axons to two areas in the brain and Eph/Ephrin is involved in the process of the correct guidance of these branches to the appropriate target areas (Boyle *et al.*, 2006). *Dscam1* is another cell recognition molecule involved in axon branching and guidance in the development of the mushroom body (Wang *et al.*, 2002, Zhan *et al.*, 2004) by homophilic repulsion. Here binding between identical molecules expressed on different branches of the same neuron promotes branch segregation by inducing signalling events that leads to repulsion. *Dscam2* has been shown to play an important role in neuronal tiling (Millard *et al.*, 2007) and synaptic specificity (Millard *et al.*, 2010), which will be discussed in more detail in section 1.5.2.

During development of the sensory systems, neurons are exposed to a wide range of guidance cues. Some of these, such as Fas II, act in an adhesive way for fasciculation of specific axons. Others, such as *Dscam2* are involved in the generation of boundaries between cellular processes. The concert of guidance cues each neuron is exposed to, plays an essential role in brain wiring and potentially also behavioural state.

1.5.2 *Dscam2* in the fly visual system

Motion detection relies on the modularity of the visual system as it compares activation of neighboring facets. Down Syndrome Cell Adhesion Molecule 2 (Dscam2), a homologue of human DSCAM, is a cell recognition molecule crucial for the formation of connections between neurons and the development of the modularity of the visual system (Millard *et al.*, 2007). Dscam proteins in all species mediate homophilic binding, but Dscam2-Dscam2 interactions in the fly have been shown to induce repulsion, at least in the neurons studied thus far. During development, *Dscam2* generates boundaries between neighboring modules in the visual system through the process of cell-type-specific homophilic repulsion. For example, *Dscam2* restricts L1 lamina neuron axons to a single column in the medulla (Millard *et al.*, 2007). When *Dscam2* is removed from these cells, they form

inappropriate connections in adjacent columns (figure 1.7, box 4). L2 dendrites exhibit a similar phenotype when they lack *Dscam2*, as mutant dendritic arbors project into adjacent lamina cartridges (Lah *et al.*, 2014; figure 1.7, box 3). Given that identical synaptic targets for L1 axons and L2 dendrites exist in adjacent columns and cartridges, respectively, these mutant cells are likely forming synapses in neighboring regions of the optic lobe, thereby reducing the number of independent modules. Direct evidence for this has been observed at photoreceptor synapses in *Dscam2* homozygous mutant flies (Millard *et al.*, 2010). In the lamina of the *Dscam2* mutant, cartridges frequently fuse. An L2 dendrite from each of the two cells within the fused cartridge participates in the same photoreceptor synapse, something that never occurs in wild-type flies. Approximately 40% of the synapses within these fused cartridges contain two L2 dendrites and no L1 (figure 1.7, box 2). Thus, a visual stimulus that would normally engage one of the cartridges, engages two in the mutant. Lastly, R7 and R8 axons are disorganized in *Dscam2* mutant flies. R7 and R8 frequently cross over into adjacent medulla columns; this non-autonomous phenotype (Millard *et al.*, 2007) also results in a reduction of modularity (figure 1.7, box 5). Together, these morphological and synaptic phenotypes in the optic lobe suggest that Dscam2 plays a major role in establishing modularity; behavioral consequences of this, however, have not been investigated.

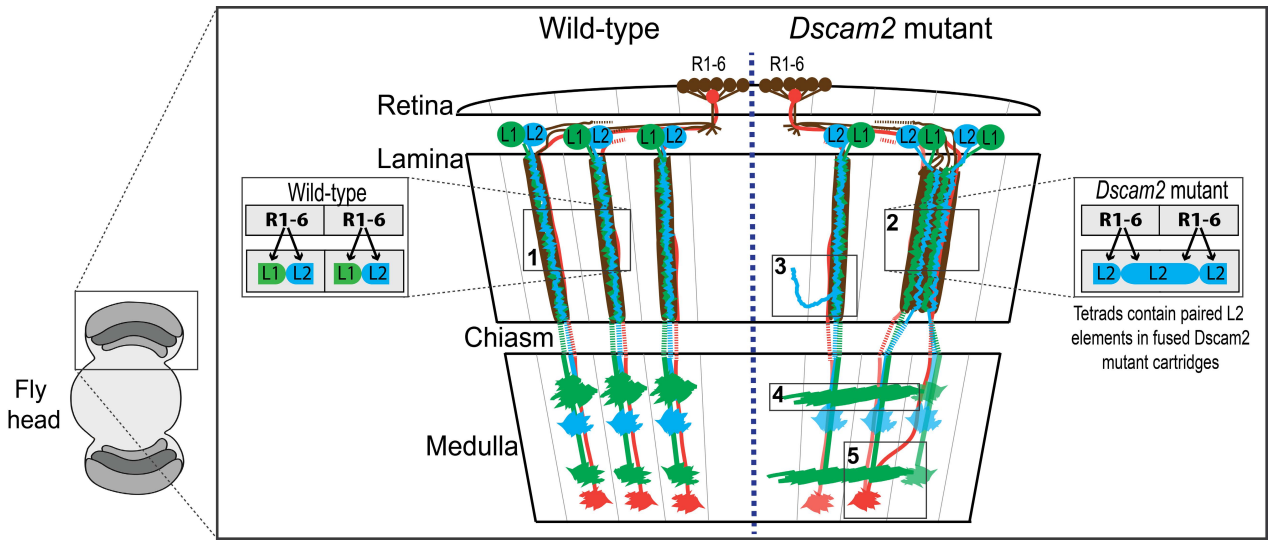

Figure 1.7. Wiring diagram of the optic lobes of wild type and the *Dscam2* mutant.
Schematic of wild-type (left side) and *Dscam2* mutant (right side) optic lobes with wiring details highlighted in boxes. Photoreceptors R1-6 (brown) in the retina form synapses with a postsynaptic complex that includes L1 (green) and L2 (blue) lamina neurons. Photoreceptors R7 (red) and R8 (not-shown) project directly into the medulla. **(1)** In WT animals, L1 and L2 are postsynaptic at every photoreceptor synapse. **(2)** In Dscam2 mutant animals, 40% of the photoreceptor synapses within fused cartridges contain two L2 elements, one of which is from a neighbouring cartridge. **(3)** L2 dendritic arbours project into neighbouring lamina cartridges when they lack Dscam2. **(4)** Dscam2 restricts L1 lamina neuron axons to a single column in the medulla. **(5)** R7 and R8 axons are disorganized in *Dscam2* mutant flies and frequently cross over into adjacent medulla columns; this phenotype is non-autonomous.

1.6 Thesis outline

Although we are slowly gaining a better understanding of the neurodevelopment of the brain as well as visual behaviours, behavioural consequences of miswiring due to the lack of a cell recognition molecule, such as Dscam2, are not well understood. This thesis describes three visual behaviour assays which can be used to identify phenotypes in different mutants. *Dscam2*^{null} flies have wiring defects in the visual system and provide a unique opportunity to study the behavioural consequences of miswiring in the brain.

This chapter serves as a general introduction to the overall research aim and provides context for the experiments. Chapter 2 describes how a population and single tethered-fly assay have been optimized and used to explore motion perception by assessing the visual response to a wide range of psychophysical parameters of black/green moving gratings. In both assays, wild-type flies demonstrate strong optomotor responses to a wide range of visual stimuli, each in their own visual context. The assays complement each other for an in-depth assessment of visual system acuity to identify different severities of acuity impairments. Chapter 3 describes how a single tethered-fly virtual reality assay has been set-up and used to explore object-orientation preference and attention-like tracking mechanisms. In this assay, wild-type flies display fixation and anti-fixation behaviour to specific bar contrasts and widths. In addition, there attention-like behaviour to bar displacements demonstrated that the displacement corrections are dependent on whether the bar is displaced clockwise or counter-clockwise. Assays from chapter 2 and 3 were used in chapter 4 and 5 to study visual perception in *Dscam2*^{null} flies. In the *Dscam2* mutant, the modularity of the visual system is disorganized and in chapter 4 it is demonstrated that motion detection is affected. In several conditions, *Dscam2*^{null} flies responded opposite from control. In chapter 5, it is demonstrated that also object orientation is affected in these mutants. In addition, attention-like behaviour in this mutant was studied in detail and found to be altered. In chapter 6, it is described how the phenotypes found in chapter 4 and 5 can be used as a starting point to study other *Dscam2* related mutants such as *Dscam2* single isoform and trisomic mutants. Both mutants did not display any optomotor phenotypes but were found to have changes in their orientation behaviour. Chapter 7 serves as a general discussion and is used to explore how the combined experimental results further our knowledge of the research topic.

Chapter 2

Optomotor assays:

population and single fly paradigms

2.1 Chapter overview

In order to better understand the influence of genes on motion perception in *Drosophila*, assays that allow a detailed characterization of motion detection are required. Here, it is described how two different visual paradigms, a population assay and single tethered-fly assay, provide a means to explore the visual response to a wide range of psychophysical parameters. The assays used in this study measure visual responses in different ways. The population assay is high-throughput, ideal for screening purposes but does not control well for visual context, whereas the single tethered-fly assay is the opposite. In this chapter, we investigate whether both assays provide similar results and can be used to efficiently dissect motion detection in *Drosophila*.

2.2 Methods and results

2.2.1 A population assay for monitoring optomotor responses

2.2.1.1 Fly preparation

Wild-type flies that have an X chromosome from laboratory-reared wild-type *Canton-S* flies and a second and third chromosome from w^{1118} background were used and will be indicated as wild-type in chapter 2 and 3. Flies were reared on standard *Drosophila* yeast-based media and kept at 22 - 25°C under 12-hour light and 12-hour dark cycles.

The day prior to the experiment, female flies were collected (n = 27-33) which were between four and 12 days after eclosion. Flies were anesthetized by CO_2. The collected flies were starved at room temperature for 19-22 hours in modified disposable polyethylene “jumbo” transfer pipettes (Thermo Fisher Scientific, Waltham, Massachusetts) containing 10 µl of water. Previous studies showed that starved flies had an increased responsiveness to visual stimuli compared to non-starved flies. All

experiments were conducted between early and mid-afternoon to reduce variation between different groups.

2.2.1.2 Experimental setup

In the population visual response assay, a group of flies had to traverse an eight-point choice maze (J&M Specialty Parts, San Diego, California, USA) while being exposed to a moving visual stimulus (figure 2.1). The maze has eight tiers and flies choose to turn left or right at each tier (figure 2.1C). At the end of the maze, flies are collected at one of nine different exit points. This assay is similar to a previously published assay (Evans *et al.*, 2011, Van Swinderen & Flores, 2007) with the main difference being that the cathode-ray tube (CRT) monitors have been replaced by light emitting diode (LED) panels (Shenzchen Sinorad Medical Electronics; figure 2.1C) due to their higher refresh rate (200 Hz), which is above the flicker fusion frequency for *Drosophila* vision (Heisenberg, 1984) and allows the fly to perceive the stimulus as moving smoothly. The tube containing the flies was tapped once to startle the flies and then inserted into the maze entrance. It was found that startling the flies increased their walking speed in the maze. On average, it took a group of 30 flies 2.5 minutes to reach one of the nine exit points of the maze. Here, they were automatically counted using infrared sensors (modified *Drosophila* Activity Monitors, Trikinetics, Waltham, Massachusetts; Evans *et al.* (2011). Visual stimuli were programmed in VisionEgg (Straw, 2008) using Python 2.5 programming language which allows for control of visual stimulus specifics such as colours, bar sizes, motion speed, luminance and contrast. The grating stimulus was a moving grating of black and green bars (peak wavelength of 518 nm) with a contrast of 1, a luminance level of 93.5 lux, a spatial frequency of 0.018 cycles/degrees, a temporal frequency of 3 Hz and a velocity of 164.4 degrees/second unless stated otherwise. The contrast used was defined as the difference between light (LED on) and dark (LED off) values (I_{max}, I_{min}, respectively) divided by the sum of light and dark values. The condition with a contrast of 1 had an I_{max} of 93.5 lux and an I_{min} of 0 lux. The grating is a pattern of green and black bars that is repeated endlessly with the length of a single green and black bar defined as spatial period. The spatial frequency used was defined as 1 divided by the spatial period and is used to describe the moving grating. The visual response of wild-type flies was tested to a range of luminance levels (1.4 – 1100 lux, i.e. low to high level of luminance) and spatial frequencies (0.01-0.04 cycles/degree, i.e. wide to narrow bars).

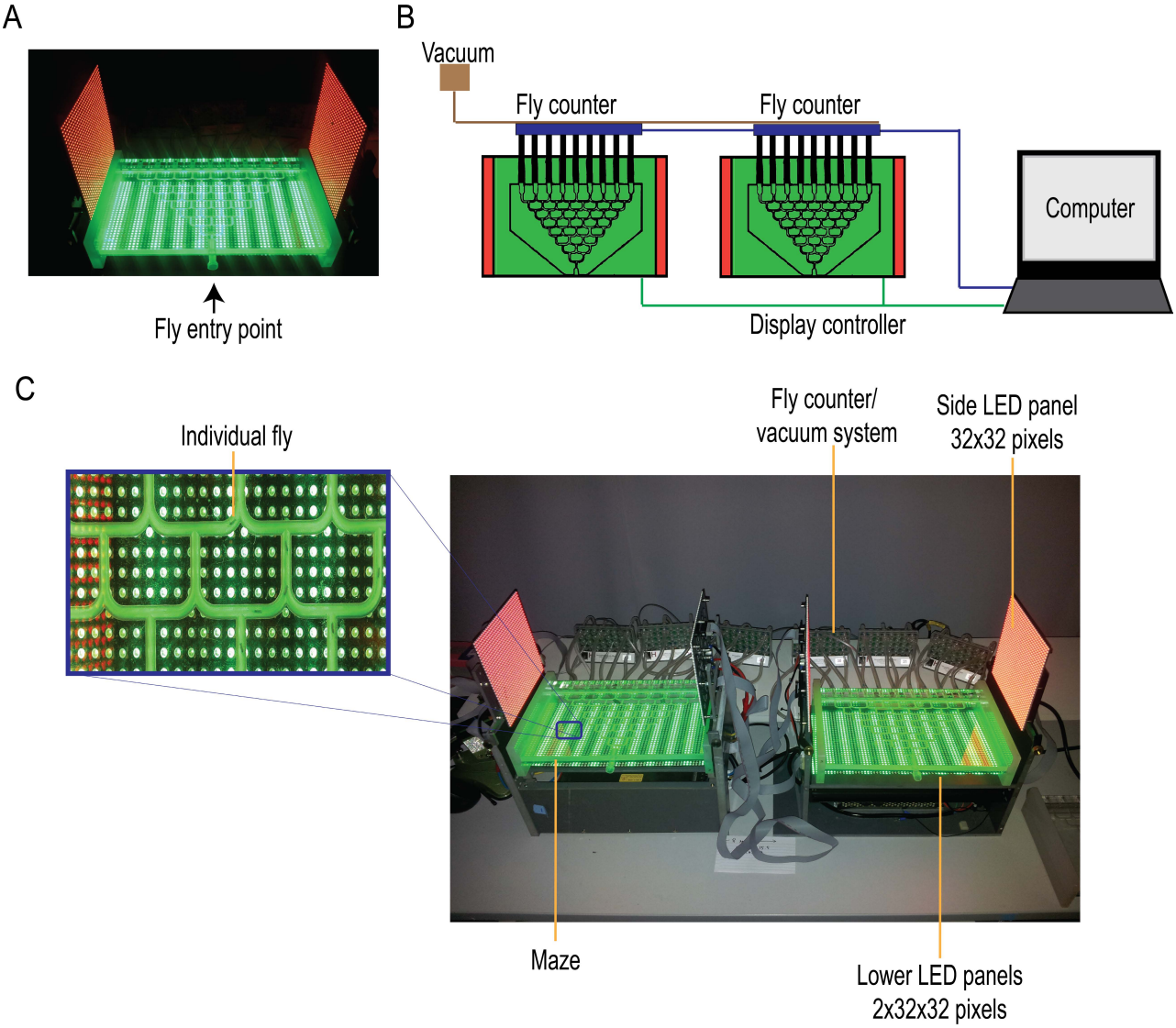

Figure 2.1. The maze visual response assay.
(A) A maze over a LED box where visual stimuli are displayed. The two red LED side panels provided a standard surrounding luminosity without colour cues (flies are unable to see red). **(B)** A schematic of the complete set-up consisting of two LED boxes controlled by a computer. Fly counter automatically counts the flies as they enter the exit tubes. Flies are vacuumed out of the set-up after being counted. **(C)** A photo of the complete set-up consisting of the two LED boxes controlled by a computer. Each LED box consists of two LED side and lower panels of which each panel contained one blue, green, and red LED in a 32 x 32-pixel configuration. The fly counters automatically count the flies as they enter the exit tubes. Flies are vacuumed out of the set-up after being counted. Inset shows close-up of individual flies in the maze channels.

2.2.1.3 Data analysis and statistics

The visual response was calculated from fly counts with custom-written MATLAB (MATLAB and Statistics Toolbox Release 2013b, The MathWorks, Inc., Natick, Massachusetts, United States) scripts as a weighted average of the number of flies in each exit point of the maze (Eqs. 1).

$$\text{Visual Response} = \frac{(\#\text{ flies in tube number}) * \text{tube number}}{(\text{total \# of flies})} \qquad \text{(Equation 1)}$$

In this equation, the tube number is -4 to +4 (Van Swinderen & Flores, 2007). The visual response was defined as positive when flies followed the direction of motion and negative when they moved against the direction of motion. One experiment consisted of the visual stimulus presented right-to-left to one group of flies and left-to-right to a different group of flies to prevent bias. A minimum of four experiments with eight mazes and approximately 30 flies each were performed per visual stimulus, thus resulting in at least 240 flies per data point.

Data was analysed using custom-written MATLAB scripts and GraphPad Prism 5.00 for Windows (GraphPad software, San Diego California USA). For all stimuli an average and standard error of the mean (SEM) visual response was calculated, based on individual visual response experiments performed over multiple days. A Lilliefors test (Lilliefors, 1967) was used to test for normality of the dataset. To compare between visual responses at different grating luminance levels, a Student's *t*-test was performed for normally distributed data and a Mann-Whitney for non-normally distributed data. When multiple groups were compared, we performed a two-way ANOVA. Group size varied from N = 28-62 per group.

2.2.1.4 Wild-type flies follow the direction of motion

When wild-type flies were exposed to the grating of black and green stripes, they followed the direction of the motion, resulting in a visual response of 0.64 ± 0.08 (figure 2.2A). This response was similar to previously published results (Evans *et al.*, 2011). Flies followed rightward and leftward motion with similar magnitudes, as expected.

Commonly, LED panels are much brighter than CRT monitors are. In order to assess differences in visual response at varying levels of luminance, *Drosophila* visual responses at a range of luminance levels was assessed. When wild-type flies were exposed to the same grating at different luminance levels, they followed the direction of the motion at most luminance levels except at the lowest level

of 1.4 lux, where flies did not respond (Student's *t*-test, $p < 0.05$; figure 2.2B). The luminance level of 93.5 lux showed the lowest variation in visual response and was chosen for future experiments.

Previous experiments with CRT monitors demonstrated a negative relationship between visual response and spatial frequency (Evans *et al.*, 2011). In order to assess whether a similar trend is observed with LED panels, the spatial frequency of the grating was varied without changing the velocity of the stimulus. Wild-type flies followed the direction of the motion at most spatial frequencies (figure 2.2C), but they did not respond to gratings with a spatial frequency greater than 0.036 cycles/degree (Student's *t*-test, $p < 0.05$; figure 2.2C). This was similar to results from Evans *et al.* (2011) demonstrating that similar responses were produced by the LED and CRT displays.

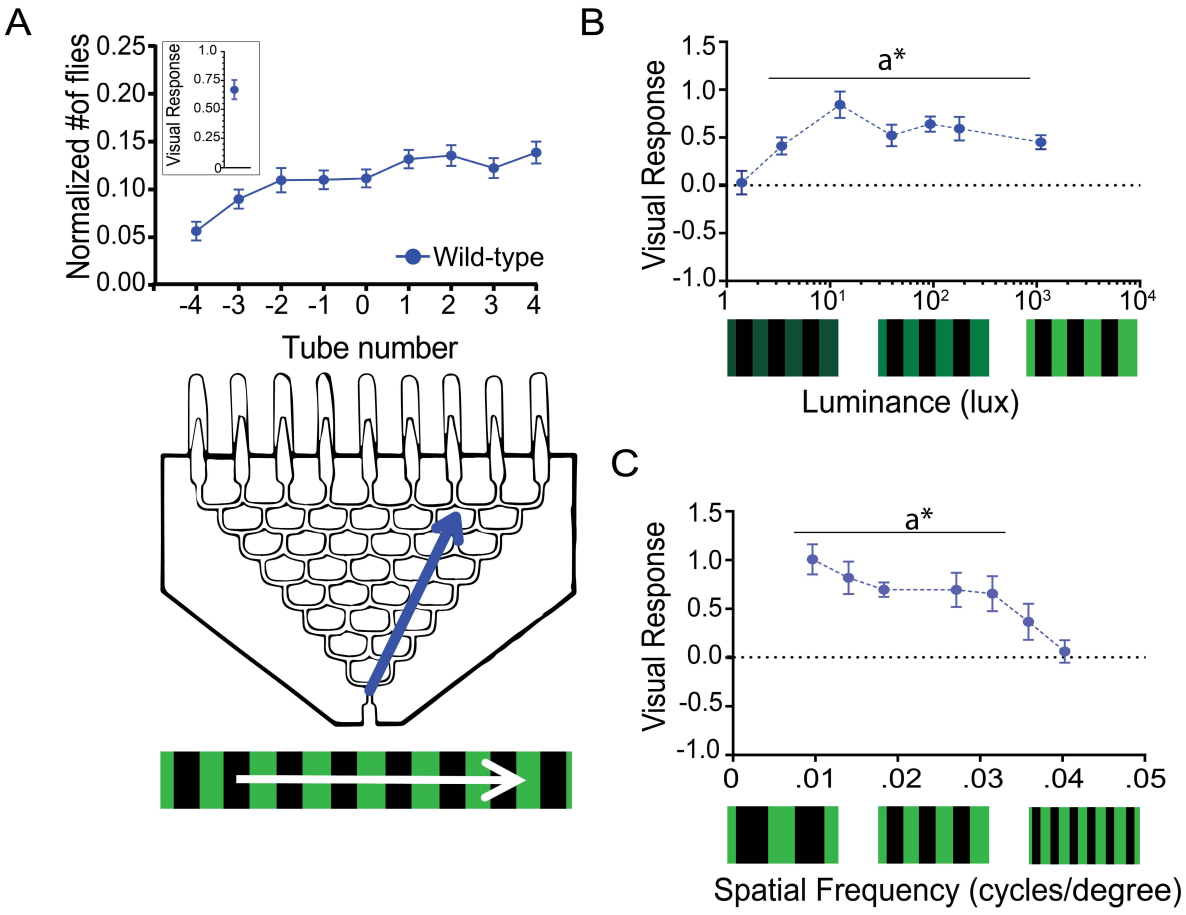

Figure 2.2. Wild-type flies respond to motion in the population visual response assay.
(A) Population visual response assay. An eight-choice maze was placed on LED panels displaying moving gratings. The line graph displays the normalized distribution of flies in the maze. On average, wild-type flies follow the direction of motion, resulting in a positive visual response. The inset represents the calculated visual response for wild-type flies. **(B)** Visual responses of wild-type flies to different grating luminance levels. **(C)** Visual responses of wild-type flies to different spatial frequencies. At least 28 mazes of approximately 30 flies each were run for every condition. Error bars indicate SEM. a* indicates significance from zero (Student's *t*-test, $p < 0.05$).

2.2.2 A single tethered-fly assay for monitoring optomotor responses

The population assay described above is ideal for testing motion behaviour in large populations of flies. Over 7000 flies were assessed in a relatively short period of time, yielding large volumes of data (figure 2.2) and making this assay very useful for high-throughput screening purposes. One limitation of the population visual response assay lies in the difficulty to control the flies' visual context. For example, the perception of the speed of the moving grating depends on the flies' own motion. In addition, population effects such as social interactions could influence a fly's decision to turn left or right. Therefore, it was decided to set up a single tethered-fly assay in which it is possible to carefully control the flies' visual context without the influence of self-motion and social interactions on the visual response. In these experiments, the fly is unable to turn. Its body and wings are glued in a horizontal position to a tungsten wire and its head is fixed to the thorax (Paulk *et al.*, 2015). It is able to move its legs but will not receive most sensory feedback usually experienced during free walking. This assay can be used in conjunction with the population visual response assay to assess flies' visual system sensitivity.

2.2.2.1 Fly preparation

Prior to the experiment, female adult flies were collected between one and six days after eclosion using CO_2 anaesthesia, two to four days before the experiment and placed in a vial with fresh food. In contrast with the visual response maze assay, flies were not starved but kept on fresh food at room temperature. In the morning on the day of the experiment, three to 10-day-old female flies were cold anesthetized. The head, thorax, and wings were tethered to a 0.1mm thick tungsten rod with blue light activated dental cement (Whaledent AG, Switzerland). Prolonged bright blue light exposure could render flies temporally motion blind due to depolarization of R1 – 6 cells even after termination of the exposure (Broda & Wright, 1978). To overcome this together with the effects of cold-anaesthesia, the flies were allowed recover for two to five hours with access to food and water. After recovery, the flies were placed in the single fly assay. All the experiments were performed between early and mid-afternoon to reduce variation.

2.2.2.2 Experimental setup

In the single tethered-fly assay, a single fly walks on an air-supported Styrofoam ball (~37 mg, radius 7.5 mm; Pioneer-Craft, painted with black and red pattern using a Sharpie pen) in an LED arena (figure 2.3A). A 50 ml Falcon tube held the ball in a mold made of plaster of paris and was connected to a small tube leading from the side of the base to provide an airflow at ~1 L/min regulated with an

air flow meter (EZI-FLOW). The LED arena consists of four LED panels on which visual stimuli were displayed. These panels were identical to the ones used in the population assay to allow a direct comparison between a population and single fly assay. This set-up is similar to that used in Paulk *et al.* (2014), except that ball movement was monitored by a camera (60 frames/second, 0.3MP B&W Firefly MV USB2.0 camera, Point Grey, Richmond BC, Canada), rather than infra-red sensors (Moore *et al.*, 2014; figure 2.3A).

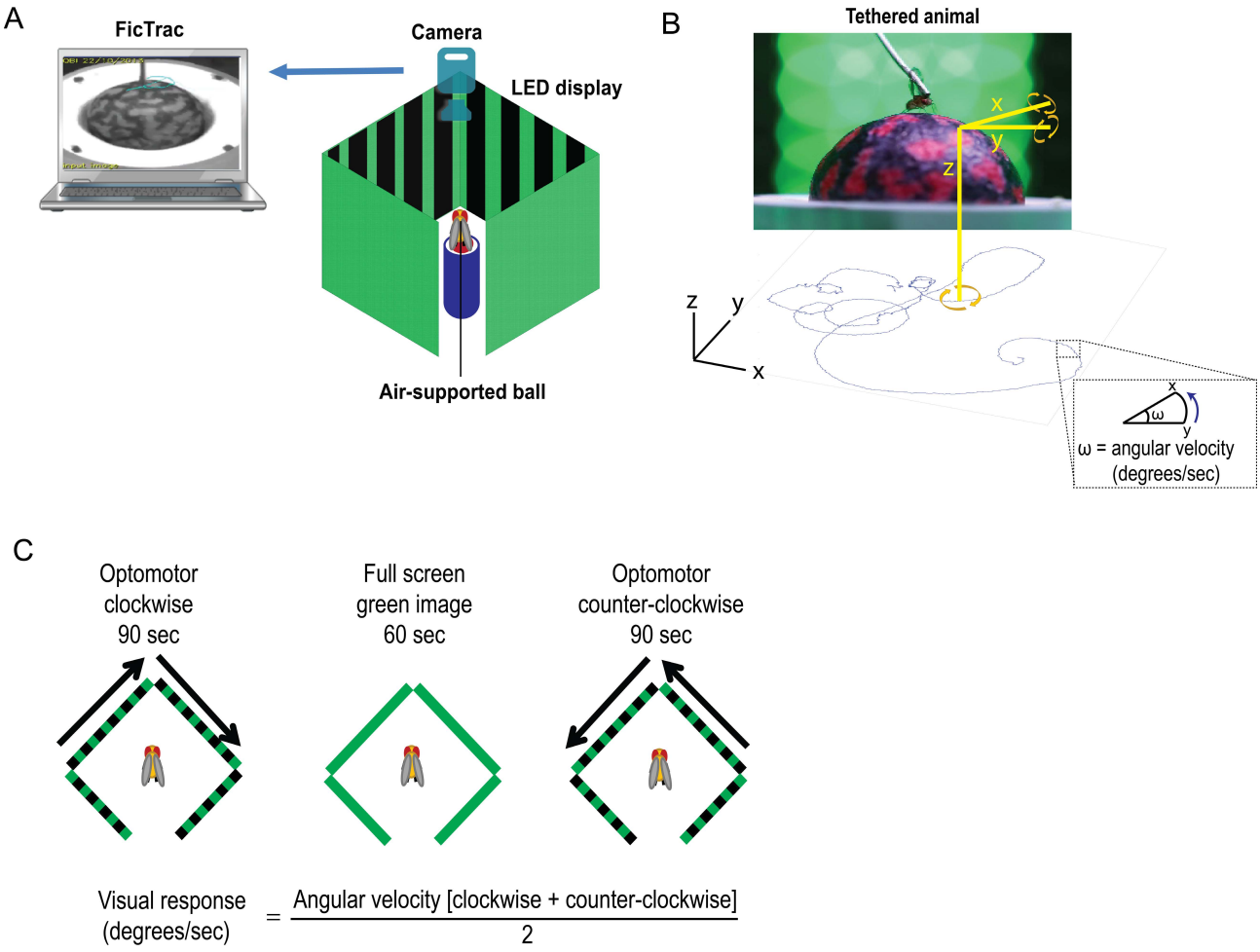

Figure 2.3. Single tethered-fly assay for assessment of motion tracking in flies.
(A) A single fly assay to assess motion tracking in flies. In this assay, a tethered fly is walking on an air-supported ball surrounded by LED panels displaying apparent motion. **(B)** The movement of the ball is tracked by a camera and the computer software program FicTrac which translates rotation of the ball into a 2D fictive path. From the 2D fictive path, the angular velocity can be determined and used as a measure of the response to the visual stimulus. **(C)** The visual response is calculated by the summation of the angular velocity for the optomotor clockwise and optomotor counter-clockwise stimulus, divided by two. The optomotor stimuli are separated by a full screen green image for 60 seconds to compensate for the after effect.

Similar to the visual response maze, the single fly assay used a moving grating composed of green and black bars as the visual stimulus (figure 2.3C). Visual stimuli were programmed in VisionEgg (Straw, 2008) using Python 2.5 programming language which allows for control of visual stimulus specifics such as colours, bar sizes, speed, luminance and contrast. The grating stimulus had a contrast of 1, a spatial frequency of 0.051 cycles/degrees, temporal frequency 3 cycles/second, and a velocity of 58.8 degrees/second unless stated otherwise. The contrast was defined as described above (section 2.2.1.2). The spatial frequency was calculated based on the distance from the front of the fly to the middle of the two front panels (13 cm). The distance from the fly to the LED panels is larger in the single fly assay compared to the population assay. This means that bars with the same spatial frequency in the single fly assay will be perceived as smaller and slower than the bars in the population assay. This allows for measurement of a finer range of spatial frequencies. This is of particular interest when mutants with a lower visual acuity are tested. Due to the configuration of the arena, the distance from the fly to the middle of the two back panels was 8 cm. This leads to a difference in spatial period between front and back panels. For example, a visual stimulus with a spatial frequency of 0.051 cycles/degree would have bars with a spatial period of 19.6 degrees in the front and 33.4 degrees in the back of the arena. Wild-type flies were tested with a range of spatial frequencies (0.026-0.102 cycles/degree, i.e. wide to narrow bars); similar to what was done in the maze.

2.2.2.3 Data analysis and statistics

To monitor fly locomotion on the air-supported ball, FicTrac on a computer with Linux Ubuntu 12.10, was used, which tracks spherical motion of the moving ball. From these data points a two-dimensional fictive path can be generated (Moore *et al.*, 2014; figure 2.3B). This information can be used to graph the turning of the ball over time, and an average angular velocity (the response to the optomotor stimulus). The optomotor response is calculated based on the speed and direction of the ball in the presence of the moving grating and is expressed as an average angular velocity. A fly that is not walking will have no response whereas a fly that responds well to the stimulus will move the ball at a high angular velocity. As in the maze, following the motion stimulus results in a positive optomotor response. One experiment consisted of a clockwise optomotor stimulus presented for 90 seconds followed by 60 seconds of a full screen green image and then by 90 seconds of counter-clockwise stimulus.

Data analysis was performed with custom-written MATLAB scripts and statistical analysis using Graphpad Prism 5.00 (Graphpad software, San Diego California USA). For all stimuli an average and standard error of the mean (SEM) visual response was calculated, based on individual visual response

experiments performed over multiple days. A Lilliefors test (Lilliefors, 1967) was used to test for normality of the dataset. To compare the visual response to zero, we performed the Student's *t*-test for normally distributed data and a Mann-Whitney for non-normally distributed data. Group size was N = 49.

2.2.2.4 Wild-type flies turn with the direction of motion in a tethered-fly assay

In wild-type flies exposed to the moving grating described above, the average angular velocity from multiple flies was 63 ± 14.0 degrees/second (Mean ± SEM; figure 2.4A). This is interesting because flies in the population assay stopped responding to gratings with a spatial period below 27.9 degrees whereas in this assay flies respond to a grating with a spatial period of 19.6 degrees (figure 2.4B). This response was dependent on motion since a stationary grating did not elicit a directional response that was different from zero (-5.6 ± 10.6 degrees/second, Student's *t*-test $p = 0.61$). Flies followed clockwise and counter-clockwise motion with similar efficiencies.

Similar to what was done in the population assay; the visual response of wild-type flies to different spatial frequencies was assessed. Interestingly, wild-type flies followed the direction of the motion at all spatial frequencies tested, including those that did not elicit a response in the population assay (figure 2.3C/2.4B).

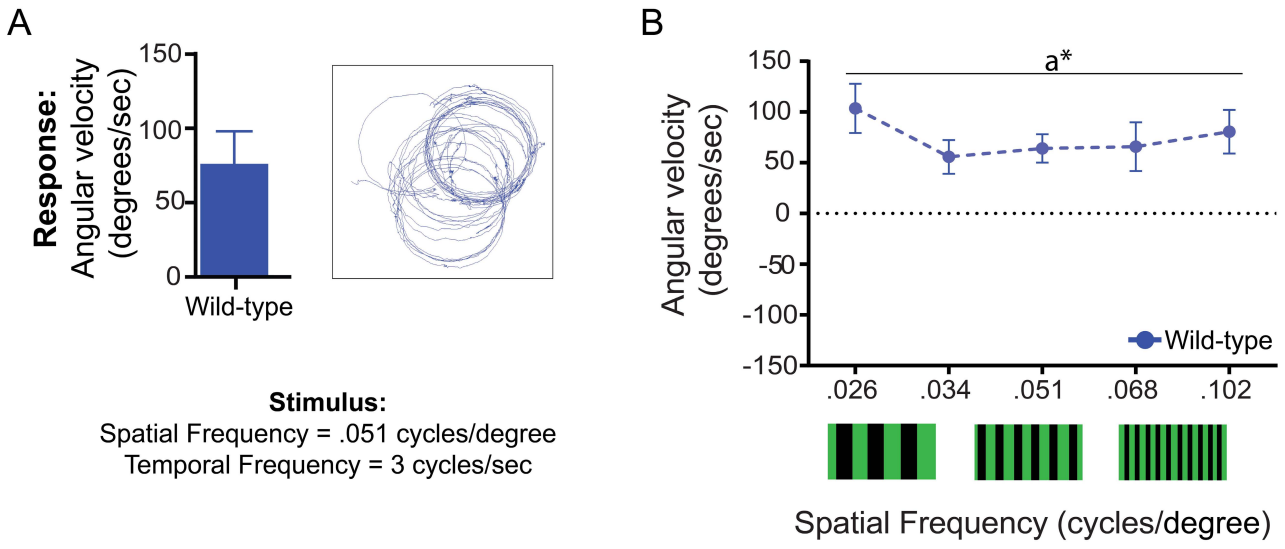

Figure 2.4. Wild-type flies respond to motion in the single fly assay.
(A) Visual response of wild-type flies to a grating with a contrast of 1, a spatial frequency of 0.051 cycles/degree and a temporal frequency of 3 cycles/second. Inset represent the 2D fictive walking path of a single wild-type fly exposed to the grating, visualizing the rotational response. **(B)** Visual responses of wild-type flies to different grating spatial frequencies. N = 49. Error bar indicates SEM. a* indicates significance from zero (Student's *t*-test, $p < 0.05$).

2.3 Discussion

In this chapter, it is demonstrated that wild-type flies turn in response to black/green gratings in a population and tethered single fly assay. This behaviour is dependent on the spatial frequency of the grating and type of assay. Both assays complement each other and thereby provide a foundation for studying motion detection in these two different visual contexts.

2.3.1 A population assay to assess motion detection

As no tethering of flies is required in the population visual response assay, groups of flies can be analysed quickly in a high-throughput fashion making it well suited for screening purposes. The population visual response assay has been used in the past to screen for mutants with motion detection problems (Calcagno *et al.*, 2013, Evans *et al.*, 2011, Van Swinderen & Brembs, 2010, Van Swinderen & Flores, 2007). In these experiments, CRT monitors where used to display visual stimuli, which have a refresh rate (60 Hz), much lower than the flicker fusion frequency for *Drosophila* vision (Heisenberg, 1984). This means that visual stimuli presented on these monitors are likely to be perceived as flickering, and movements of the bars might appear irregular. To overcome this problem, the CRT monitors were replaced by LED panels which have a refresh rate (200 Hz) above the flicker fusion frequency for *Drosophila* vision (Heisenberg, 1984). It was found that in this optimized assay, wild-type flies follow the motion in the maze as a group, when exposed to luminance levels above 3.4 lux and spatial frequencies greater than 0.036 cycles/degree and higher. Results to different luminance and spatial frequency levels are similar that observed with the use of CRT monitors (Evans *et al.*, 2011) and therefore it can be concluded that a higher refresh rate does not change the visual response of wild-type flies to these conditions. However, it is still possible that more challenging visual stimuli may affect the visual response and therefore the use of LED panels over CRT monitors is justified.

2.3.2 A single tethered-fly motion detection assay

Compared to the population assay, in which different groups of flies are required to assess the visual response to different visual stimuli, many different visual parameters can be tested on the same fly in the tethered-fly assay. Here, the fly is able to rotate the ball but unable to move its upper body, thereby eliminating perception of self-motion. The LED panels used in this assay are identical to the ones used in the population assay to allow a comparison between the assays. Due to the configuration of the arena, the distance from the fly to the front and back of the arena is different. This could be a

potential disadvantage considering some literature suggests that the rear part of the visual field in flies evokes different responses than the front part (Tammero *et al.*, 2004). However, under the conditions at which the wild-type flies were tested in this section, strong visual responses were measured for all conditions. Similar to the population assay, it was found that wild-type flies follow the motion at different spatial frequencies.

2.3.3 Comparison between a population and single fly assay

Interestingly, a difference in response between the assays was found at some spatial frequencies. It was found in the population assay that wild-type flies did not respond to gratings with a spatial period below 27.9 degrees. This is surprising considering wild-type flies should be able to respond to gratings with a spatial period of higher than 9.2 degrees (Götz, 1964). In the single tethered-fly assay, wild-type flies responded strongly to spatial periods between 9.8 and 39.2 degrees so it is unclear why flies in the population assay did not respond. This can potentially be explained by a difference in visual context. Due to the nature of the design of the population assay, it not possible to control how the flies perceive the visual stimulus. A fly may respond to reflections of the stimulus within the maze, it could walk down the channels both upright and upside down and other flies in the maze can influence the fly's visual response. Previous research demonstrated that in single choice population assays, a group of mixed gender flies walked in the opposite direction of the moving grating (Lee *et al.*, 2001, Zhu & Frye, 2009). In the population assay described in this chapter, flies have to make a multitude of left/right choices while exposed to a moving grating and female flies respond by following the moving grating (Bosch *et al.*, 2015, Evans *et al.*, 2011, Van Swinderen & Flores, 2007). Flies are social animals and are attracted to each other regardless of sex (Lefranc *et al.*, 2001, Navarro & Del Solar, 1975) and this aggregation behaviour could influence the flies' decision-making. Although a leading fly could have a strong influence on followers, flies do not all aggregate in the same tube, which is demonstrated by the tailed distribution along the nine tubes (figure 2.2A). These confounding factors could contribute to the finding that flies in the population assay do not respond to gratings with a spatial period less than 27.9 degrees.

To summarize, flies follow the direction of the moving stimulus in both assays described in this chapter (Bosch *et al.*, 2015). These assays provide a foundation for studying motion detection in two different visual contexts and will be used in order to better understand the influence of gene manipulations on visual behaviours in *Drosophila* in chapter 4 and 6. In addition, the single fly assay will also function as platform to study more complex visual processes in chapter 3, 5, and 6.

Chapter 3

Operant behaviour and attention-like mechanisms

3.1 Chapter overview

In order to better understand the influence of genes on attention in *Drosophila*, it is important to have assays that allow a detailed characterization of these complex behaviours are required. These assays measure orientation preference in a freely moving or tethered fly that is in control of the angular position of a visual panorama with or without competing stimuli. Here, it is described how the single fly assay (chapter 2) can be used to assess operant and attention-like behaviour in *Drosophila*. In the tethered setup, a fly walks on a ball, the movement of which controls the position of the visual panorama. This gives the fly control of the angular position of the panorama (closed loop) and allows for analysis of orientation preference and object tracking of which the latter involves attention-like mechanisms.

3.2 Methods and results

3.2.1 Control flies display contrasting orientation preferences

In this section, the single fly assay described in 2.2.2 was modified into a virtual reality assay by the introduction of a closed-loop system in which the fly can turn the air-supported ball to control the angular position of the bar in the arena (Paulk *et al.*, 2014). This assay can be used to assess object-orientation preference in flies.

3.2.1.1 Fly preparation and experimental setup

Flies were prepared as described in 2.2.2.1 and used in the single fly virtual reality assay. Flies were able to control the angular position of a single bar. The bar was either light (green LED on, peak wavelength of 518 nm and 168 lux) and presented on a dark (LED off) background or dark and presented on a light background (3102 lux). The size of the bars was calculated based on the distance from the front of the fly to the middle of the two front panels (13 cm). Due to the configuration of the arena, the distance from the fly to the middle of the two back panels was 8 cm. This leads to a

difference in bar size between front and back panels. For example, a bar size of 29.4 x 58 degree, will be 50.1 x 114.6 degree in the back. All bar sizes are measured from the front unless stated otherwise.

3.2.1.2 Data analysis and statistics

Similarly as in 2.2.2, the fly's locomotion on the air-supported ball was monitored by FicTrac. From these data points a two-dimensional fictive path can be generated (Moore *et al.*, 2014). This information can be used to determine the angular position of the bar. One experiment was three minutes long and consisted of multiple trials in which the bar was perturbed 84° (at 280 degree/second) at random times by the computer (figure 3.1B). To ensure that the flies orientation response to the bar displacement was independent of the optomotor response (in which the fly follows a moving grating); the bar was programmed to move in the opposite direction of the flies turning response. In other words, the flies were using the ball as a joystick to control the angular position of the bar, in which a left turn of the ball resulted in a left turn of the angular position of the bar and is caused by the fly walking to the right (figure 3.1A). From individual flies, the bar position in pixels is converted to an angular position in degrees. The angular position of a group of flies is graphically represented in a radial histogram (polar plot), generated using a custom-written MATLAB script to visualize the distribution. In this plot, the histogram length represents the weighting of each position (i.e. the longer the histogram, the longer the bar was held in that direction) (figure 3.1C). From individual flies, the bar position in degrees was used to calculate a mean direction (vector angle) and shape of distribution (resultant vector length, response strength) using the Circular Statistical Toolbox in MATLAB (Berens, 2009). From these data, a group mean direction and group vector length was calculated (figure 3.1D). A Rayleigh test was used to test if the distribution was non-uniform. The group mean and group shape of distribution were only calculated if the distribution was non-uniform. If the distribution was non-uniform, then the group mean direction is graphically represented in the polar plot with a yellow arrowhead if the direction was towards the front of the arena or with a red arrowhead if the direction was towards the back. The shape of distribution is represented in a boxplot (figure 3.1D). In figures, the radial histogram is calculated as in figure 3.1C and the group mean direction and vector length as in 3.1D. In figures and the text, "N" refers to the number of flies.

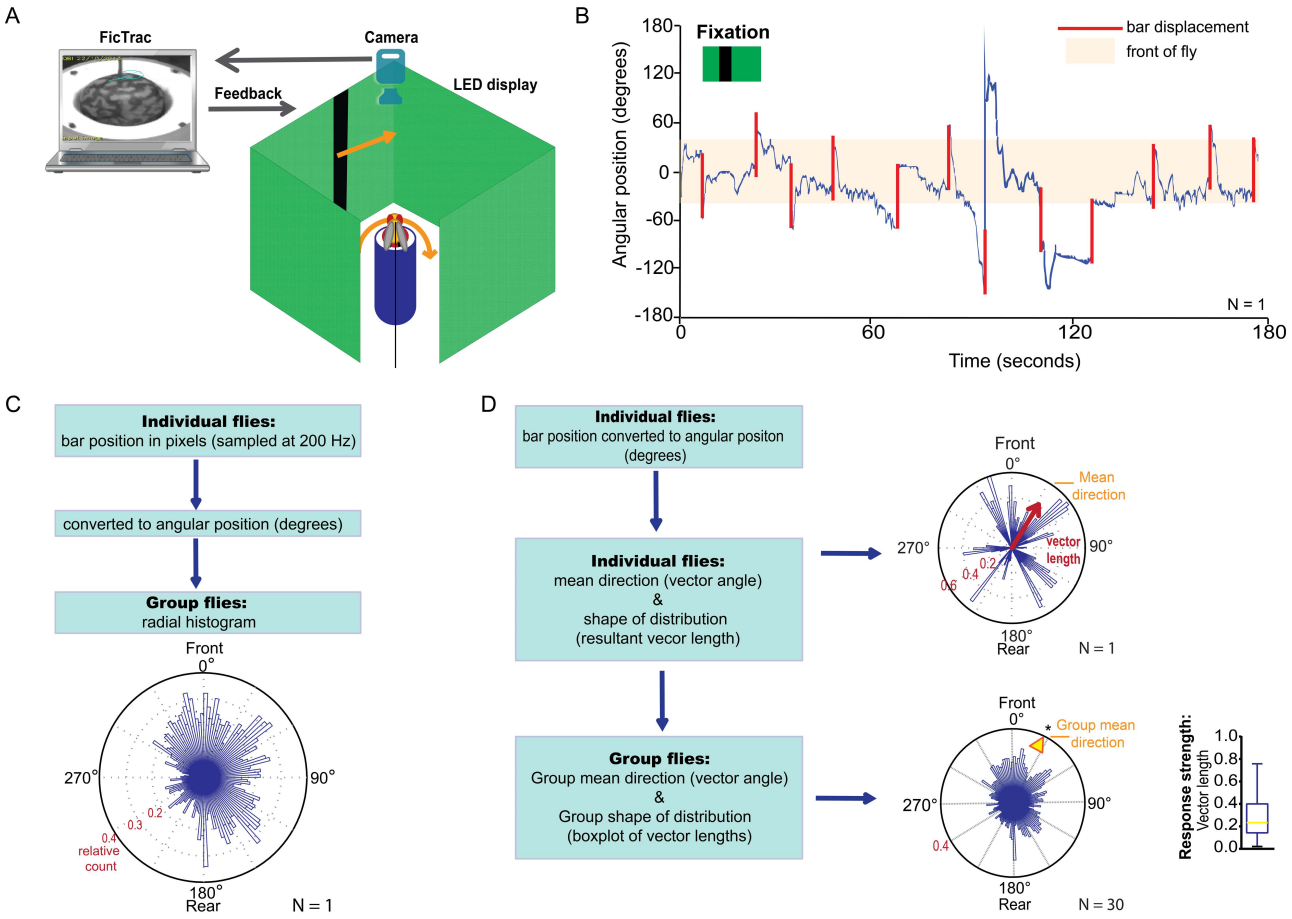

Figure 3.1. Data analysis in the single fly virtual reality assay.
(A) A tethered fly walks on an air-supported ball and uses the ball to control the angular position of the bar. The fly's locomotion on the air-supported ball was monitored by a camera and software program FicTrac that fed the movement of the ball back into the LED displays (closed-loop behaviour). **(B)** Each experiment was 3 minutes long and consisted of multiple trials in which the bar was displaced 84° at random times by the computer (red bars). On average, the fly maintains the bar to the front (light orange shading). **(C)** From individual flies, the bar position in pixels was converted to an angular position in degrees. The angular position of a group of flies is graphically represented in a radial histogram (polar plot) to visualize the distribution. **(D)** A mean direction (red arrow) and resultant vector length was calculated for each fly based on the bar position in degrees and overlayed on a polar plot calculated as in 3.1C. From these data, a group mean direction (indicated with a yellow arrowhead) and group vector was calculated, of which the latter was presented in a box plot with min to max whiskers. The colour of the median line in the box plot corresponds with the colour of the arrowhead. The polar plot itself was calculated as in 3.1C.

3.2.1.3 A single fly virtual reality assay for monitoring orientation preferences

First, the response of wild-type flies to a 29.4 x 58 degree dark bar on a light background was tested. The bar elicited variable responses from wild-type flies, but on average they placed the bar towards the front of the arena (28°, 0° = front; figure 3.2A). To determine if the distribution was non-uniform, a Rayleigh test was performed on the group mean direction. This showed a non-uniform distribution ($p < 0.01$, figure 3.2A). To visualize the strength and variation of the responses, this data was displayed in a box plot (figure 3.2B).

Next, the flies' response to a light bar of similar size was tested. Previous studies using painted visual cues rather than LEDs demonstrated that wild-type flies elicit an anti-fixation response to a light bar, however, this response is very assay dependent (Bülthoff, 1980, Heisenberg & Wolf, 1979, Maimon *et al.*, 2008, Tuthill *et al.*, 2013, Wolf & Heisenberg, 1980). That similar anti-fixation behaviour could be achieved in an LED arena with a light bar on a dark background is demonstrated by the response of wild-type flies, which placed the light bar 184° from the front on average (figure 3.2B). Rayleigh tests on the group mean direction showed a non-uniform distribution for control flies ($p < 0.05$, figure 3.2C). To visualize the strength and variation of the responses, this data was displayed in a box plot (figure 3.2D).

In conclusion, a dark bar elicited fixation and a light bar anti-fixation in wild-type flies. Interestingly, the LED arena described here produced similar results to the paper/plastic drum assay described by Heisenberg and colleagues (Bülthoff, 1980, Heisenberg & Wolf, 1979, Wolf & Heisenberg, 1980).

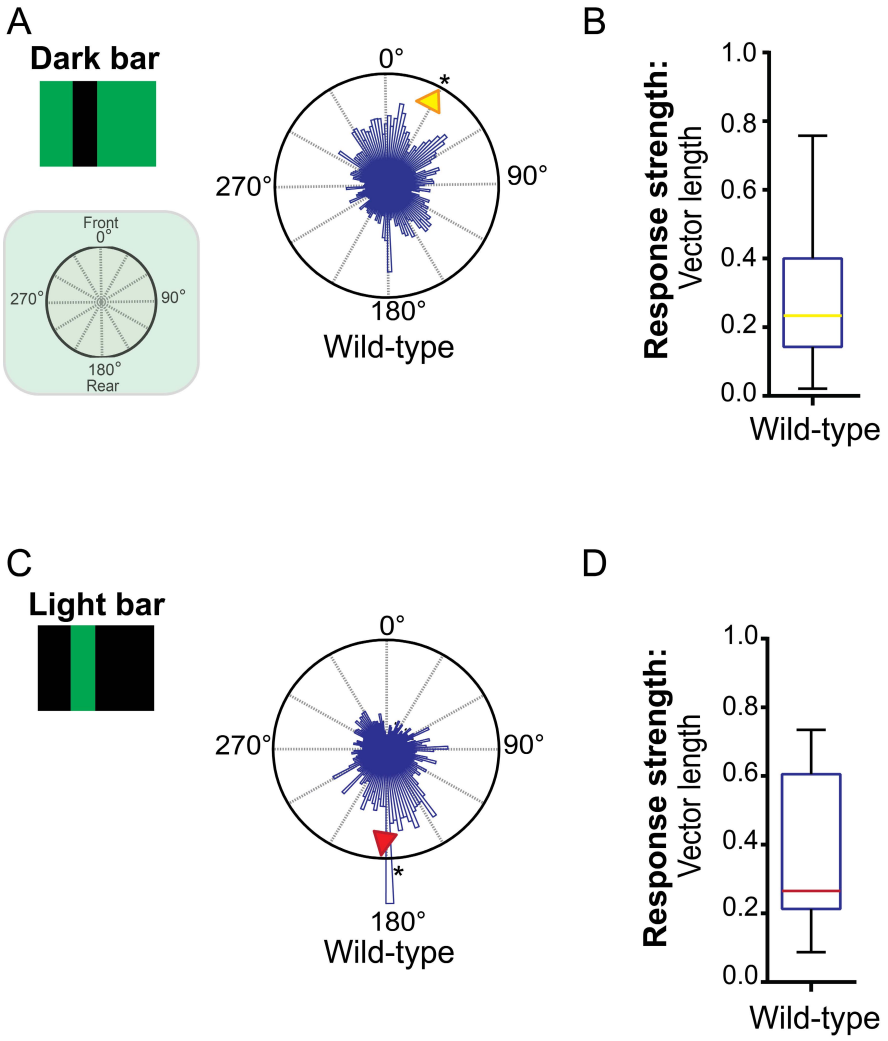

Figure 3.2. Wild-type flies display distinct object-orientation preferences.
Object-orientation preference assay. Flies were presented with a bar in a closed-loop condition and their preference for the bar position was recorded. The histograms within the 360° circular plots represent a weighted value for each bar position derived from all flies of each genotype as described in figure 3.1C. For each fly an average bar angle was calculated, as well as a group mean direction which is graphically represented in the radial histogram as a yellow arrowhead for a bar position towards the front of the arena or red arrowhead for a bar position towards the back as described in figure 3.1D. A Rayleigh test confirmed the distributions were non-random * $p < 0.05$. **(A)** Wild-type flies fixate on a dark bar on a light background. **(B)** Wild-type flies demonstrate variable response strengths (indicated with min to max whiskers in the boxplot) and variation for the dark bar stimulus. The colour of the median line corresponds with the colour of the arrowhead (indicating direction) in A. **(C)** Wild-type flies place a light bar on a dark background towards the back of the arena. **(D)** Wild-type flies demonstrate variable response strengths and variation for the light bar stimulus. As in **B,** the variation in strength of the response is visualized in a boxplot with min to max whiskers. For all groups at least 20 flies were tested for every condition.

3.2.2 Wild-type flies correct automated bar perturbations

In the previous section, the summed angular position of the bar of all flies was plotted in a radial histogram. In addition, the mean vector length and direction for each fly was calculated with a resulting group mean vector length and direction. Another way of looking at this is to focus on the computer initiated bar perturbations that occur randomly over the time period of the assay and the flies' response to them. The perturbation causes the fly to elicit a motor response that provides information about attention-like processes. The bar was perturbed 84 degrees either clockwise or counter-clockwise at random times (section 3.2.1.2) resulting in four to 12 perturbations per experiment. The response before, during, and after perturbations which started in either the front 90 degrees of the arena (fixation) or the rear 90 degrees (anti-fixation) of the arena were averaged and presented as red and blue lines in figure 3.3. The shading of the same colour indicates the standard deviation of the points.

For fixation and anti-fixation, in the majority of cases, flies returned the bar to the front or rear of the arena, for fixation and anti-fixation respectively (indicated by the horizontal dashed line, figure 3.3) within the three seconds post-perturbation. Interestingly, in both cases counter-clockwise perturbations were more consistently corrected to the starting position compared to clockwise perturbations (figure 3.3). Considering clockwise perturbations were in most cases not corrected, it could explain why the fixation response is orientated to the right of the front though it would not explain why this is not the case for anti-fixation (figure 3.2A/D).

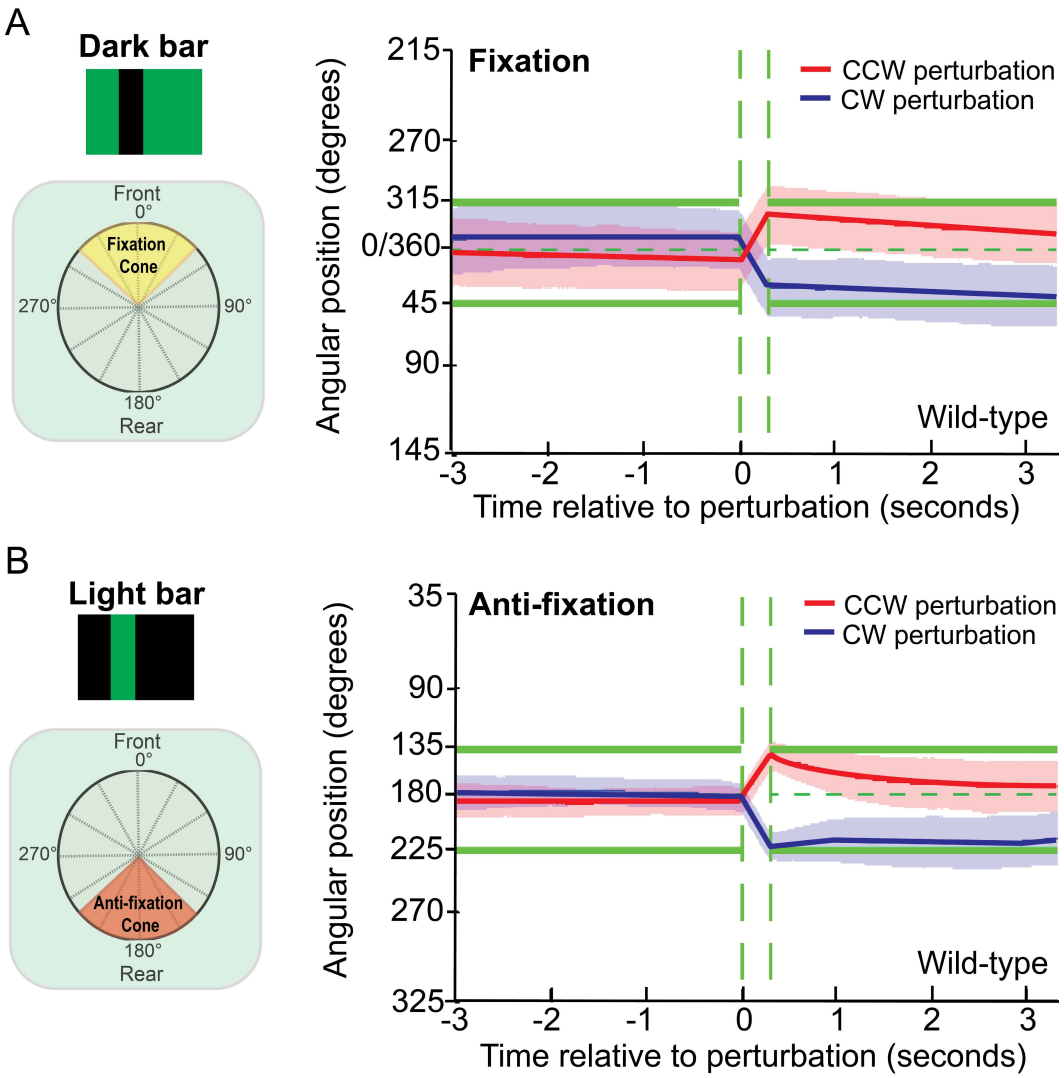

Figure 3.3. Wild-type flies correct bar perturbations.
From the data presented in section 3.2.1, the response before, during and after perturbations was isolated and divided into clockwise and counter-clockwise perturbations. The line represents the mean response with the same colour shading presenting the standard deviation from the points. The fixation cone subtends 90 degrees in the front and the anti-fixation cone subtended 90 degrees in the back of the arena (indicated by the green lines with the dashed green line indicating the direct front or rear of the fly for fixation and anti-fixation respectively. The open-loop displacement event is indicated by dashed vertical lines. Random perturbations took place anywhere in the arena but only events taking place in the fixation or anti-fixation cone were used in the calculations ($n \geq 91$). **(A)** Wild-type flies correct perturbations of a dark bar with counter-clockwise perturbations corrected closer to the direct front of the fly compared to the clockwise perturbations. **(B)** Although the outcome is different, i.e. anti-fixation, wild-type flies correct clockwise and counter-clockwise perturbations of a light bar similar to how they respond to dark bar perturbations. For all groups at least 20 flies were tested for every condition.

3.2.3 Wild-type object-orientation preferences depends on bar width

Wild-type flies display distinct orientation preferences to a single 29.4 degree wide bar depending on its visual parameters with a dark bar eliciting fixation and a light bar eliciting anti-fixation responses. Interestingly, although a light bar elicits anti-fixation responses in other assays (Bülthoff, 1980, Heisenberg & Wolf, 1979, Wolf & Heisenberg, 1980), fixation responses to this stimulus have also been reported (Maimon *et al.*, 2008, Reiser & Dickinson, 2008). It is unclear why these differences have been observed and therefore further exploration into this response is required. It was noticed that the fixation response of wild-type flies was slightly off-centred and it was questioned if the flies focus on the object itself or its edges. To answer this question, the bar width was systematically changed while other parameters were kept constant. It was expected that if flies focus on the object itself, that the orientation of the responses would not change with a change in bar width. If the flies would focus on the edges of the object however, a bimodal distribution would be expected when bar width is increased.

First, the response of wild-type flies to dark bars of different widths was tested. It was found that the fixation response was lost when the bar width was reduced from 29.4 to 9.8 degrees (Rayleigh test, $p = 0.71$; figure 3.4A). In addition, fixation behaviour was found to be improved when the bar width was increased to 58.8 and 88.2 degrees (bar location: 0.2° and 5.5° respectively, 0° = front, Rayleigh test, $p < 0.001$; figure 3.4A). The response from flies was to the centre of the bar and not bimodally orientated towards the edges, suggesting flies did not focus on the edges but on the object itself. Response strengths for the non-uniform distributions are similar between different conditions (figure 3.4B)

Next, the flies' response to a light bar of different widths was tested. It was found, similar to the dark bar, that the response was lost when the bar width was reduced to 9.8 degrees (Rayleigh test, $p = 0.87$; figure 3.4C). Interestingly, when the width of the light bar was increased to more than 29.4 degrees, anti-fixation behaviour did not get stronger but rather changed into an uniform response (Rayleigh test, $p = 0.95$ and $p = 0.16$ respectively; figure 3.4C). Indeed, it seems that only one very specific condition leads to anti-fixation behaviour (figure 3.4C/D). This is additional evidence that the flies orientate towards the object rather than edges because if flies were responding to edges, the same result for dark and light bars would be expected.

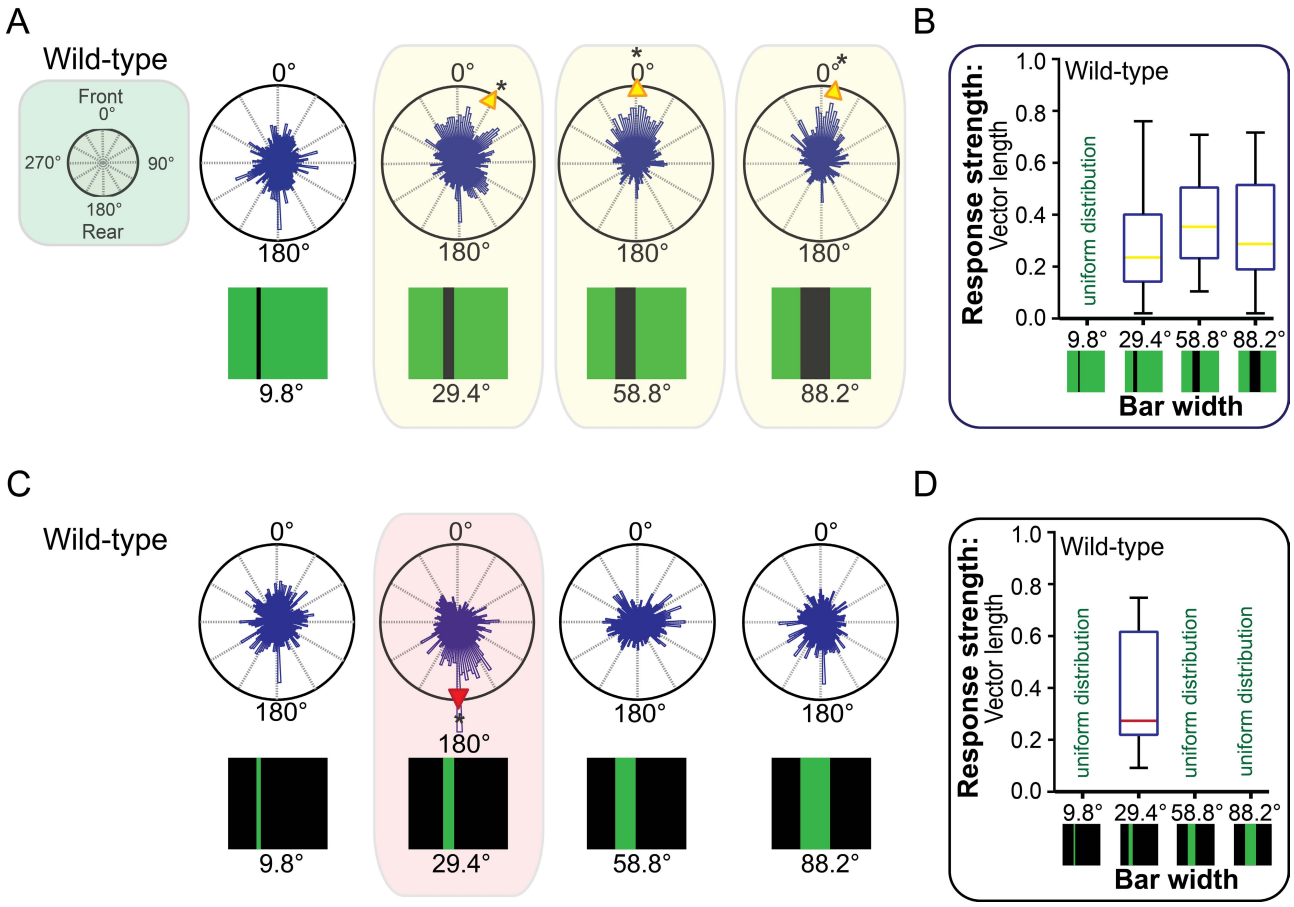

Figure 3.4. Object-orientation preference of wild-type flies depends on bar width.
Object-orientation preference assay with different bar widths. Flies were presented with a bar of different widths in a closed-loop condition. Their preference for the bar position was recorded as in figure 3.2. For each fly an average bar angle was calculated, as well as a group mean direction which is graphically represented in the radial histogram as a yellow arrowhead for a bar position towards the front of the arena or red arrowhead for a bar position towards the back. A Rayleigh test confirmed the distributions were non-random * $p < 0.05$. **(A)** Wild-type flies fixate on bars of 29.4 degree and wider and Rayleigh tests show a lower p value with an increase in bar width, indicating a more non-uniform distribution. **(B)** The variation in strength of the response of non-uniform distributions is visualized in a boxplot with min to max whiskers. The colour of the median line corresponds with the colour of the arrowhead (indicating direction) in **A**. **(C)** Wild-type flies place a 29.4-degree wide light bar towards the back of the arena but do not demonstrate an orientation preference at other bar widths. **(D)** The variation in strength of the response of non-uniform distributions is visualized in a boxplot with min to max whiskers. The colour of the median line corresponds with the colour of the arrowhead (indicating direction) in **C**. For all groups at least 20 flies were tested for every condition.

3.3 Discussion

In this chapter, it is demonstrated that wild-type flies fixate on a dark bar and anti-fixate on a light bar. Both behaviours are dependent on the width of the bar, with the flies focussing on the object itself and not the edges. Together, this provides a foundation for studying complex visual behaviours in *Drosophila*.

3.3.1 Different responses to dark and light bars

That wild-type flies display fixation and anti-fixation behaviour to a dark and light bar respectively (figure 3.2) is in line with results from other behavioural paradigms (Bülthoff, 1980, Heisenberg & Wolf, 1979, Wolf & Heisenberg, 1980) but two points require further discussion. First, the fixation response in the single fly virtual reality assay is not as strong as that shown by other groups (Bahl *et al.*, 2013, Reiser & Dickinson, 2008). Flies display besides fixation also non- and anti-fixation behaviour, what dilutes the fixation response. One reason for this variability could be attributed to the height of the bar. Maimon *et al.* (2008) demonstrated that flies fixate well to a bar that is 90 degrees high, but as the bar height decreases the flies exhibit more "spinning" and "anti-fixation" behaviours. The perceived bar height by the fly in our arena is 58 degrees high in front of the arena and 115 degrees high in back of arena (section 3.2.1.1). In the Maimon *et al.* (2008) paper, wild-type flies exhibited some spinning and anti-fixation for bars of around 60 degrees height, which is consistent with the obtained results in this chapter. Secondly, the anti-fixation behaviour to a light bar has been shown by some but not all researchers. Heisenberg (1984) demonstrated that wild-type flies (of another strain) are attracted to dark stripes but anti-fixate on light stripes in a tethered fly setup. This difference in responses to light and dark stripes by control flies has not been shown in other assays (Maimon *et al.*, 2008, Reiser & Dickinson, 2008). In addition, studies involving orientation preference experiments often focus solely on a dark bar on a light background without gathering data on a light bar on a dark background, thereby it is unclear if anti-fixation would have been observed in these assays (Bahl *et al.*, 2013, Götz, 1987). It is possible that anti-fixation has not always been observed due to differences in closed-loop feedback gain, closed-loop apparatus, visual presentation, genetic background of flies tested, and rearing conditions (Maimon *et al.*, 2008). Indeed, the Heisenberg (1984) study was performed with another wild-type strain and a backlit drum instead of LED panels. In the assay used it in this chapter, LED panels are used and anti-fixation behaviour by wild-type flies is found at a very specific light bar width (figure 3.4). Thus, anti-fixation appears to be an alternative behaviour to fixation, but the exact visual parameters and optic circuits that lead to this response are not well understood. To conclude, the single tethered-fly virtual reality assay can be

used to measure robust anti-fixation behaviour in wild-type flies and will therefore be useful for dissecting this behaviour in the future. In addition, this assay can be used to identify mutants that lack the ability to fixate or anti-fixate.

3.3.2 Wild-type flies correct perturbations

To investigate flies' attention-like processes, a focus was placed on the behaviour elicited by the random bar perturbations when the fly is walking on the ball in closed loop. This is a small subset of the larger data set considering only perturbations which started within the fixation or anti-fixation cone were analysed. Counter-clockwise bar perturbations triggers in most cases a motor response in which the fly brings the bar back to the centre of the frontal area for a dark bar and rear area of the arena for a light bar. This may be considered an attention-like process in which the fly detects the displacement and responds to it. Interestingly, for the dark and light bar condition, clockwise perturbations elicit limited correction and were found to be biased to the right side of the arena (figure 3.3). This is unlikely due to a bias in ball rotation considering no significant difference between clockwise and counter-clockwise optomotor responses were found. Considering the bar stays within the fixation or anti-fixation cone, one possibility is that the fly focusses on the left edge of the object. However, it is unclear why the fly would focus on the left but not right edge of the object. In conclusion, the perturbations elicit in cases an attention-like process that triggers the fly to correct the perturbation. Some of these corrections are biased to the right side and although this data is a small subset of the larger data set, it is possible that this clockwise bias introduces the variability seen in the polar plots.

3.3.3 Fixation and anti-fixation response is bar width dependent

Wild-type flies respond to the dark bar with fixation and light bar with anti-fixation behaviour, however, it is unclear if flies focus on the centre of the object or its edges. Free-walking flies have been shown to fixate on bar edges in bright conditions (Osorio *et al.*, 1990) and from the polar plot and perturbation data presented in this thesis it was unclear if flies orient towards the centre or edges of the bar. By increasing the dark bar size, fixation behaviour was maintained and orientated towards the centre of the bar. Increasing the light bar size resulted in a loss of anti-fixation behaviour (figure 3.4). It was unexpected to find that only one very specific condition leads to anti-fixation behaviour but this potentially explains why some studies did not find anti-fixation in wild-type flies in similar setups (Maimon *et al.*, 2008, Reiser & Dickinson, 2008). It is unclear if this anti-fixation behaviour is a consequence of the artificial simple environment the fly is presented with under tethered

circumstances. Normally, a flies' environment is more visually complex consisting of a wide range of objects with different levels of luminance, contrast, spatial and temporal characteristics. In this artificial environment, a light object of 29.4 x 58 degrees appears to trigger repulsion in the fly.

Chapter 4

Motion detection phenotypes of Dscam2^{null} flies

4.1 Chapter overview

Dscam2 has been shown to be required for establishing modularity in the visual system (Millard *et al.*, 2007). Wiring defects in the visual system of *Dscam2* mutant flies have been described in detail with key findings indicating an essential role for *Dscam2* in neuronal connectivity and visual system modularity (Lah *et al.*, 2014, Millard *et al.*, 2007, Millard *et al.*, 2010). However, behavioural consequences of these wiring defects have not been studied. In this chapter, an initial focus was placed on identifying potential sensory impairments in the *Dscam2* mutant by measuring their overall fitness and responsiveness followed by a thorough analysis of motion detection.

4.2 Materials and methods

4.2.1 Fly husbandry

Dscam2 mutant stocks (*Dscam2*$^{null-1}$, *Dscam2*$^{null-2}$ and *Dscam2*$^{null-3}$, previously generated by homologous recombination, (Millard *et al.*, 2007)) were isogenized in a w^{1118} background through eight backcrosses. After isogenization, the w^{1118} X chromosome was replaced with w^{+}. The final genotype contained an X chromosome from *Canton-S* and a second chromosome from w^{1118} background. The third chromosome was either from the w^{1118} background, for the control flies (making the flies identical to the wild-type flies used in chapter 2 and 3), or a recombinant w^{1118} third chromosome that contained the *Dscam2*^{null} allele. *Dscam2*^{null} heterozygous flies were generated by crossing *Dscam2*$^{null-1}$ to control flies. *Dscam2*^{null} transhomozygous flies were generated by crossing specific *Dscam2*^{null} flies to each other. Initial experiments started with the use of *Dscam2*$^{null-1}$ and *Dscam2*$^{null-2}$ flies. However, some experiments were complimented with *Dscam2*$^{null-3}$ flies after a difference in response between *Dscam2*$^{null-1}$ and *Dscam2*$^{null-2}$ flies was found. Flies were reared on standard *Drosophila* yeast-based media and kept at 22-25°C under 12-hour light and 12-hour dark cycles.

4.2.2 General behaviours

Sensory responses in *Dscam2*^{null} flies were studied by measuring their geotactic, chemotactic, and phototactic behaviours.

4.2.2.1 Response to gravity: geotaxis

Fly preparation

Female flies were collected (n = 10/experiment/strain) between four and 12 days after eclosion by CO_2 anaesthesia, the day before the experiment. Flies were kept on standard *Drosophila* yeast-based media at 22-25°C under 12-hour light and 12-hour dark cycles.

General procedure

A climbing apparatus (figure 4.1A) was prepared using an empty polystyrene vial with a cotton stopper (VWR, Radnor, PA, USA). Each vial was marked at a vertical distance of 10 cm above the bottom surface. On the day of the experiment, 10 female flies were gently transferred to the climbing apparatus where they were allowed to acclimatize to the new setting for 5 min. Geotaxis was measured by tapping the flies to the bottom of the vial and measurement of the proportion of flies that could climb above the 10 cm mark within 10 and 20 seconds after the tap. Each session consisted of 4 trials, with a 10 min rest periods between each trial.

Data analysis

The proportion of flies per group that passed the 10 cm mark was recorded for each trial and served as the statistical replicate. A Student's *t*-test was performed using GraphPad Prism version 6.0 for Windows (GraphPad Software, San Diego California, USA) to compare different strains.

4.2.2.2 Response to non-volatile attractants: chemotaxis

Fly preparation

Female flies were collected (n = 10/experiment/strain) between four and 12 days after eclosion by CO_2 anaesthesia, the day before the experiment.

General procedure

An olfactory acuity trap apparatus (figure 4.2A) was prepared based on a trap assay developed by Woodard *et al.* (1989) with a polystyrene vial containing 1 ml 1% agarose closed with a cotton stopper. The traps were constructed from a 1.7 ml flat capped microfuge tube (Labadvantage, USA),

one blue 1000 µl and one yellow 200 µl pipet tip (Labadvantage, USA). The microfuge tube was severed with a scalpel blade approximately 2.5 mm from its terminus to create and an aperture with an internal diameter of 4 mm. A blue 1000 µl pipet tip was severed at 1.6 cm from the top and 1.5 cm from the terminus. This twice-cut tip was inserted in the cut off end of the microfuge tube, with its small end inside. A yellow 200-µl pipet tip was severed at 1.5 cm from the bottom to create a large enough aperture for flies to enter, and fitted tightly over the large end of the twice-cut tip with its small bottom outside. The microfuge tube contained 300-µl water with or without 0.03 g dried yeast. The trap was placed in the agarose containing polystyrene vial together with 10 flies for 18 hours at RT. After the incubation, the proportion of flies per group trapped in the Eppendorf tube was recorded.

Data analysis

The proportion of flies per group that entered the olfactory acuity trap was recorded and served as the statistical replicate. A Student's *t*-test was performed using GraphPad Prism version 6.0 for Windows (GraphPad Software, San Diego California, USA) to compare different strains.

4.2.2.3 Response to light: fast phototaxis assay

Fly preparation

Female flies were collected (n = 27-33/experiment) between four and 12 days after eclosion by CO_2 anaesthesia, the day before the experiment. Flies were starved at room temperature for 19-22 hours prior to experimentation in modified disposable polyethylene "jumbo" transfer pipettes (Thermo Fisher Scientific, Waltham, Massachusetts) containing 10 µl of water. All experiments were conducted between early and mid-afternoon to reduce variation between different groups.

General procedure

Classical phototaxis experiments consist of setup such as a Y-maze or a horizontal tube in which the fly is exposed to a no-light and light condition at the same time. This is a simple way of testing a fly's response to phototaxis but has a limited resolution considering the nature of a 2-choice experiment consists of a 50% change element. Therefore an eight-point choice maze (J&M Specialty Parts, San Diego, California, USA) with nine exit points was used (described previously in (Van Swinderen & Flores, 2007), as well as in chapter 2). The maze has eight tiers and the flies make a choice to turn left or right at each tier (figure 4.3A). A UV (360 - 363nm), green (528nm) or blue (472nm) LED light (NS360L-3RIQ, B3B-443-B525, B3B-447-1x Rothner Lasertechnik, Vienna, Austria), powered by a standard 9-volt battery, was used as the light source and placed to the left or the right of the maze exit points. At the end of the maze, flies were collected at one of nine different exit points. The tube

containing the flies was tapped once to startle the flies and then inserted into the maze entrance. On average, it took a group of 30 flies 2.5 min to reach one of the nine exit points of the maze. Here, they were automatically counted using infrared sensors (modified *Drosophila* Activity Monitors, Trikinetics, Waltham, Massachusetts) (Evans *et al.*, 2011). A single experiment consisted of two cohorts of flies that were shown the light stimulus on opposite sides of the maze. At least five experiments with 10 mazes and approximately 30 flies each were performed per stimuli, resulting in at least 300 flies per data point. The light source was removed for the negative control. A visual response was calculated from fly counts with custom-written MATLAB (version R2013b, MathWorks, Natick, MA) scripts as a weighted average of the number of flies in each exit point of the maze (Eq. 1, section 2.2.1.3 and figure 4.3A).

Data analysis

Data analysis was performed with custom-written MATLAB scripts and statistical analysis using Graphpad Prism 6.0 for Windows (Graphpad software, San Diego, California, USA). For all stimuli an average and standard error of the mean (SEM) visual response was calculated, based on individual visual response experiments performed over multiple days. A Lilliefors test (Lilliefors, 1967) was used to test for normality of the dataset. To compare the average visual response of the mutant with that of control, a Student's *t*-test was performed for normally distributed data and a Mann-Whitney for non-normally distributed data. A two-way ANOVA was used to compare multiple groups. Group size varied from n = 8-62 per fly strain and per experiment.

4.2.3 Population visual response assay

The fly preparation and experimental procedure were as described in section 2.2.1. A range of contrasts (0.1-1, i.e. low to high level of contrast), temporal frequencies (1-16 cycles/second, i.e. slow to fast moving), and spatial frequencies (0.01 to 0.04 cycles/degrees, i.e. wide to narrow bars) were tested. The velocity of the grating was kept constant at 164.4 degrees/second for the different spatial frequencies.

4.2.4 Single tethered-fly assay

The fly preparation and experimental procedure were as described in section 2.2.2. A range of different temporal frequencies (9.8-104.4 degrees/second) and spatial frequencies (0.026-0.102 degrees/cycle) were tested. The velocity of the grating was kept constant at 58.8 degrees/second for the different spatial frequencies.

4.3 Results

4.3.1 General behaviours

4.3.1.1 *Dscam2* mutant flies have an impaired geotactic response

Drosophila flies exhibit anti-geotactic behaviour, whereby they walk up against the Earth's gravitational field after being tapped down in a vial (Desroches *et al.*, 2010, Inagaki *et al.*, 2010, Sun *et al.*, 2009). It was unknown whether *Dscam2*^{null} flies have defects in geotaxis or locomotion which is useful information for visual behaviour experiments which rely heavily on locomotion. Control flies responded strongly, with approximately 40% and 75% of flies crossing the 10 cm mark after 10 and 20 seconds after knockdown, respectively. Two different strains of *Dscam2*^{null} flies displayed a significantly lower (Student's *t*-test, $p < 0.05$) response, with 10-20% and 20-40% of the flies crossing the 10 cm mark after these time points (figure 4.1, panel A and B respectively). These results demonstrate a mild impairment of the geotactic response in *Dscam2*^{null} flies. This is consistent with the broad expression pattern of this gene which includes areas of the peripheral nervous system involved in movement (Grace Lah, personal communication).

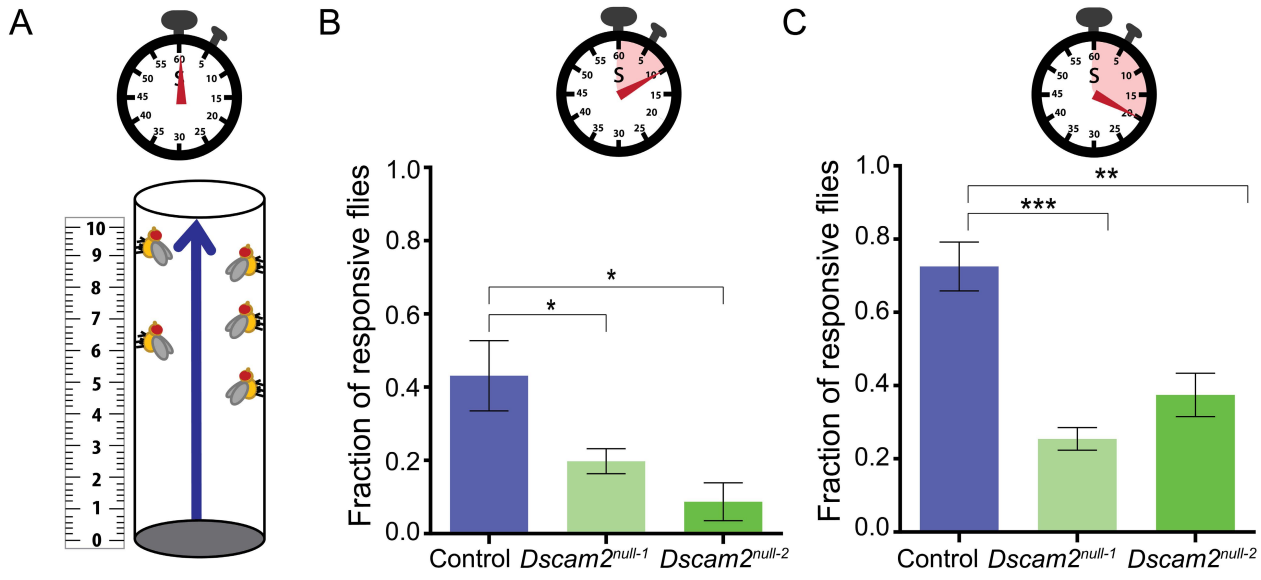

Figure 4.1. *Dscam2* mutants have an impaired geotactic response.
Geotactic response of control and *Dscam2*^{null} flies. **(A)** Geotaxis assay in which knocked down flies walk up a vial. **(B)** Proportion of control (blue) and *Dscam2*^{null} flies (light and dark green) reaching the 10 cm mark 10 seconds after knockdown of flies to the bottom (C) and 20 seconds after knockdown. For all groups at least nine flies per trial and a total of four trials were run for every condition. Error bars indicate SEM. A student's *t*-test was performed to compare control *vs* *Dscam2*^{null}. Significance between groups are indicated by asterisks in which * $p < 0.05$, ** $p < 0.01$, and *** $p < 0.001$.

4.3.1.2 *Dscam2* mutant flies can detect odours

Drosophila uses chemosensory systems in order to orientate themselves in their chemical environments. It was unknown whether *Dscam2*^{null} flies have defects in their ability to detect odours, which is key for potential odour learning experiments. To determine whether *Dscam2*^{null} flies are able to detect odours, an olfactory acuity apparatus was set up based on a trap assay developed by Woodard *et al.* (1989). In this assay, flies can enter a trap they cannot escape from, which contains either water (control) or water with food. Control flies enter the food-containing trap but not the water-containing trap (approximately 80% *vs* 5% respectively, see figure 4.2B). Two different strains of *Dscam2*^{null} flies displayed similar behaviour in which they would enter the food containing trap but not the water containing trap (approximately 70-90% *vs* 0-5% respectively, see figure 4.2B). Significant differences were found for control *vs Dscam2*$^{null-1}$ and *Dscam2*$^{null-1}$ *vs Dscam2*$^{null-2}$ flies (Student's *t*-test, $p < 0.05$), but presumably these differences would decrease if more flies were tested. For all groups, the proportion of flies trapped in the food containing trap was significantly higher (Student's *t*-test, $p < 0.001$) compared to the amount of flies in the only water containing trap. The significant increase for mutant flies (Student's *t*-test, $p < 0.05$) compared to control is likely caused by the small sample size. Together, these results demonstrate that flies enter the trap due to the attraction of the food odour.

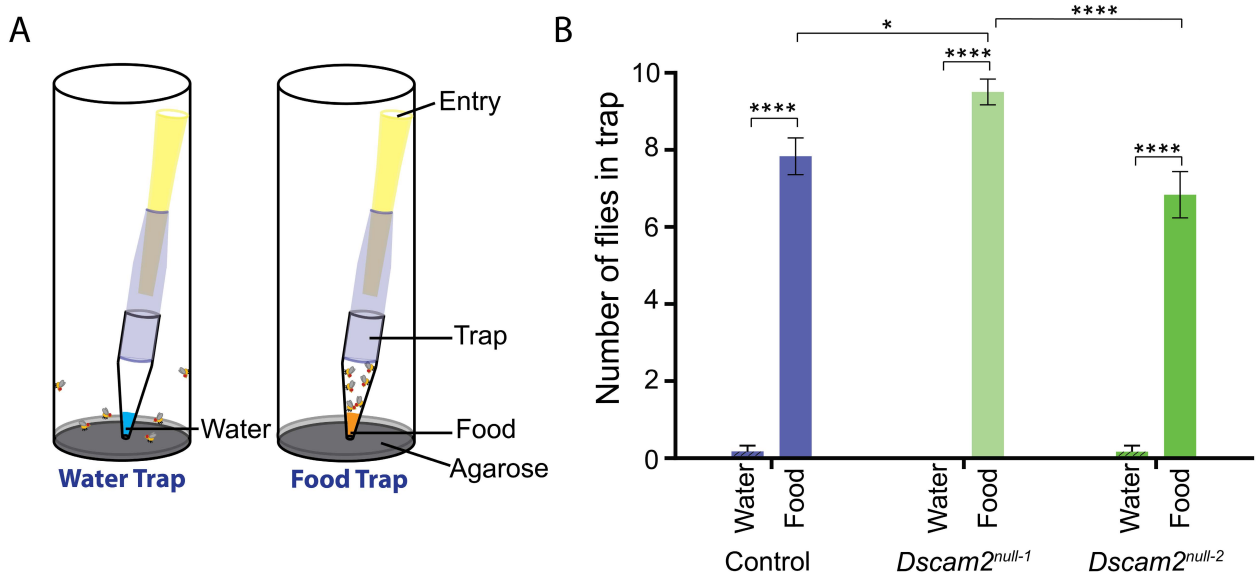

Figure 4.2. *Dscam2* mutants have normal odour detection.
Chemotactic response of control and *Dscam2*^{null} flies. **(A)** Olfactory acuity assay. Flies can enter but not exit the trap. **(B)** The proportion of control (blue) and *Dscam2* mutants (different shades of green) in the food trap (solid colour) was significantly higher compared to the trap with only water (striped). For all groups at least nine flies were run for every condition. Error bars indicate SEM. Student's *t*-test was performed to compare control *vs Dscam2*^{null} flies. Significance between groups are indicated by asterisks in which * $p < 0.05$, and **** $p < 0.001$.

4.3.1.3 *Dscam2* mutant flies exhibit reduced phototaxis

Many insects including *Drosophila* exhibit positive phototaxis, whereby they are attracted to a light source (Benzer, 1967). This is a hard-wired behaviour but is influenced by environmental factors, such as desiccation (Perttunen, 1963). It is also influenced by normal behavioural variation within a fly strain (Kain *et al.*, 2013). For example, Kain *et al.* (2013) demonstrated by repeated measure that individual flies will choose the light over dark on average 80% of the time. It was unknown whether the synaptic defects in the lamina of $Dscam2^{null}$ flies lead to any phototactic defects. This is useful information because future visual behaviour experiments rely on the ability to detect light. Phototaxis towards green, blue and UV light was measured and a visual response was calculated (Eq. 1, section 2.2.1.3 and figure 4.3A). Control flies responded strongly to all three wavelengths by walking towards the light, resulting in a skewed distribution of flies towards the light source at the end of the maze (figure 4.3B). Approximately 60% of the flies ended up in the three exit tubes closest to the light source. In control experiments where no light was present, flies distributed evenly along the exit tubes, resulting in a visual response close to zero. Two different strains of $Dscam2^{null}$ flies displayed a significant response to all three light sources with between 30 and 45% of the flies choosing the three exit tubes closest to the light source (figure 4.3B). The responses of the $Dscam2^{null}$ flies to the three wavelengths were not significantly different from each other (Student's *t*-test, $p > 0.05$) and no response was evoked without light (figure 4.3B). For all three wavelengths, the magnitude of the response in the mutants was significantly reduced compared to control (Student's *t*-test, $p < 0.05$; figure 4.3B). These results suggest that the circuitry that controls light detection is functional, but impaired, in $Dscam2^{null}$ flies.

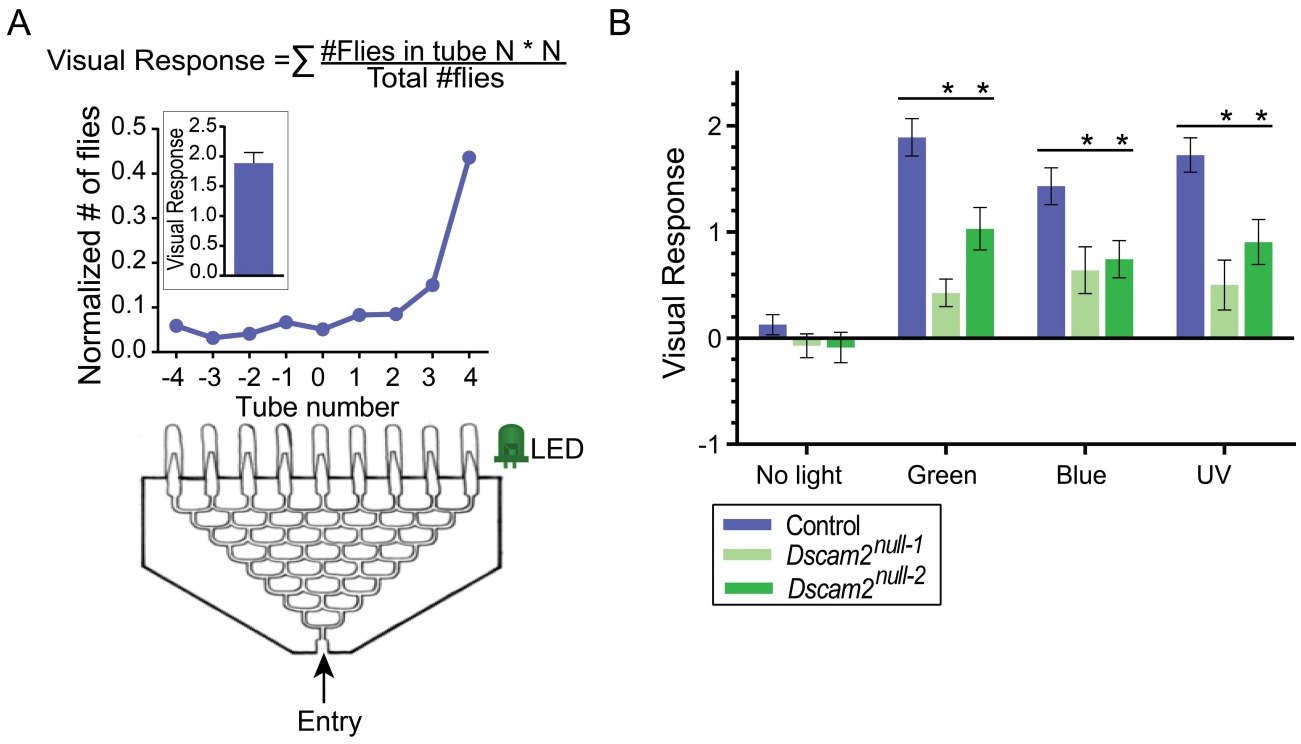

Figure 4.3. *Dscam2* mutants exhibit reduced phototaxis.
Phototaxis assay. **(A)** Flies (~30 per maze) enter the maze and end up in one of the nine end tubes (-4 to 4). The normalized distribution of flies from one maze is shown in the line graph. This was calculated by dividing the number of flies in each tube by the total. The visual response formula is at the top of the panel, corresponding with Eq. 1, section 2.2.1.3, and the response of the flies shown is plotted in the inset. **(B)** Phototaxis of control (blue), $Dscam2^{null\text{-}1}$ (light green) and $Dscam2^{null\text{-}2}$ (green) flies to different light sources. The mutant response is impaired compared to control. A student's *t*-test was performed for normal distributed data and a Mann-Whitney test for non-normal distributed data, * $p < 0.05$. For all groups at least nine mazes of approximately 30 flies each were run for every condition. Error bars indicate SEM.

4.3.2 *Dscam2* mutant flies in a population assay

A population assay (described in section 2.2.1) was used to assess motion detection. Here, a maze is placed on top of LED panels displaying moving visual stimuli. A visual response is calculated based on the distribution of flies at the maze exits; this response is positive when flies followed the direction of motion and negative when they moved against the direction of motion. As described in section 2.2.1.4, wild-type flies follow a moving grating of green and black stripes and their response is negative correlated to the bar size. In the next three sections, the visual response of control and $Dscam2^{null}$ (section 4.4.2.1) heterozygous (section 4.4.2.2) and transhomozygous mutant (section 4.4.2.3) flies to moving stimuli was explored.

4.3.2.1 *Dscam2*^{null} flies turn against the direction of motion in a population assay

In contrast to control flies which follow the moving grating, mutant flies moved against the direction of the motion, resulting in a negative visual response of -0.16 ± 0.12 and -0.54 ± 0.17 for *Dscam2*$^{null-1}$ and *Dscam2*$^{null-2}$ respectively (figure 4.4A). Control and mutant flies followed rightward and leftward motion with similar magnitudes, as expected.

To further investigate how the absence of *Dscam2* affects visual behaviours, the visual system of the flies was challenged by altering the contrast, spatial frequency, and temporal frequency of the grating. Each of these parameters contributes to how well an image is detected and therefore provides a means for testing the sensitivity and acuity of the visual system.

Control flies show a contrast-dependent behavioural response to moving gratings, with no response to a low contrast stimulus (0.1) and a maximal response at higher contrasts (0.7) (figure 4.4B). *Dscam2* mutant flies also responded to changes in contrast, but moved against the moving grating (figure 4.4B). Similar results were obtained when the spatial frequency (the width of the bar) was varied at a fixed contrast and velocity. Control flies responded well to low spatial frequencies (wider bars) but this response reduced to zero at higher spatial frequencies (narrower bars). The responses of the two *Dscam2* mutants was weaker than the controls and in the opposite direction (figure 4.4C). Finally, a constant spatial frequency was maintained, while the speed of the bars was varied in order to explore the temporal sensitivity of the visual system. Control flies responded to all tested temporal frequencies by following the moving grating. Neither of the two *Dscam2* mutants responded to lower temporal frequencies, but both elicited significant responses to faster moving bars (Student's *t*-test, $p > 0.05$). Consistent with the other tested parameters, the responses of both mutants were reversed compared to controls (figure 4.4D).

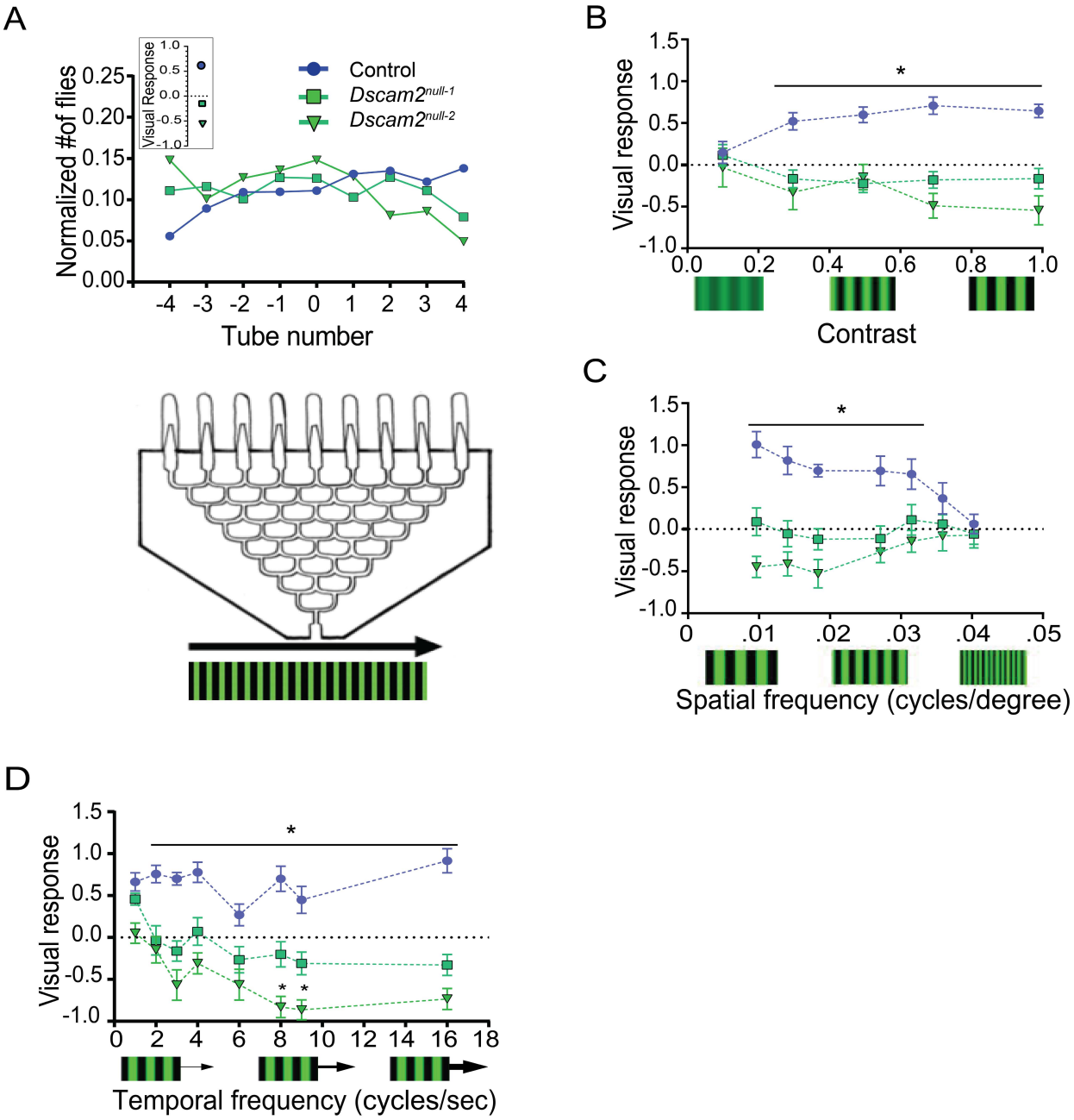

Figure 4.4. *Dscam2* mutants have a weakened and inverted response to motion in the population visual response assay.

Population visual response assay. **(A)** The same maze that was used for the phototaxis assay (figure 4.3) was placed on LED panels displaying moving gratings. The line graph displays the normalized distribution of flies in the maze. On average, control flies follow the direction of motion, resulting in a positive visual response. *Dscam2*^{null} flies exhibit the opposite behaviour, resulting in a negative response. The inset represents the calculated visual response for each genotype (see section 2.2.1.3). **(B-D)** Visual responses of control, *Dscam2*$^{null-1,}$ and *Dscam2*$^{null-2}$ flies to different **(B)** grating contrasts, **(C)** spatial frequencies and **(D)** temporal frequencies. A student's *t*-test was performed for normal distributed data and a Mann-Whitney test for non-normal distributed data, * $p < 0.05$ (control *vs* mutants). For all groups at least eight mazes of approximately 30 flies each were run for every condition. Error bars indicate SEM.

Although both *Dscam2* mutant strains showed a similar trend towards a negative visual response, the magnitude of their responses was different for most stimuli (figure 4.4B-D). This was surprising given that these lines were backcrossed into the same genetic background as the control flies in 2011 and the *Dscam2* mutations in the two strains were identical (Millard *et al.*, 2007). These data raised the possibility that one of the fly lines contained a genetic modifier linked to the *Dscam2* mutation that was not removed during backcrossing. To address this, the response of a third line with an identical *Dscam2* mutation (*Dscam2*$^{null\text{-}3}$), was tested at selected visual parameters. *Dscam2*$^{null\text{-}3}$ flies turned against the direction of motion, like the two other mutants but the magnitude of their response was more similar to *Dscam2*$^{null\text{-}1}$ than *Dscam2*$^{null\text{-}2}$ flies (figure 4.5A/B). Although the responses of *Dscam2*$^{null\text{-}1}$ and *Dscam2*$^{null\text{-}3}$ were not significantly different from zero at lower temporal frequencies, the stimuli that induced the highest responses in control and *Dscam2*$^{null\text{-}2}$ flies resulted in significant responses from these two lines as well (figure 4.5A/B). Thus, all three mutants turn against the direction of motion even though the magnitudes of the responses are variable. It is concluded that there is likely a genetic modifier independent of *Dscam2* in the *Dscam2*$^{null\text{-}2}$ line that increases the magnitude of the visual response in the maze paradigm. In the next section, it is assessed if one copy of functional *Dscam2* rescues the optomotor phenotype.

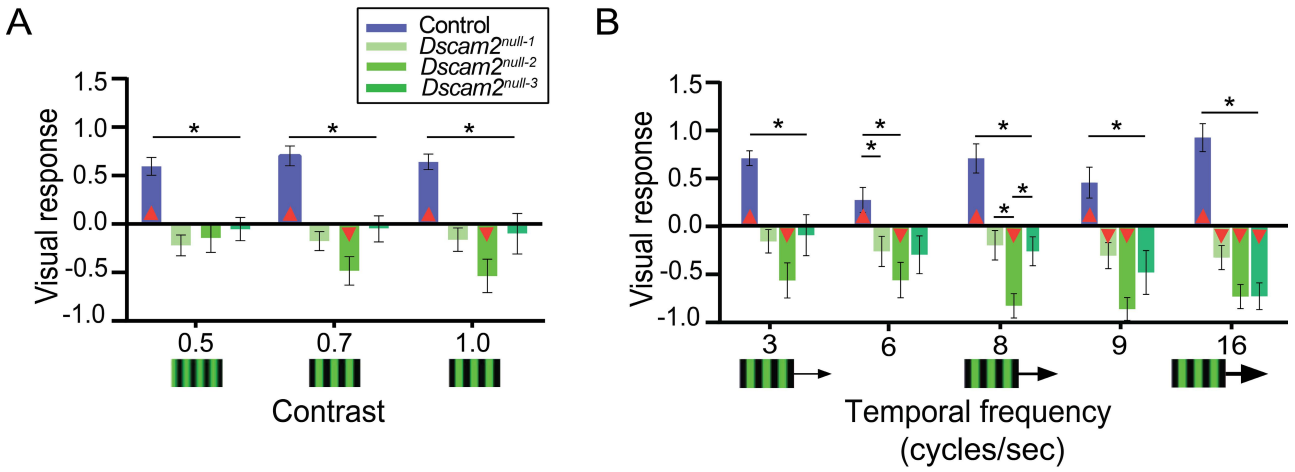

Figure 4.5. Differences between *Dscam2* mutants in the population visual response assay. Comparison of a third *Dscam2* mutant with the two other *Dscam2* mutants**. (A-B)** Visual responses of control, *Dscam2*$^{null\text{-}1}$, *Dscam2*$^{null\text{-}2,}$ and *Dscam2*$^{null\text{-}3}$ flies to different grating **(A)** contrasts and **(B)** temporal frequencies. Data presented from control, *Dscam2*$^{null\text{-}1}$, *Dscam2*$^{null\text{-}2}$ flies is reprinted from figure 4.4 to compare the visual response to a third *Dscam2* mutant (*Dscam2*$^{null\text{-}3}$, dark green bar). This mutant behaves most similarly to *Dscam2*$^{null\text{-}1}$ over different contrast levels and temporal frequencies. A bar graph was chosen to emphasize the magnitude differences in visual response between the lines. A student's *t*-test was performed for normal distributed data and a Mann-Whitney test for non-normal distributed data, * $p < 0.05$. Red triangles within bars indicate a significant difference from zero. For all groups at least eight mazes of approximately 30 flies each were run for every condition. Error bars indicate SEM.

4.3.2.2 *Dscam2* gene dosage affects the optomotor response

Dscam2 homozygous flies respond opposite to control flies in the population assay: can this optomotor phenotype be rescued by introduction of one functioning copy of the *Dscam2* gene? Studies in a mouse model for Down syndrome demonstrated circuit refinement in the eye was *DSCAM* dosage dependent (Blank *et al.*, 2011). Their results suggested that an increase in *DSCAM* dosage results in more repulsion, while a decrease in *DSCAM* dosage results in insufficient repulsion (Blank *et al.*, 2011). To investigate how *Dscam2* dosage affects the optomotor response, $Dscam2^{null-1}$ homozygous flies ($Dscam2^{null-1/null-1}$) were compared to $Dscam2^{null-1}$ heterozygous ($Dscam2^{null-1/+}$) and control flies.

The visual system was challenged by altering the contrast and temporal frequency of the moving grating. This is a similar approach as in section 4.3.2.1 but limited to five different conditions. When heterozygous flies were exposed to a grating with a contrast level of 1 (see section 4.2.3), a spatial frequency of 0.051 cycles/degree and a temporal frequency of 3 Hz, they followed the direction of the motion, resulting in a visual response of 0.66 ± 0.22 (figure 4.6A). This response was similar to control flies and opposite from homozygous mutant flies (figure 4.6A). Control, $Dscam2^{null-1/+}$ and $Dscam2^{null-1/null-1}$ flies followed rightward and leftward motion with similar magnitudes, as expected.

In general, the heterozygous flies perceived changes in these visual parameters similarly to control flies and their responses were significantly different from homozygous mutant flies under most conditions. However, at a temporal frequency of 8 Hz, heterozygous flies failed to respond similar to the homozygous mutants (Two-way ANOVA, Tukey's multiple comparison test and Student's *t*-test, $p < 0.05$; figure 4.6B).

From these experiments it can be concluded that one copy of *Dscam2* is sufficient to rescue most optomotor phenotypes. However, the lack of a response at 8 Hz indicates that *Dscam2* is haploinsufficient to some degree.

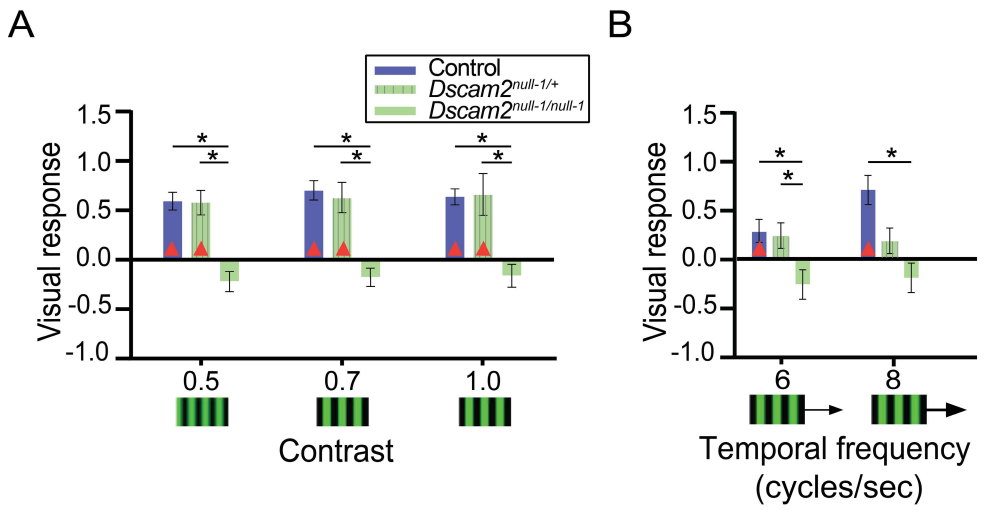

Figure 4.6. *Dscam2* heterozygotes respond similarly to control flies under most conditions. Influence of *Dscam2* dosage on the visual response. **(A-B)** Visual responses of control, $Dscam2^{null\text{-}1}$ heterozygous ($Dscam2^{null\text{-}1/+}$, grey striped on light green bars) and homozygous ($Dscam2^{null\text{-}1/null\text{-}1}$, light green bars) flies to different grating **(A)** contrasts and **(B)** temporal frequencies. Data presented from control and $Dscam2^{null\text{-}1}$ is reprinted from figure 4.4. *Dscam2* heterozygotes behave similar to control flies under most conditions, but perform similar to the mutants at 8 cycles/sec. A bar graph was chosen to emphasize the magnitude differences in visual response between the lines. A student's *t*-test was performed for normal distributed data and a Mann-Whitney test for non-normal distributed data, * $p < 0.05$. Red triangles within bars indicate a significant difference from zero. For all groups at least eight mazes of approximately 30 flies each were run for every condition. Error bars indicate SEM.

4.3.2.3 The $Dscam2^{null\text{-}2}$ line carries an assay-specific modifier

In section 4.3.2.1 it was reported that although all three *Dscam2* mutant strains showed a similar trend towards a negative visual response, the magnitudes of their responses were different, for most stimuli. To further explore the difference between the different $Dscam2^{null}$ flies, $Dscam2^{null\text{-}2}$ flies were crossed with $Dscam2^{null\text{-}1}$ and $Dscam2^{null\text{-}3}$ to generate *Dscam2* transhomozygous mutant flies, allowing for an assessment of whether the modifier is dominant or recessive. The visual response of these mutants was tested with a selection of visual stimuli similar to section 4.3.2.2.

When transhomozygous mutant flies were exposed to a grating with a contrast level of 1, a spatial frequency of 0.051 cycles/degree and a temporal frequency of 3 Hz, they moved against the direction of the motion, resulting in a visual response of -0.33 ± 0.28 and -0.26 ± 0.25 for $Dscam2^{null\text{-}2/null\text{-}1}$ and $Dscam2^{null\text{-}2/null\text{-}3}$ respectively (figure 4.7A). This response was between the response of $Dscam2^{null\text{-}2}$ (-0.54 ± 0.17) and $Dscam2^{null\text{-}1}$ (-0.16 ± 0.12) or $Dscam2^{null\text{-}3}$ (-0.10 ± 0.22) respectively (figure 4.7A) but not significantly different from each other.

Altering contrast and temporal frequency levels resulted in similar responses between the *Dscam2* transhomozygous and homozygous flies. A two-way ANOVA combined with a Tukey's multiple

comparisons test did not reveal any significance between groups and conditions. However, focusing on each visual stimulus individually and testing the difference in visual response between fly strains with a Student's *t*-test (without assuming a consistent standard deviation) revealed a significant difference between transhomozygous *Dscam2*$^{null\text{-}2/null\text{-}1}$ and *Dscam2*$^{null\text{-}1}$ and *Dscam2*$^{null\text{-}2}$ for the temporal frequency of 8 Hz ($p < 0.05$; figure 4.7).

Thus, transhomozygous mutants turn against the direction of motion similarly to *Dscam2*^{null} flies even though the magnitudes of the responses are variable. In the contrast experiment, the results are consistent with a recessive trait; transhomozygotes generally have a decreased magnitude compared to *Dscam2*$^{null\text{-}2}$ homozygous flies. However, in the temporal frequency experiment, the magnitudes are similar to *Dscam2*$^{null\text{-}2}$, suggesting that the modifier could be dominant. Due to the variability in these experiments, it is therefore difficult to definitively conclude whether the modifier is dominant or recessive. Interestingly, no differences between strains have been found to affect optomotor responses in the tethered-walking assay (see section 4.3.3).

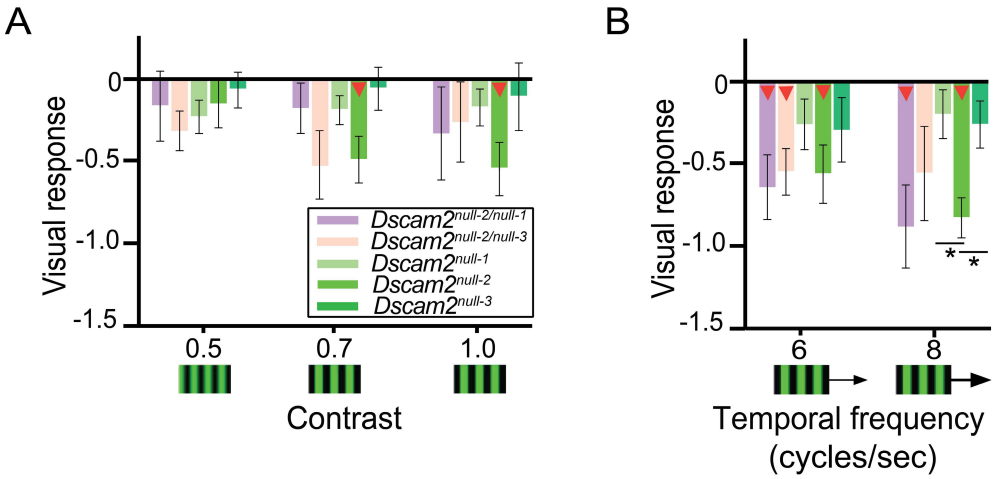

Figure 4.7. *Dscam2* transhomozygotes respond similarly to *Dscam2*^{null} flies under most conditions.

The response of *Dscam2* transhomozygotes to different visual parameters. **(A-B)** Visual responses of *Dscam2* transhomozygous (*Dscam2*$^{null\text{-}2/null\text{-}1}$, purple and *Dscam2*$^{null\text{-}2/null\text{-}3}$, rose coloured bars) and homozygous (*Dscam2*$^{null\text{-}1}$, *Dscam2*$^{null\text{-}2}$ and *Dscam2*$^{null\text{-}3}$) flies to different grating **(A)** contrasts and **(B)** temporal frequencies. Data presented from control and *Dscam2* homozygous mutants is reprinted from figure 4.4. Transhomozygous mutant flies do not respond significantly different from homozygous flies at all conditions. A bar graph was chosen to emphasize the magnitude differences in visual response between the lines. A student's *t*-test was performed for normal distributed data and a Mann-Whitney test for non-normal distributed data, * $p < 0.05$. Red triangles within bars indicate a significant difference from zero. For all groups at least eight mazes of approximately 30 flies each were run for every condition. Error bars indicate SEM.

4.3.3 *Dscam2* mutant flies in a single fly assay

4.3.3.1 *Dscam2* mutants are able to detect motion but perceive it in the opposite direction at a specific visual parameter

The weak behavioural response of *Dscam2* mutant flies in the population assay raised the concern that these flies could be partially motion blind. Although the population assay is ideal for testing motion behaviour in large populations of flies, the stimulus in the maze is complex. Light can be scattered by the glass and plastic from which the maze is constructed, flies have the ability to walk upside down in the maze channels, and social interactions with other flies can influence their decision at each choice point. Thus, the inverted and reduced visual response of *Dscam2* mutant flies in the maze could involve many confounding factors. The single tethered-fly assay was used to address these issues, by carefully controlling the visual field of the fly.

It was demonstrated in chapter 2 that wild-type flies respond well to a moving grating stimulus with a contrast of 1, a spatial frequency of 0.051 cycles/degree, and a temporal frequency of 3 Hz with a group average of 63 ± 14.0 degrees/second (Mean ± SEM) (figure 2.4/4.8B). In contrast to the results from the maze, the three $Dscam2^{null}$ strains responded to the optomotor stimulus with positive angular velocities that were not significantly different from controls (figure 4.8B). This demonstrated that the mutant flies are able to elicit an optomotor response similar to control flies under optimal conditions, and eliminated the possibility that they are motion blind.

As was done in the population assay, the capacity of the flies' visual system was investigated by presenting stimuli that are more difficult to detect to uncover detection limits. Control flies responded well to a wide range of spatial frequencies with angular velocities of 55-104 degrees/second to each condition (figure 4.8B). *Dscam2* mutants responded comparably to the different spatial frequencies with the exception of the highest spatial frequency, to which they did not respond (figure 4.8B and 4.8C). The limited range of the mutant's motion detection system is consistent with the data from the population assay. To explore this finding further, the spatial frequency where *Dscam2* mutant flies were not responding was fixed and a range of temporal frequencies were tested. Control flies had some difficulty detecting the different temporal frequencies, responding to only two of the five conditions tested (figure 4.8C). *Dscam2* mutant flies responded to one of the same conditions that the control flies did, but interestingly, they responded in the opposite direction (figure 4.8C and 4.8D). Thus, a specific visual parameter that caused the mutant flies to turn against the moving grating was found, consistent with the results from the population assay. To explore this finding further, the temporal frequency where *Dscam2* mutant flies were not responding was fixed and a range of spatial

frequencies were tested. Control and mutant flies followed similar trends except for the specific visual parameter that caused the mutant flies to turn against the moving grating. Altogether, from these experiments, it was concluded that the *Dscam2* mutant flies detected motion as well as control flies under optimal conditions. However, they were unable to detect more challenging visual stimuli and they perceived motion in the opposite direction at a specific temporal frequency. These data make a strong argument that changes in visual system modularity can affect both the sensitivity and the perception of the visual system.

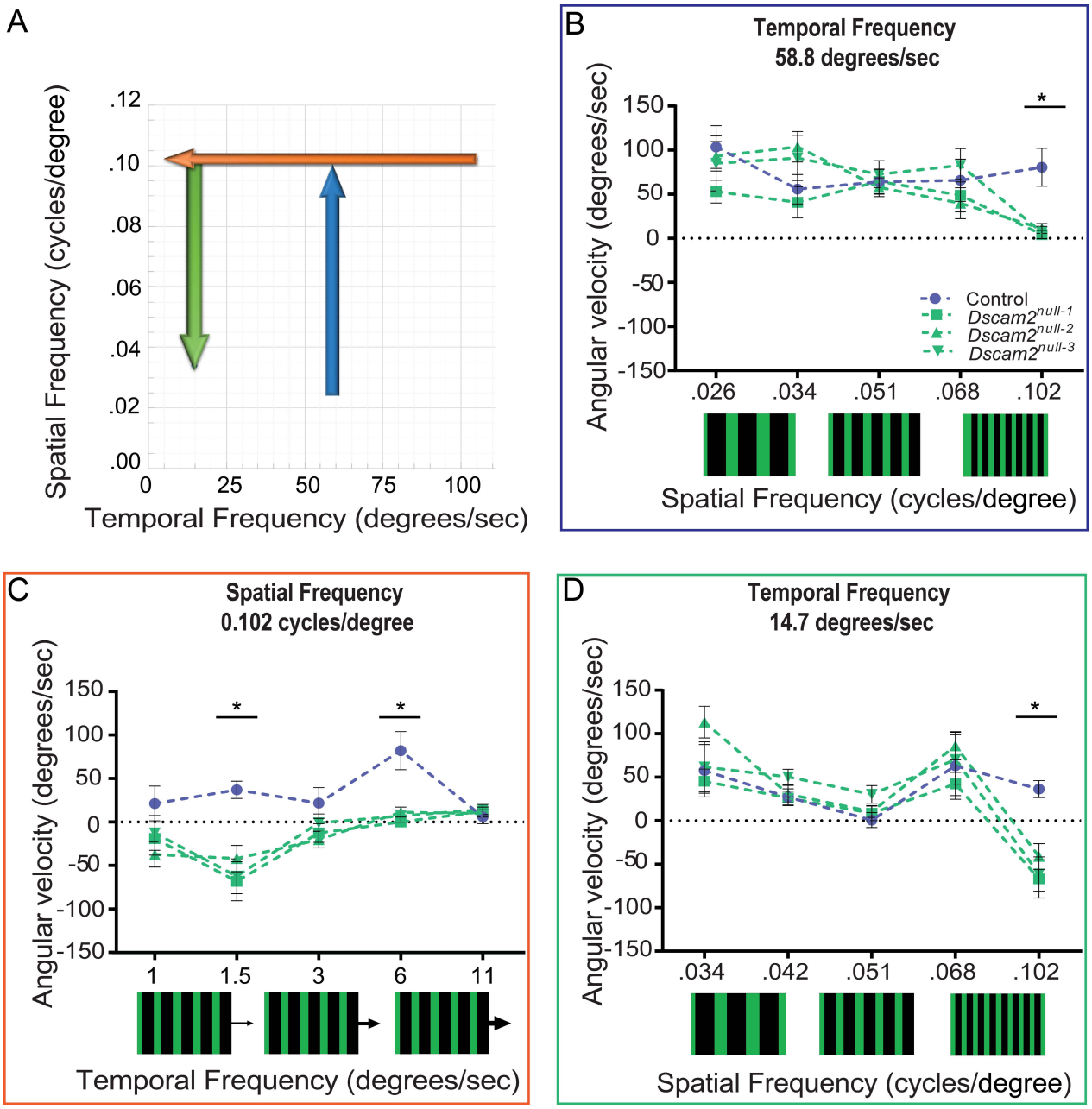

Figure 4.8. *Dscam2* mutant flies have conditional responses to motion in the single fly assay. Visual response of *Dscam2* mutant flies to a range of visual parameters. **(A)** A schematic of the different spatial and temporal frequencies explored in this experiment, colours correspond to the outlines of the graphs**. (B-E)** Visual responses of control (blue), *Dscam2*$^{null-1}$ (green squares), *Dscam2*$^{null-2}$ (green up-pointing triangles) and *Dscam2*$^{null-3}$ (green down-pointing triangles) flies to gratings with different spatial and temporal frequencies. **(B)** Visual response to different spatial frequencies at a constant grating velocity of 58.8 degrees/second; **(C)** various temporal frequencies at a constant spatial frequency of 0.102 cycles/degree and **(D)** various spatial frequencies at a constant grating velocity of 14.7 degrees/second. A student's *t*-test was performed for normal distributed data and a Mann-Whitney test for non-normal distributed data, * $p < 0.05$. For all groups at least eight flies were tested for every condition. Error bars indicate SEM.

4.3.3.2 *Dscam2* mutants respond to clockwise but not counter-clockwise translational stimuli

A behavioural specialization of L1 and L2 in motion detection has also been shown with translational stimuli such as front-to-back and back-to-front motion (Duistermars *et al.*, 2012, Rister *et al.*, 2007, Tuthill *et al.*, 2013). Duistermars *et al.* (2012) demonstrated that wild-type flies respond to translational motion in a contrast dependent manner, with a maximal response to a high contrast front-to-back stimulus and a minimal response to a high contrast back-to-front (figure 4.9A). It has been suggested that L2 plays a role in front-to-back motion (Rister *et al.*, 2007, Tuthill *et al.*, 2013). Considering that the *Dscam2* mutant flies have wiring defects directly related to L2 (Millard *et al.*, 2010), the response of *Dscam2* mutants to translational stimuli was tested. The visual stimulus was similar to the rotational stimulus that was used in the previous section, except that it was displayed on either the left or right side of the arena. A fly's optomotor response was calculated from the average angular velocity of the ball during the motion phases of the experiment.

Control flies responded to the front-to-back stimulus by following the motion (46.7 ± 21.0 degrees/second and 42.2 ± 10.1 degrees/second respectively, figure 4.9B). Interestingly, the response of $Dscam2^{null}$ flies to the front-to-back stimulus did not differ significantly from zero when presented to the left eye. However, the mutants follow the motion similarly to control flies when the front-to-back stimulus was presented to the right eye (figure 4.9B).

Based on the study of Duistermars *et al.* (2012) no response was expected for the back-to-front motion stimulus. This was true for the left eye, but control flies moved against the direction of the motion when it was presented to the right eye (-32.7 ± 14.7 degrees/second, figure 4.9C). $Dscam2^{null}$ flies respond well to the back-to-front stimulus when presented to the left eye by moving against the direction of the motion but did not respond when it was presented to the right eye (figure 4.9C). This is opposite from control flies.

These data demonstrate that *Dscam2* mutant flies do not respond to counter-clockwise orientated stimuli but do to clockwise stimuli (figure 4.9B-C). This is something that has not been observed in rotational optomotor response but could suggest a change in how they perceive visual stimuli.

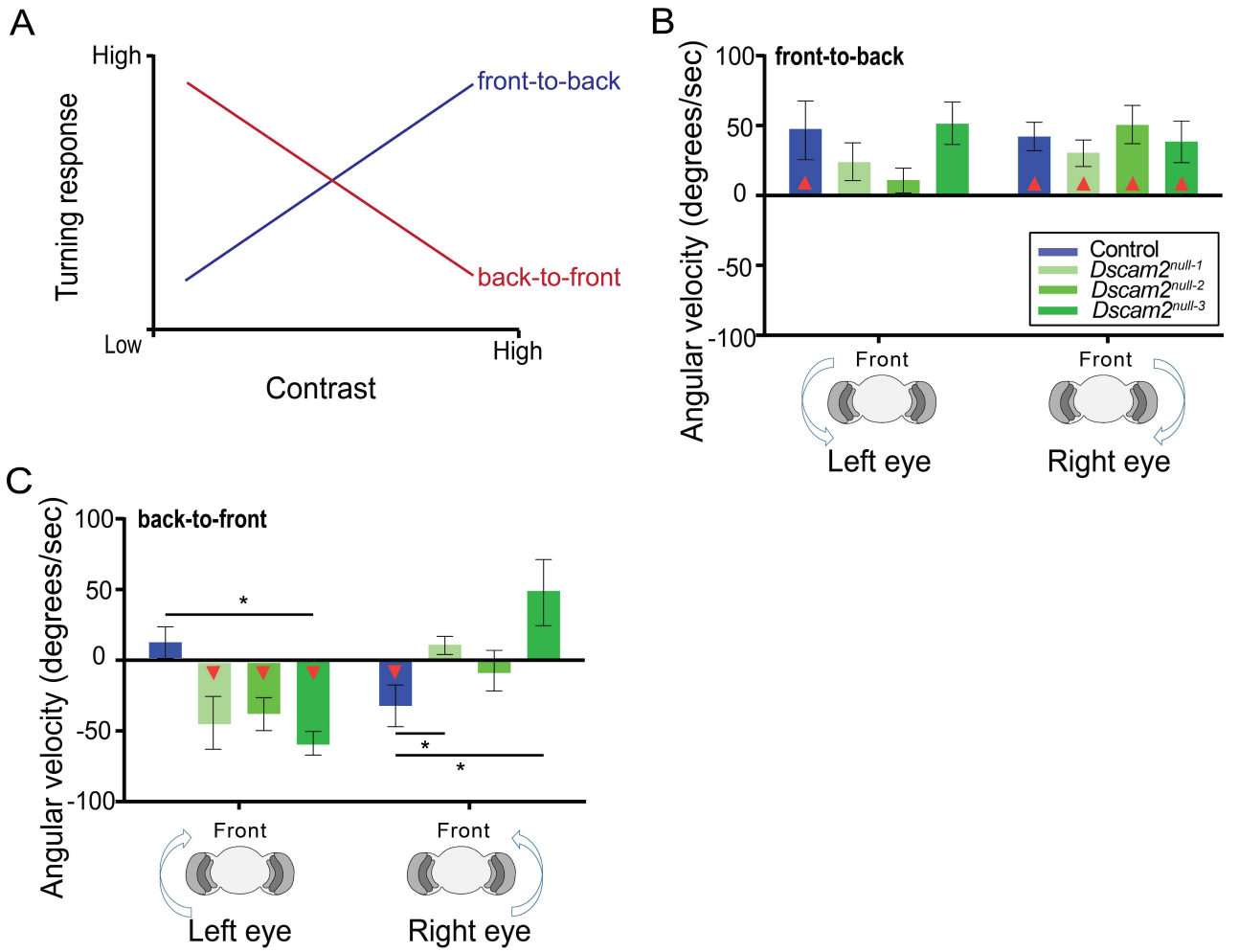

Figure 4.9 *Dscam2* mutants do not respond to counter-clockwise translational motion.
Visual response of control and *Dscam2* mutant flies to translational motion. **(A)** Summary results from Duistermars *et al.* (2012) for front-to-back and back-to-front stimuli at different contrast levels with tethered flying flies. **(B)** Angular velocities of control (blue) and $Dscam2^{null\text{-}1}$ (light green), $Dscam2^{null\text{-}2}$ (green) and $Dscam2^{null\text{-}3}$ (dark green) flies to high contrast front-to-back and **(C)** back-to-front stimuli. *Dscam2* mutants respond to back-to-front motion when presented to the left eye and front-to-back when presented to the right eye. A student's *t*-test was performed for normally distributed data and a Mann-Whitney test for non-normally distributed data. For all groups at least nine flies were tested for every condition. Error bars indicate SEM. Red triangles within bars indicate a significant difference from zero. Significance between groups are indicated by asterisks in which * $p < 0.05$.

4.4 Discussion

Dscam2 plays an important role in neuronal connectivity during *Drosophila* development (Millard *et al.*, 2007, Millard *et al.*, 2010) and the absence of *Dscam2* has been shown to result in synaptic defects in the visual system (Millard *et al.*, 2007, Millard *et al.*, 2010). In this chapter, different behavioural responses of *Dscam2* mutant flies were characterised and it was found that many of them were perturbed.

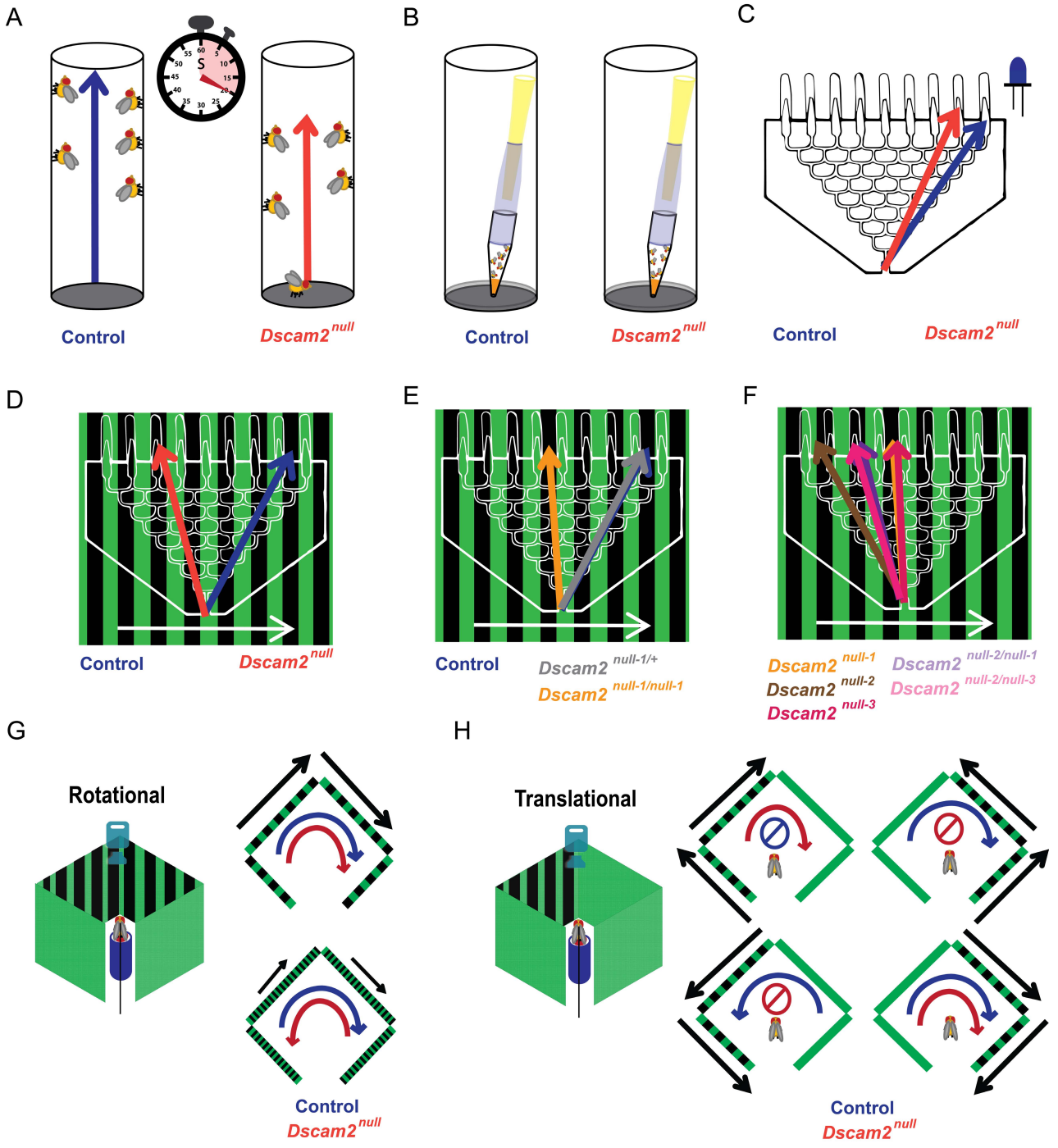

Figure 4.10 *Dscam2* mutant visual behaviour is conditionally perturbed.
Simplified schematic summarizing the average responses of *Dscam2* mutants compared to control flies. Details on the assays can be found in section 4.2. **(A)** Geotaxis is partially impaired in *Dscam2*^{null} flies. **(B)** *Dscam2*^{null} flies can detect odours. **(C)** Phototaxis is partially impaired in *Dscam2*^{null} flies. **(D)** *Dscam2*^{null} flies turn against the direction of motion in a population assay. **(E)** *Dscam2* gene dosage affects the optomotor response. **(F)** *Dscam2*$^{null\text{-}2}$ flies carry an assay-specific modifier affecting the magnitude of their optomotor response. **(G)** Specific motion parameters such as slowly moving small bars in a tethered single fly assay elicit a negative optomotor response from *Dscam2*^{null} flies. **(H)** *Dscam2*^{null} flies respond to clockwise but not counter-clockwise translational stimuli.

4.4.1 The geotactic response is impaired in *Dscam2* mutant flies

Flies display negative geotaxis similar to many other flying insects (Davenport & Perkins, 1897). Although genes involved in geotaxis behaviour have been identified, little is known about the exact neuronal mechanism (Kamikouchi *et al.*, 2009). As described earlier, geotaxis includes both locomotor and motivational components. One unique aspect of this behaviour is that geotaxis functions as a trigger for the fly to walk. This is not the case in other locomotion assays where a fly is motivated to walk by a mechanical stimulus. Geotaxis is impaired in *Dscam2* mutant flies (figure 4.1B and 4.10A), and there are several possible interpretations of this phenomenon. *Dscam2* mutant flies might walk slower, resulting in less flies reaching the 10 cm mark or they might have a specific problem with detection gravity. Locomotion problems in the mutants have not been observed in other assays (see section 4.4.2 and 4.4.3), making the latter option more likely. *Dscam2* is expressed in motor neurons (Grace Lah, personal communication) so subtle defects which only are elicited during walking vertically could also contribute to this phenotype. An alternative option is that *Dscam2* mutant flies could have motivational impairments leading to a reduced geotactic response. Addressing the cause of this phenotype is beyond the scope of this thesis, as a detailed investigation is required.

4.4.2 *Dscam2* mutant flies can detect odours

For survival, flies need to be able to find food sources. They are able to do this using their chemosensory systems in order to orient themselves in their chemical environments. *Dscam2* mutant flies have a normal odour response (figure 4.2B and 4.10B), demonstrating that some sensory systems are unaffected by the *Dscam2* mutation. This makes testing olfactory learning in the mutant a possibility for future studies.

4.4.3 Phototaxis is impaired in *Dscam2* mutant flies

Flies use photoreceptors in the retina to detect light, as was described in Chapter 1. Photons activate photoreceptors specialised for motion detection (R1-6) and colour vision (R7-8) (Anderson & Laughlin, 2000, Bausenwein *et al.*, 1992, Meinertzhagen & Sorra, 2001). The positive phototactic behaviour found in adult *Drosophila*, in which they are attracted to light over dark (Benzer, 1967) is influenced by internal and external factors. Gorostiza *et al.* (2015) demonstrated that phototaxis is a value-based choice depending on the flies' internal neurochemical state. The neurochemical state is suggested to be the underlying cause of 'normal' behavioural variation within a fly strain in which for example flies choose the light over dark on average 80% of the time in a phototaxis assay (Kain

et al., 2013). External factors such as a dry environment can switch positive phototactic behaviour into negative (Perttunen, 1963). This demonstrates flexibility in this behaviour.

As discussed in depth in chapter 1, six different visual pigments are found in the photoreceptors located in ommatidia. R1-6 contain blue-green absorbing rhodopsin Rh1 which gives these photoreceptors a broad spectral sensitivity (Salcedo *et al.*, 1999). R7 and R8 have a more specific spectral sensitivity to UV and green light, respectively (Chou *et al.*, 1996, Chou *et al.*, 1999, Papatsenko *et al.*, 1997). It was demonstrated that phototaxis to green, blue and UV light is equally impaired in *Dscam2* mutant flies (figure 4.3B and 4.10C) and there are two different interpretations possible to this result. Firstly, it is possible that the sensitivity of the visual system in *Dscam2* mutant flies is reduced causing less activation of the light detection circuitry. This would result in a lowering of the phototactic response. Secondly, it is possible that the severity of wiring defects in *Dscam2* mutant flies varies, rendering a subpopulation unable to detect light at all. The latter case is unlikely considering in the single fly assay none of the flies were found to be non-responsive (section 4.3.3.1).

4.4.4 *Dscam2* mutant flies move against the direction of the motion in the population visual response assay

After demonstrating that *Dscam2* mutant flies are not blind, motion detection was assessed. The *Drosophila* optomotor response has been key for testing models of motion detection. The Hassenstein-Reichardt EMD model has been used to explain motion detection in *Drosophila* (Hassenstein & Reichardt, 1956a). It relies on the modularity of the visual system for motion detection and given the reduced modularity in *Dscam2* mutants (figure 1.7), it was expected that their acuity would be compromised. The observed behaviours confirm this expectation; these flies had attenuated motion tracking compared to controls (figure 4.4B-D and 4.10D).

Unexpectedly, *Dscam2* mutants respond to motion in an opposite manner compared to controls. Moving gratings of alternating dark and light bars have classically been used to elicit an optomotor response from flies. The response varies depending on the particular assays, as discussed in section 1.3.1. In assays where the fly is tethered, individuals turn or walk in the direction of the motion, a response that is thought to stabilize their visual world (Götz, 1964, Götz, 1968). In free walking assays, flies respond to a moving grating by turning with or against the direction of motion (Evans *et al.*, 2011, Lee *et al.*, 2001, Zhu & Frye, 2009). What regulates this behavioural switch between following and moving against motion is not known. Data presented here suggests that *Dscam2* plays a crucial role in the perception of these motion stimuli.

4.4.5 One copy of *Dscam2* is sufficient to rescue most optomotor phenotypes in the population visual response assay

A *DSCAM* dosage-dependent effect on eye circuit refinement was found in in a mouse model for Down syndrome (Blank *et al.*, 2011). Considering that mouse *DSCAM* and *Drosophila Dscam2* share conserved functions, it was questioned whether the amount of repulsive interactions in the eye is *Dscam2* dosage dependent. In the previous section, *Dscam2* mutants were exposed to a wide range of visual stimuli with alterations of contrast and temporal frequency to challenge the visual system. From this, five stimuli were selected in which the response of *Dscam2* homozygous flies was compared to heterozygous and control flies. $Dscam2^{null\text{-}1}$ homozygotes responded to all but one visual stimulus similarly to control flies (figure 4.6A-B and 4.10E), demonstrating that one copy of *Dscam2* is sufficient to rescue most optomotor phenotypes. However, the lack of a response at 8 Hz indicates that *Dscam2* is haploinsufficient to some degree. This suggests that some of the motion detection circuitry is affected by the lack of one copy of *Dscam2* but that it only affects a very specific condition.

4.4.6 An unidentified modifier in the $Dscam2^{null\text{-}2}$ line affects the magnitude of the visual responses

It was expected that all three *Dscam2* mutant strains would respond similarly. They were backcrossed into the same genetic background as the control flies and have identical *Dscam2* mutations (Millard *et al.*, 2007). However, differences in response magnitudes where found, suggesting a genetic modifier independent of *Dscam2* in the $Dscam2^{null\text{-}2}$ line that increases the magnitude of the visual response in the maze paradigm. Transhomozygous mutants were generated and turned against the direction of motion at different contrast and spatial frequencies. Unfortunately, due to the variability in the experiments, no clear conclusion can be drawn if the modifier is dominant or recessive, however no differences between strains have been found to affect optomotor responses in the tethered-walking assay (see section 4.3.3).

4.4.7 *Dscam2* mutant flies are able to track motion but respond opposite from control flies at specific conditions

In the population assay, *Dscam2* mutants responded to motion weakly and opposite to controls, leaving it unclear whether the flies were partially motion blind. Therefore, a single tethered-fly assay was used to address motion detection in *Dscam2* mutant flies. It was found that they are able to elicit

an optomotor response to rotational stimuli similar to control flies under optimal conditions (figure 4.8A-D and 4.10G). This eliminates the possibility that they are motion blind. *Dscam2* mutant flies have a reduced range of motion detection, consistent with the data from the population assay. *Dscam2* mutant flies did not respond to narrow bars at the standard temporal frequency, indicating a change in visual system acuity. Interestingly, when this spatial frequency was fixed and the temporal frequency was altered, it was found that *Dscam2* mutant flies responded opposite to control flies to a slow moving grating with narrow bars. This result will be discussed in more detail in chapter 7 and a comparison will be made between the population and single fly assay.

4.4.8 *Dscam2* flies respond to clockwise stimuli only

Duistermars *et al.* (2012) demonstrated that wild-type flies show a maximal response to a high contrast front-to-back stimulus and minimal response to a high contrast back-to-front in a tethered flying fly assay (figure 4.9A). Together with the finding that L2 plays a role in front-to-back motion (Rister *et al.*, 2007, Tuthill *et al.*, 2013), it was expected that the *Dscam2* mutant flies which have wiring defects directly related to L2 (Millard *et al.*, 2010), would respond differently to the high contrast front-to-back stimulus compared to control

In line with Duistermars *et al.* (2012), control flies responded to the high contrast front-to-back stimulus when presented either to the left or right eye (figure 4.9B and 4.10G). Interestingly, *Dscam2*^{null} flies only responded to the front-to-back stimulus when presented to the right eye (figure 4.9B). Although no response from control flies was expected for a high contrast back-to-front motion stimulus based on the study of Duistermars *et al.* (2012), control flies showed a response to a high contrast back-to-front stimulus when presented to the right eye but did not respond when it was presented to the left eye (figure 4.9C and 4.10G). *Dscam2*^{null} flies responded to this stimulus well when presented to the left eye but not when it was presented to the right eye (figure 4.9C). This is opposite from control flies.

The difference in response between left and right eye for these stimuli was unexpected. This could be attributed to either the flies or the assay. The left and right eye have been reported to be equally functional and sensitive to pattern motion in any direction (Götz, 1968) and is therefore unlikely the cause of this difference. Although the assay in this chapter is setup in a symmetrical way, the distance of the fly to the front panels differs from the distance of the fly to the rear panels, causing the bars on the rear panels to be perceived as wider. Motion perception in the frontal area differs from the rear

area as motion restricted to the rear quarter-field elicits clockwise turning responses independent of the direction of image motion (Tammero *et al.*, 2004). If flies are exposed to smaller and bigger bars at the same time then they might chose the direction of the bigger bars, in this case they would then focus more on the rear panels. Although all these options could result in a bias, it would not explain why the bias has not been observed in rotational and front-to-back stimuli.

Also the finding that control flies responded to the high contrast back-to-front stimulus was unexpected as Duistermars *et al.* (2012) found wild-type flies not responding to this condition. This could be explained by differences between the assay used by the authors and in this chapter, such as flying *vs* walking flies, differences in LED panels and visual stimulus.

When *Dscam2* mutants were tested two observations were made: (1) mutant flies only responded to clockwise stimuli and (2) mutant flies respond to a high contrast back-to-front stimulus presented on the left eye, while control flies do not (figure 4.9B-C and 4.10G). This suggests that the change in modularity in *Dscam2* mutant flies have an altered perception of counter-clockwise stimuli. This could be attributed partially to a change in contrast perception associated with the reduced modularity of the visual system, something that requires further testing of back-to-front and front-to-back stimuli at low and intermediate contrast levels. Indeed, if mutant flies perceive a high contrast back-to-front stimulus as one of an intermediate contrast, one would expect that reducing the contrast to an intermediate level would eliminate the response.

In the next chapter, object-orientation preference in *Dscam2* mutant flies will be investigated in detail.

Chapter 5

Operant behaviour and attention-like mechanisms of Dscam2^{null} flies

5.1 Chapter overview

In this chapter, it is asked whether the change in visual perception in the *Dscam2^{null}* flies is limited to motion detection or can be extended to object position detection and associated attention-like processes. Here, object-orientation behaviour of *Dscam2^{null}* flies to light and dark bars is assessed followed by an in depth analysis of how this behaviour can be modulated by bar size.

5.2 Results

To assess how *Dscam2^{null}* flies position an object in relation to themselves, a single tethered-fly virtual reality assay as described in chapter 3 was used. Here, a tethered-fly walks on an air-supported ball and is surrounded by LED panels displaying a visual stimulus which is under control by the fly.

5.2.1 *Dscam2* mutant flies anti-fixate on a dark bar

Control flies fixate on a 29.4 x 58 degree dark bar on a light background by placing the bar towards the front of the arena (28°, 0° = front; figure 3.1A/5.1A). In contrast to control flies, all three *Dscam2* mutant strains demonstrated an anti-fixation response to this stimulus, placing the bar 145-195° from the front (figure 5.1A). A Rayleigh test on the group mean direction showed a non-uniform distribution for both control and mutant flies ($p < 0.01$ and $p < 0.05$, respectively). To compare the strengths and variation of the responses, these data are displayed in a box plot and show that although the direction of the response was different between control and mutant flies, the strength and variability were not (figure 5.1B). In addition, all three mutant lines responded similarly. These data demonstrated that *Dscam2* mutant flies place a dark bar behind them, a response that is opposite to control flies.

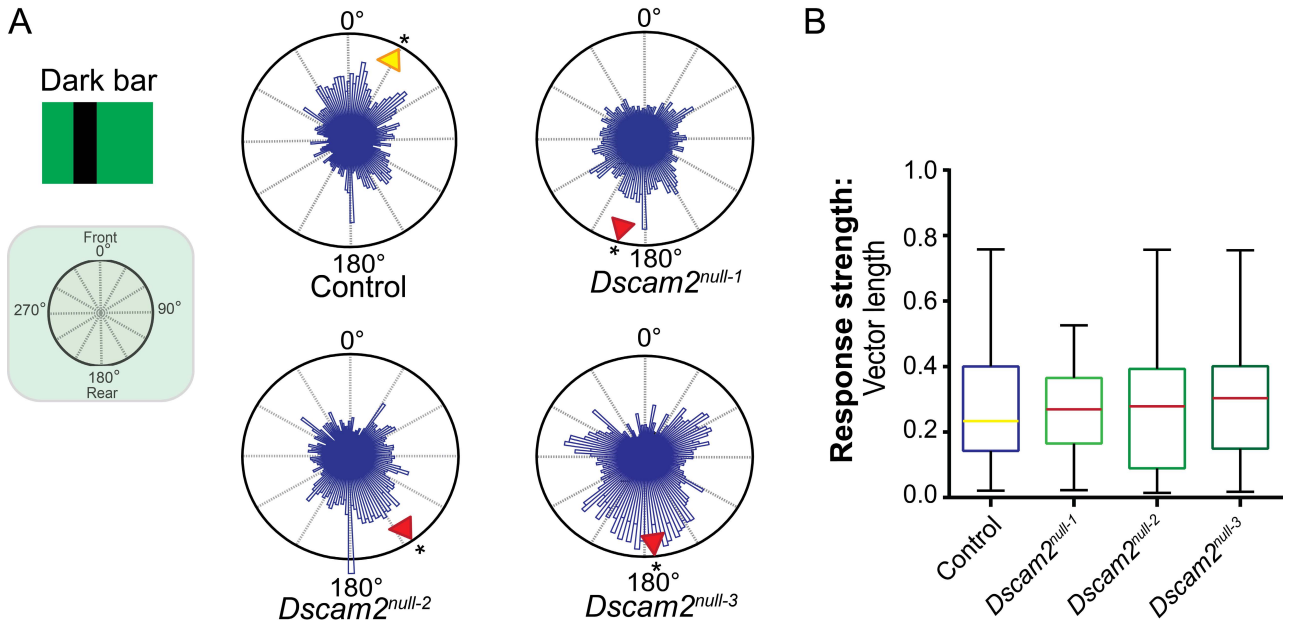

Figure 5.1. *Dscam2* mutant flies anti-fixate to a dark bar.
Object-orientation preference assay. Flies were presented with a bar in a closed-loop condition and their preference for the bar position was recorded. The histograms within the 360° circular plots represent a weighted value for each bar position derived from all flies of each genotype. A Rayleigh test confirmed the distributions were non-uniform * $p < 0.05$. If distributions were non-uniform, then for each fly an average bar angle was calculated, as well as a group mean direction which is graphically represented in the radial histogram as a yellow arrowhead for a bar position towards the front of the arena or red arrowhead for a bar position towards the back. Data from control flies is reprinted from figure 3.2. **(A)** Control flies fixate and *Dscam2* mutants anti-fixate on a dark bar. **(B)** Control and *Dscam2* mutant flies demonstrate similar response strengths (indicated with min to max whiskers in the boxplot) and variation for the dark bar stimulus. The colour of the median line corresponds with the colour of the arrowhead. For all groups at least eight flies were tested for every condition. A Kruskal-Wallis test indicated no significant difference between the vector lengths of the different fly strains.

Next, the flies' response to a light bar of similar size was tested. Control flies anti-fixate on this stimulus by placing the bar 184 degrees from the front (figure 5.2A) as shown in chapter 3. Interestingly, mutant flies behaved similar to controls with this stimulus, placing the bar 151-163 degrees from the front (figure 5.2A). A Rayleigh test on the group mean direction showed a non-uniform distribution for both control and mutant flies ($p < 0.05$). The vector lengths and variability were similar in mutant and control flies (figure 5.2B).

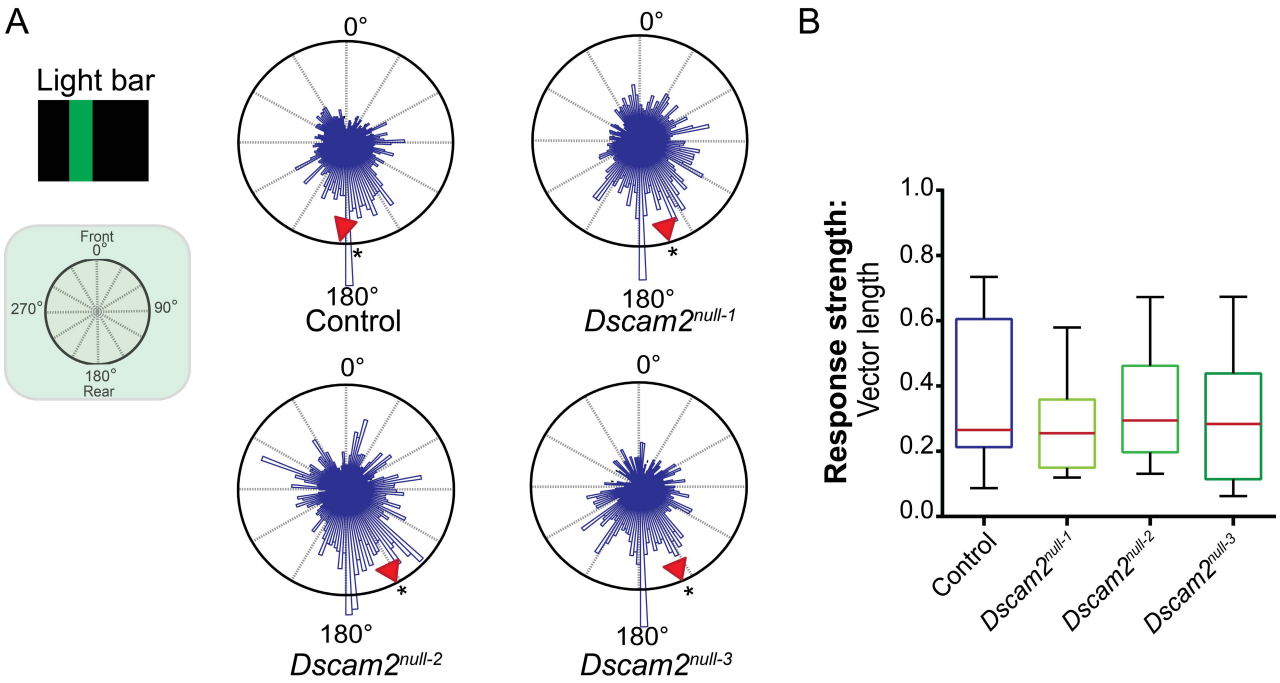

Figure 5.2. *Dscam2* mutant flies anti-fixate to a light bar.
Object-orientation preference assay. Flies were presented with a bar in a closed-loop condition and their preference for the bar position was recorded. The histograms within the 360° circular plots represent a weighted value for each bar position derived from all flies of each genotype. A Rayleigh test confirmed the distributions were non-uniform * $p < 0.05$. If distributions were non-uniform, then for each fly an average bar angle was calculated, as well as a group mean direction which is graphically represented in the radial histogram as a red arrowhead for a bar position towards the back. Data from control flies is reprinted from figure 3.2. **(A)** Control and *Dscam2* mutant flies both place a light bar towards the back of the arena. **(B)** Control and *Dscam2* mutant flies demonstrate similar response strengths (indicated with min to max whiskers in the boxplot) and variation for the light bar stimulus. The colour of the median line corresponds with the colour of the arrowhead. For all groups at least eight flies were tested for every condition. A Kruskal-Wallis test indicated no significant difference between the vector lengths of the different fly strains.

Both a light and dark bar elicits anti-fixation behaviour in mutant flies. This finding was surprising and questioned whether a light and dark bar was perceived similarly. To investigate this in more detail, position information was combined with movement information using a slow moving single bar in an open loop experiment (figure 5.3A). The angular velocity of control and mutant flies in response to this stimulus was measured. The bar was 29.4 x 58 degrees and circulated at 3 Hz in the arena for 90 seconds in a clockwise direction followed by 90 seconds counter-clockwise. Both light and dark bars were tested. Control flies followed the moving bars similar to the optomotor assay (figure 5.2B/C and section 2.2.2.4). Interestingly, mutant flies responded in a similar way (figure 5.3B/C). Two conclusions can be drawn from these results: (1) *Dscam2* mutants are able to detect the single bar and (2) considering the control and mutant flies track a moving dark bar similar to a light bar it demonstrates that motion tracking and fixation are very different responses, and suggest that without the motion cue, mutant flies perceive the dark bar differently. In the next section, the

responses to bar perturbations will be analysed in order to investigate whether it provides additional information on how the mutants perceive the dark bar.

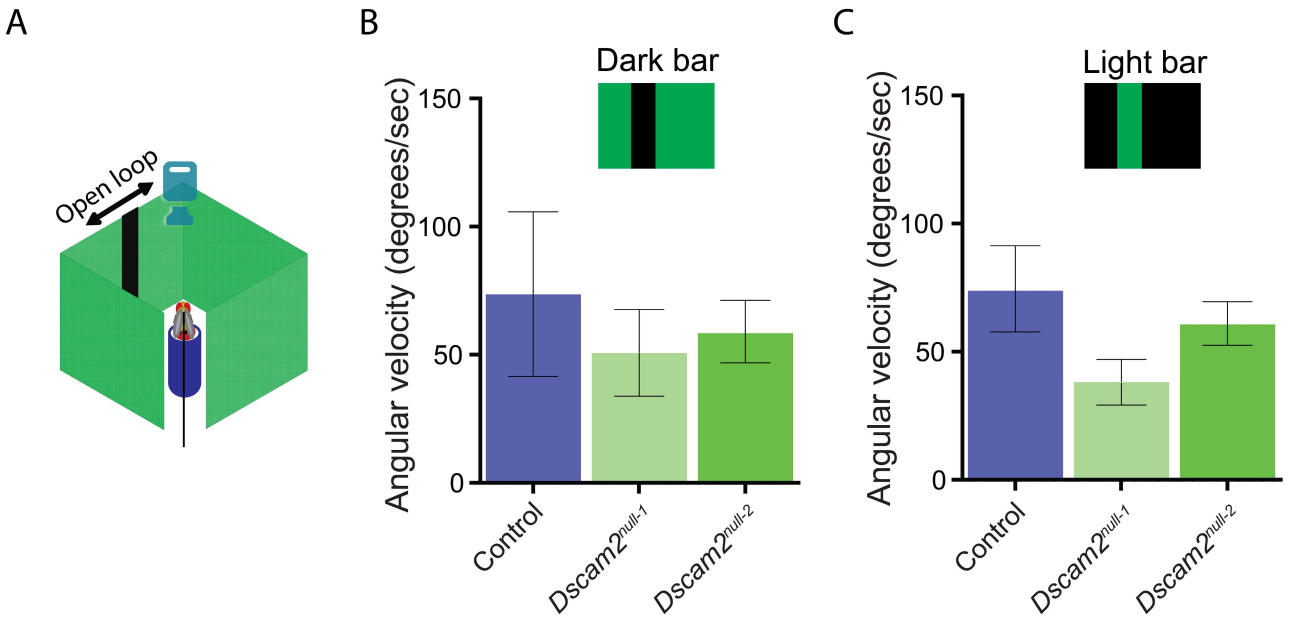

Figure 5.3. *Dscam2* mutant flies follow a single rotating bar similarly to control flies.
Open-loop single bar experiments. (A) Flies were presented with a bar in an open-loop condition and the angular velocity was recorded. (B) Control and *Dscam2* mutant flies demonstrate similar angular velocities and directional responses to a dark and (C) light bar. A Student's *t*-test was performed for normally distributed data and a Mann-Whitney test for non-normally distributed data. For all groups at least six flies were tested for every condition. Error bars indicate SEM.

5.2.2 *Dscam2* mutant flies correct automated bar perturbations

It is unclear whether the mutants perceive the dark bar similarly to a light bar considering they respond to both stimuli with anti-fixation. Another way of looking at the orientation preference data from section 5.3.1 is to focus on the computer initiated bar perturbations that occur randomly over the time period of the assay and the flies' response to them. In section 3.2.2 it was shown that wild-type flies respond to the perturbations with an attention-like behaviour where they return the bar back to its position prior to the perturbation. Similar to the experiment in section 3.2.2, the bar was perturbed 84 degrees either clockwise or counter-clockwise at random times resulting in four to 12 perturbations per experiment. The response before, during and after perturbations which took place in either the front 90 degrees of the arena (fixation) or the rear 90 degrees (anti-fixation) of the arena were averaged and presented as red and blue lines in figure 5.4. The shading of the same colour indicates the standard deviation of the points.

In the majority of cases, control flies returned the bar to the front or rear of the arena for fixation and anti-fixation respectively in response to perturbations (indicated by the horizontal dashed line, figure 3.3 and 5.4) within the three seconds post-perturbation. Interestingly, it was observed that clockwise perturbations were not always corrected and were biased to the right side of the arena (figure 3.3 and 5.4).

Noticeably, *Dscam2* mutant flies respond to dark bar perturbations within the three seconds post-perturbation (figure 5.4A/B) with a smaller standard deviation of the points compared to control flies. Interestingly, they respond to counter-clockwise perturbations of the light bar similar to control flies by correcting the bar to the rear of the fly. Similar to control flies, they also do not always correct clockwise perturbations (figure 5.3B). One of the mutants, $Dscam2^{null\text{-}2}$, corrected the clockwise perturbations of the light bar by moving it away from the anti-fixation cone in the direction of the perturbation (figure 5.4B).

These results demonstrate that $Dscam2^{null}$ flies respond to perturbations of a dark and light bar very similarly. Although, it looks like the mutants correct the light bar closer to the rear of the fly compared to the dark bar, it does not provide sufficient evidence whether the mutants perceive the dark and light bar similarly. Considering mutant flies are able to respond to the corrections it is questioned whether the flies actually prefer the bar behind them or whether they are just unable to fixate.

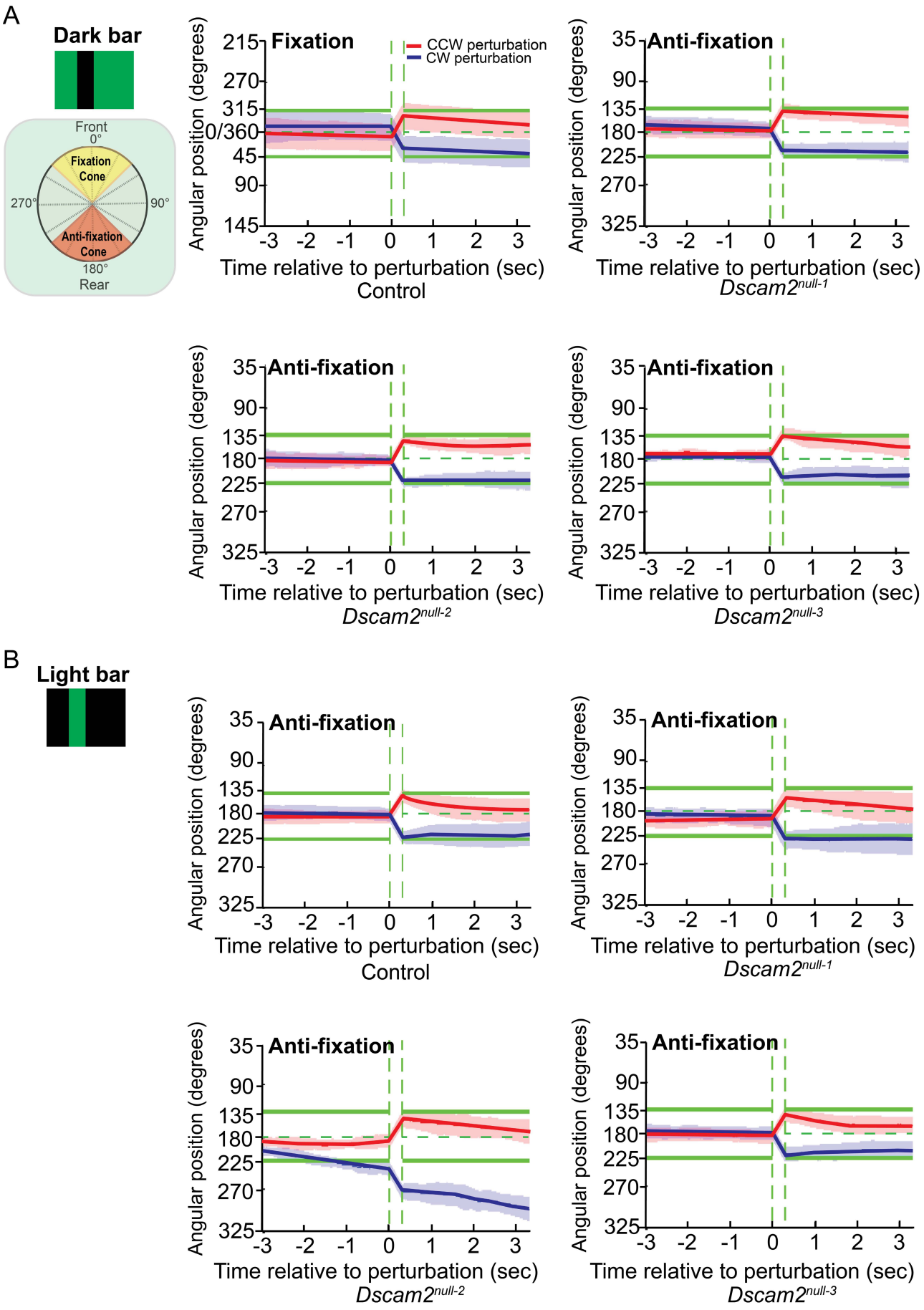

Figure 5.4. *Dscam2*^{null} flies correct perturbations only partially.
Figure legend on following page.

Figure 5.4. *Dscam2*^{null} flies correct perturbations only partially (continued).
From the data presented in section 5.3.1, the response before, during and after perturbations was isolated and divided into clockwise and counter-clockwise perturbations. The line represents the mean response with the same colour shading presenting the standard deviation from the points. The fixation cone subtends 90 degrees in the front and the anti-fixation cone subtended 90 degrees in the back of the arena (indicated by the green lines with the dashed green line indicating the direct front or rear of the fly for fixation and anti-fixation respectively). The open-loop displacement event is indicated by dashed vertical lines. Random perturbations took place anywhere in the arena but only events taking place in the fixation or anti-fixation cone were used in the calculations ($n \geq 49$). Data from control flies reprinted from figure 3.3. **(A)** Control flies correct clockwise and counter-clockwise perturbations of a dark bar in which they correct counter-clockwise perturbations closer to the direct front of the fly compared to the clockwise perturbations. Clockwise perturbations are not always corrected. *Dscam2*^{null} flies respond to a dark bar with anti-fixation and correct counter-clockwise and clockwise perturbations only partially. **(B)** Although the outcome for control flies is different for a light bar, i.e. anti-fixation, they correct clockwise and counter-clockwise perturbations of a light bar similar as they do with a dark bar. Interestingly, *Dscam2*^{null} flies respond to counter-clockwise perturbations from a light bar similar as control flies by moving the bar back toward the rear of the fly. They respond to clockwise perturbation similar to control flies by correcting the bar only in some cases, though one of the mutants, *Dscam2*$^{null\text{-}2}$, corrected the bar by moving it away from the anti-fixation cone in the direction of the perturbation. For all groups at least 14 flies were tested for every condition.

5.2.3 Object-orientation in *Dscam2* mutants depends on bar width

To further investigate how the mutants perceive dark and light bars, object-orientation preference to different bar widths was assessed. Orientation preference of control flies depends on the width of the bar as described in section 3.2.3. Different dark bar widths result in fixation responses while only one light bar condition results in anti-fixation behaviour. If mutant flies perceive a light and dark bar similarly, it is expected that they will respond similarly to changes in light and dark bar widths. The response of the mutants to a range of bar widths from 9.8 to 88.2 degrees (as used in figure 3.4) was tested while keeping other parameters constant.

First, the response to a dark bar of different widths was measured. It was found that the fixation response of control flies was lost when the bar width was reduced to 9.8 degrees but improved when the bar width was increased to 58.8 and 88.2 degrees (section 3.2.3, figure 3.4/5.5). *Dscam2* mutant flies lost their anti-fixation response when the bar width was reduced to 9.8 degrees resulting in uniform responses for $Dscam2^{null\text{-}1}$ and fixation behaviour for $Dscam2^{null\text{-}2}$ flies (Rayleigh test, p = 0.12; 327°, 0° = front, Rayleigh test, $p < 0.0001$ respectively; figure 5.5A). Anti-fixation responses in both *Dscam2* mutant strains were lost when the bar width was increased to 58.8 degrees (Rayleigh test, p = 0.06 and 0.24 for $Dscam2^{null\text{-}1}$ and $Dscam2^{null\text{-}2}$ respectively; figure 5.5C), although the response of $Dscam2^{null\text{-}1}$ was trending towards a fixation response. $Dscam2^{null\text{-}2}$ displayed fixation behaviour when the dark bar width was increased to 88.2 degrees (1.77°, 0° = front, Rayleigh test, p = 0.0026; figure 5.5D) while the other mutants displayed uniform behaviour (Rayleigh test, p = 0.28; figure 5.5D). This result is rather interesting because of the difference in response between the two mutants and because $Dscam2^{null\text{-}2}$ flies display fixation behaviour to two different bar widths.

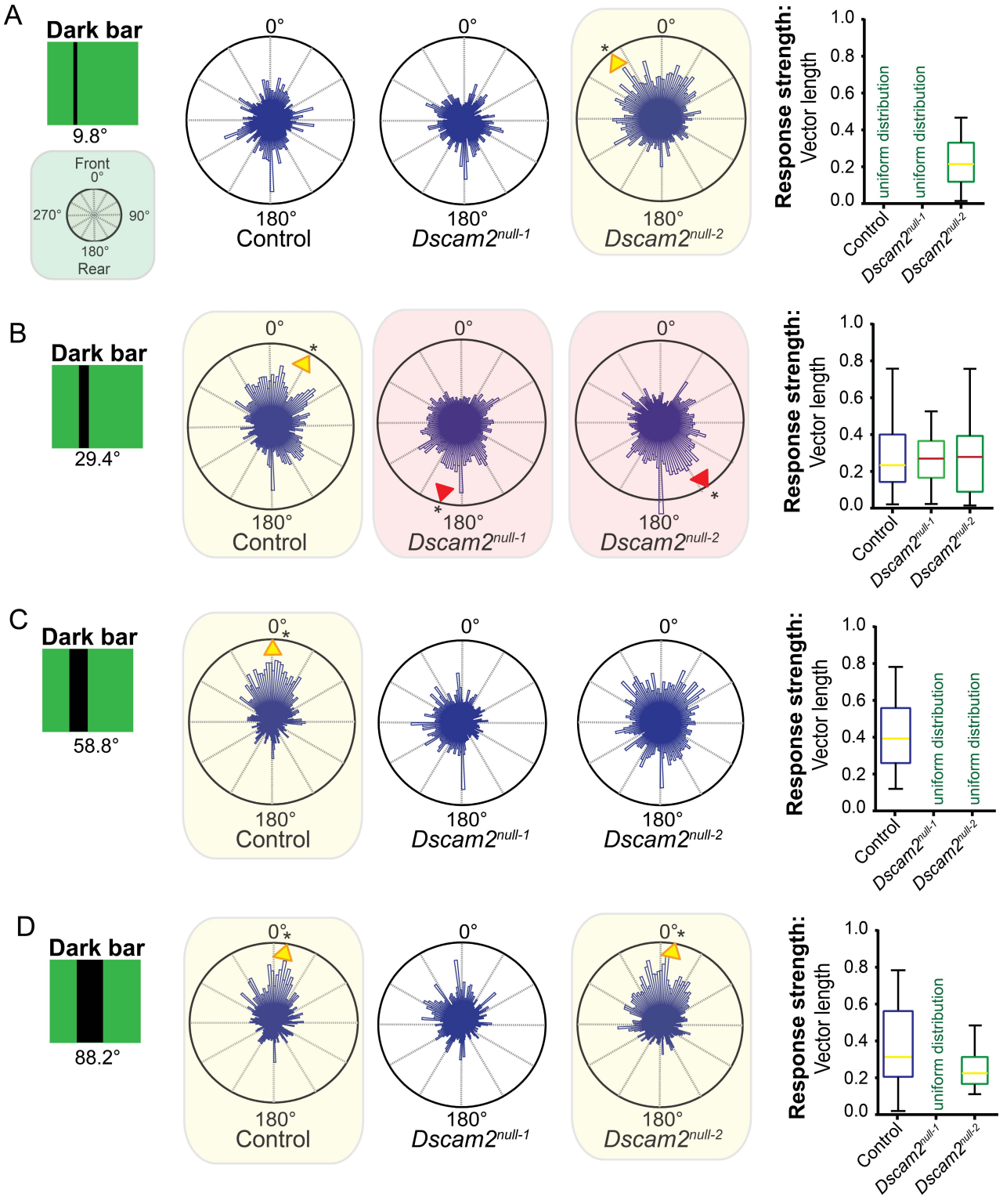

Figure 5.5. Object-orientation preference of control and *Dscam2* mutant flies depends on dark bar width.

Figure legend on following page.

Figure 5.5. Object-orientation preference of control and *Dscam2* mutant flies depends on dark bar width (continued).

Object-orientation preference assay with different dark bar widths. Flies were presented with a dark bar of varying widths in a closed-loop condition. Their preference for the bar position was recorded as in figure 5.2. The histograms within the 360° circular plots represent a weighted value for each bar position derived from all of the flies from each genotype. Rayleigh tests confirmed the distributions were non-uniform * $p < 0.05$. If distributions were non-uniform, then for each fly an average bar angle was calculated, as well as a group mean direction which is graphically represented in the radial histogram as a yellow arrowhead for a bar position towards the front of the arena or red arrowhead for a bar position towards the back. The variation in strength of the response is visualized in boxplots with min to max whiskers and with a median vector length. Data from control flies is reprinted from figure 3.4. **(A)** Control flies and *Dscam2*$^{null\text{-}1}$ flies respond uniformly and, *Dscam2*$^{null\text{-}2}$ flies fixate on a 9.8-degree wide dark bar. **(B)** Control flies fixate and *Dscam2* mutant flies anti-fixate on a 29.4-degree wide dark bar. **(C)** Control flies fixate and *Dscam2* mutant flies respond uniformly to a 58.8-degree wide dark bar. **(D)** Control flies fixate, *Dscam2*$^{null\text{-}1}$ flies respond uniformly and, *Dscam2*$^{null\text{-}2}$ flies fixate on an 88.2-degree wide dark bar. For all groups at least 20 flies were tested for every condition. Considering the three *Dscam2* mutant lines were responding similarly in section 5.3.1, this experiment was performed with only two *Dscam2* mutants, i.e. *Dscam2*$^{null\text{-}1}$ and *Dscam2*$^{null\text{-}2}$.

Next, the response to a light bar of different widths was tested. Control flies anti-fixate on a light bar of 29.4 degrees and display uniform behaviour at all other bar widths (section 3.3.3; figure 5.6A/C/D). *Dscam2* mutant flies display anti-fixation behaviour when presented with a 29.4-degree wide light bar on a dark background (figure 5.6B). Reducing the bar width to 9.8 degrees elicits uniform behaviour with $Dscam2^{null\text{-}1}$ flies and fixation behaviour with $Dscam2^{null\text{-}2}$ flies (Rayleigh test, p = 0.34, 239°, 0° = front, Rayleigh test, $p < 0.01$ respectively; figure 5.6A). This trend from anti-fixation to fixation behaviour was also observed with bar widths greater than 29.4 degrees for both mutants (figure 5.6C/D). Indeed, results indicate that anti-fixation behaviour only occurs at one specific light bar condition and that other conditions lead to fixation behaviour in the *Dscam2* mutants. This is different from the behaviour of control flies, which switch from anti-fixation to uniform behaviour (figure 5.6A-D).

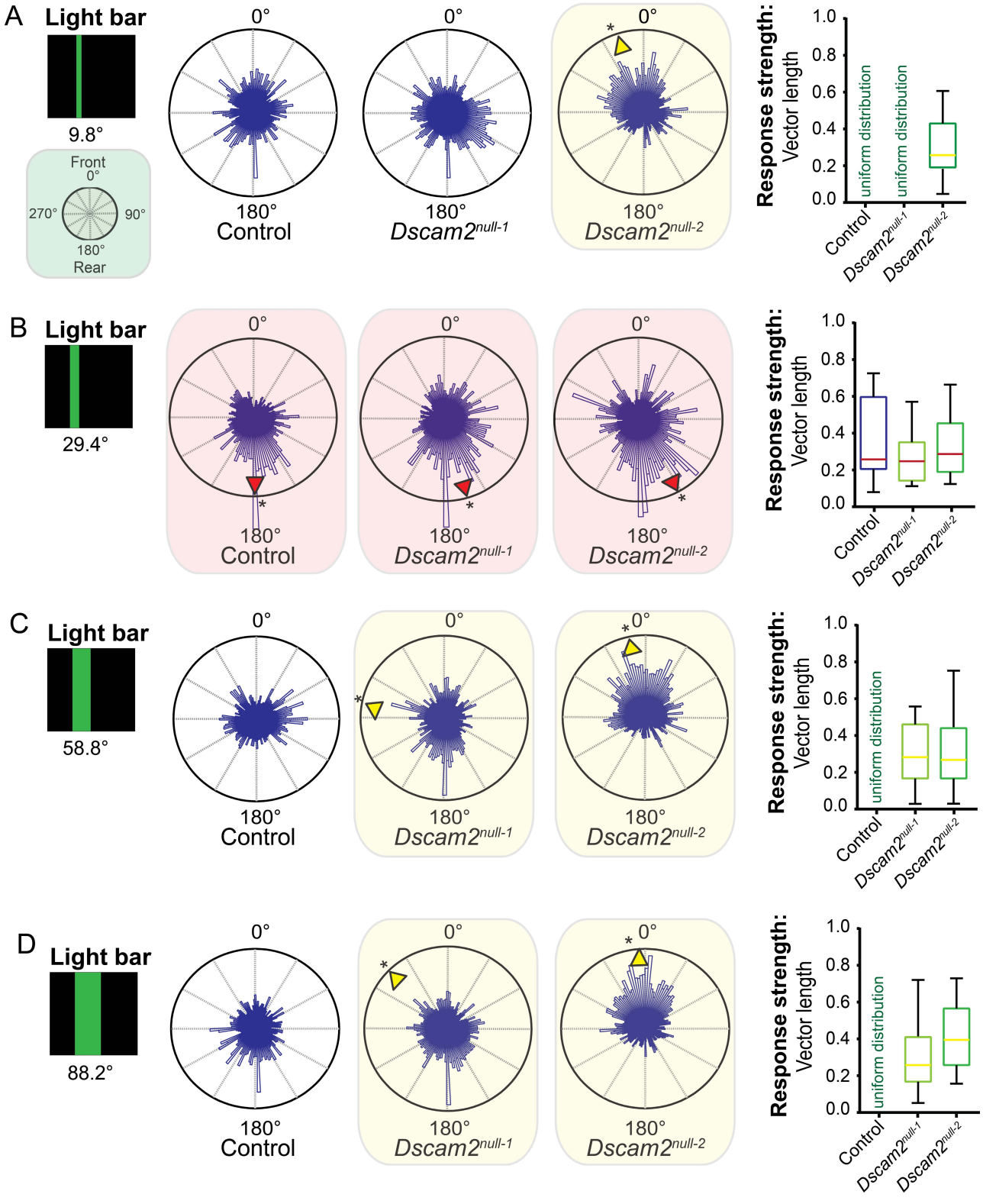

Figure 5.6. Object-orientation preference of control and *Dscam2* mutant flies depends on light bar width.

Figure legend on following page.

Figure 5.6. Object-orientation preference of control and *Dscam2* mutant flies depends on light bar width (continued).

Object-orientation preference assay with different dark bar widths. Flies were presented with a dark bar of varying widths in a closed-loop condition. Their preference for the bar position was recorded as in figure 5.2. The histograms within the 360° circular plots represent a weighted value for each bar position derived from all of the flies from each genotype. Rayleigh tests confirmed the distributions were non-uniform * $p < 0.05$. If distributions were non-uniform, then for each fly an average bar angle was calculated, as well as a group mean direction which is graphically represented in the radial histogram as a yellow arrowhead for a bar position towards the front of the arena or red arrowhead for a bar position towards the back. The variation in strength of the response is visualized in boxplots with min to max whiskers and with a median vector length. Data from control flies is reprinted from figure 3.4. **(A)** Control and *Dscam2*$^{null\text{-}1}$ flies respond uniformly while *Dscam2*$^{null\text{-}2}$ flies fixate on a 9.8-degree wide dark bar. **(B)** Control and *Dscam2* mutant flies anti-fixate on a 29.4-degree wide dark bar. **(C)** Control flies respond uniformly while *Dscam2* mutant flies fixate on a 58.8 and **(D)** 88.2 degree dark bar. For all groups at least 20 flies were tested for every condition. Considering the three *Dscam2* mutant lines were responding similarly in section 5.3.1, this experiment was performed with only two *Dscam2* mutants, i.e. *Dscam2*$^{null\text{-}1}$ and *Dscam2*$^{null\text{-}2}$.

5.3 Discussion

In this chapter, it is demonstrated that *Dscam2* mutants place a dark bar behind them, a response that is opposite to that of controls. In contrast, a light bar elicited an anti-fixation response similar to control flies. Interestingly, results suggest that they are unlikely to perceive the dark bar as a light bar and that mutant flies are able to fixate. Together, this demonstrates that *Dscam2* mutant flies have defects in visual behaviours that are unrelated to motion detection.

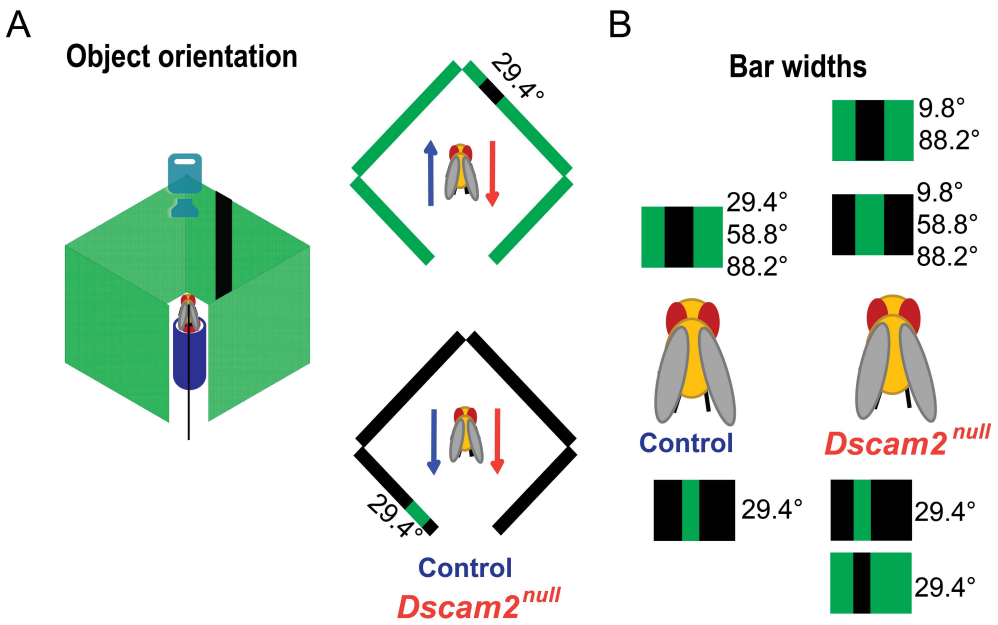

Figure 5.7. *Dscam2* mutants exhibit phenotypes for different visual behaviours.
Simplified schematic summarizing the average responses of *Dscam2*^{null} flies compared to control (wild-type) flies. Details on the assays can be found in section 5.2. **(A)**. Wild-type flies place a dark bar in the frontal area (fixation) and a light bar in the rear area of the arena (anti-fixation). *Dscam2*^{null} flies anti-fixate on both bar types. **(B)** *Dscam2*^{null} flies anti-fixate on a 29.4-degree wide light and dark bar but fixate on most other bar types.

5.3.1 *Dscam2* mutant flies anti-fixate on a dark bar

In contrast to control flies, *Dscam2* mutant flies respond with anti-fixation to a dark bar (figure 5.1/5.2/5.7A). The question arises whether the flies perceive the dark bar similarly as the light bar. *Dscam2* mutant flies did not display any differences to this bar when it was rotating in an open-loop assay, indicating that it is the visual context, not the bar *per se*, that is the source of the phenotype (figure 5.3). In general, the mutants respond very similar to control flies (figure 5.3). They correct light bar perturbations more to the centre of the back of the arena compared to dark bar perturbations. This makes it unclear if the mutant focus on the centre of the light bar and the edges of the dark bar

and questions if the mutants flies are able to fixate at all or if there response for the dark bar is slightly different from the light bar because they fail to fixate, something which will be addressed in next section.

5.3.2 The anti-fixation response to a dark bar is bar width dependent

Previous section did not provide information on whether flies perceive a dark and light bar similarly and if it is the edges of a dark bar is of interest to the flies. In addition, it also raises the question whether *Dscam2* mutant flies are able to fixate at all, something we will address by changing the bar width. Control flies fixate on dark bars greater than 9.8 degrees while *Dscam2* mutants did not respond to most bar widths except to a 29.4 degree wide dark to which they anti-fixate (figure 5.5/5.7B). Interestingly, control flies only responded to a light bar of 29.4 degree and did so with anti-fixation behaviour (figure 5.6). *Dscam2* mutants responded to different light bar widths with fixation, except for a 29.4-degree wide light bar to which they displayed anti-fixation behaviour (figure 5.6B/5.7B). These results suggest that they perceive a light a dark bar differently, at least at some bar widths. In addition, *Dscam2* mutants are able to fixate, indicating that their fixation pathway is still functional but there is something particular about the 29.4-degree wide bar that influences the flies' decision-making process. Lastly, when the mutants respond, they do so towards the centre of the object rather than its edges.

Chapter 6

Visual behaviour of other Dscam2 mutants

6.1 Chapter overview

Previous chapters demonstrated that the disrupted modularity of the *Dscam2*^{null} flies visual system lowers their visual acuity and inverts their behavioural response to specific motion and orientation stimuli. In this chapter, preliminary data is presented on the investigation whether other *Dscam2* related mutations alter behaviour in a similar way by assessment of motion detection and orientation behaviour in *Dscam2* single isoform and *Dscam2* trisomic flies.

6.2 Methods and results

6.2.1 Visual behaviour of *Dscam2* single isoform flies

Dscam2 has been shown to express two distinct isoforms, Dscam2A and Dscam2B, through alternative splicing (Lah *et al.*, 2014). They regulate repulsion between neurons in an isoform-specific homophilic manner, e.g. when two neurons express Dscam2A, they will bind, recognize and repel each other (Millard *et al.*, 2007). Dscam2A and Dscam2B are specifically expressed on L2 and L1 respectively allowing the close fasciculation of the two neurons without repelling each other (Lah *et al.*, 2014). For the *Dscam2* isoform study, two single isoform fly lines that express either Dscam2A or Dscam2B in all *Dscam2* positive cells were used (Lah *et al.*, 2014). These lines were generated by manipulating the endogenous *Dscam2* locus so that the amount of each isoform and the timing of expression were not perturbed. *Dscam2* single isoform flies have been found to cause a reduction in viability, similar to the *Dscam2*^{null} flies. Interestingly, expression of only one of the two *Dscam2* isoforms is sufficient for a proper organization of the visual system with no obvious changes in the morphological modularity (Lah *et al.*, 2014). However, a reduction in lamina cartridge size (Sarah Kerwin, personal communication) and L1 and L2 axon terminal size was found (Lah *et al.*, 2014). A more detailed analysis of the amount of photoreceptor synapses revealed an approximately 30% reduction in synapses as an expected consequence of the axon terminal size reduction (Sarah Kerwin,

personal communication). It is unclear whether this reduction in photoreceptor synapses has any behavioural consequences.

Dscam2 single isoform flies were brought into the w^+ background which was used in chapter 4 and 5. Unfortunately, Dscam2A homozygous flies were found to be non-viable in a w^+ background. They were viable in a w^{1118}/w^+ background but one copy of w^{1118} already results in optomotor phenotypes (data not shown) and demonstrates the importance of consistency in background. The Dscam2A isoform line was therefore not further used in this study. Dscam2B flies were homozygous viable in a w^+ background and were used in combination with the w^+ control which was used in chapter 4 and 5. Data for Dscam2B and w^+ control flies was collected at the same time and no significant difference was found between 'new' and 'old' collected data from w^+ control flies (data not shown) and therefore was combined for chapter 4, 5 and 6.

6.2.1.1 Phototactic behaviour of *Dscam2* single isoform flies

Phototactic behaviour of the *Dscam2* single isoform flies was assessed using a Y-maze phototaxis assay. This assay is comparable to the eight-level maze but has a lower resolution due to a theoretical limitation that is imposed by the binary-choice design. In this assay, a group of flies chooses either darkness or white light.

Fly husbandry and experimental setup

The day prior to the experiments, female flies (n = 12-18) between four and 12 days post eclosion were collected and anesthetized by CO_2. The collected flies were starved at room temperature for 19-22 hours in modified disposable polyethylene "jumbo" transfer pipettes (Thermo Fisher Scientific, Waltham, Massachusetts) containing 10 µl of water. All experiments were conducted between early and mid-afternoon to reduce variation between different groups. The Y-maze was constructed of two modified disposable polyethylene "jumbo" transfer pipettes (Thermo Fisher Scientific, Waltham, Massachusetts) connected to a polypropylene "Y" untampered connector (8 mm diameter, Kartell labware, Italy) (figure 6.1A). The light source was a white LED (RLS-5W-180-S, Rothner Lasertechnik, Vienna, Austria) and was tested in both the left or right arms to ensure that there was not a bias for one side. The fraction of responsive flies was the number of flies found in the arm with the light source divided by the total amount of flies.

Dscam2 single isoform flies respond to light

Over 90% of control flies chose the arm with the white light (figure 6.1B). $Dscam2^{null\text{-}l}$ flies showed a significantly reduced phototactic response compared to control flies, similar to what was observed

in the maze phototaxis assay (Student's t-test, $p < 0.05$; figure 6.1B). Dscam2B single isoform flies had a similar response to the controls. These results suggest that phototaxis is not perturbed in the single isoform line.

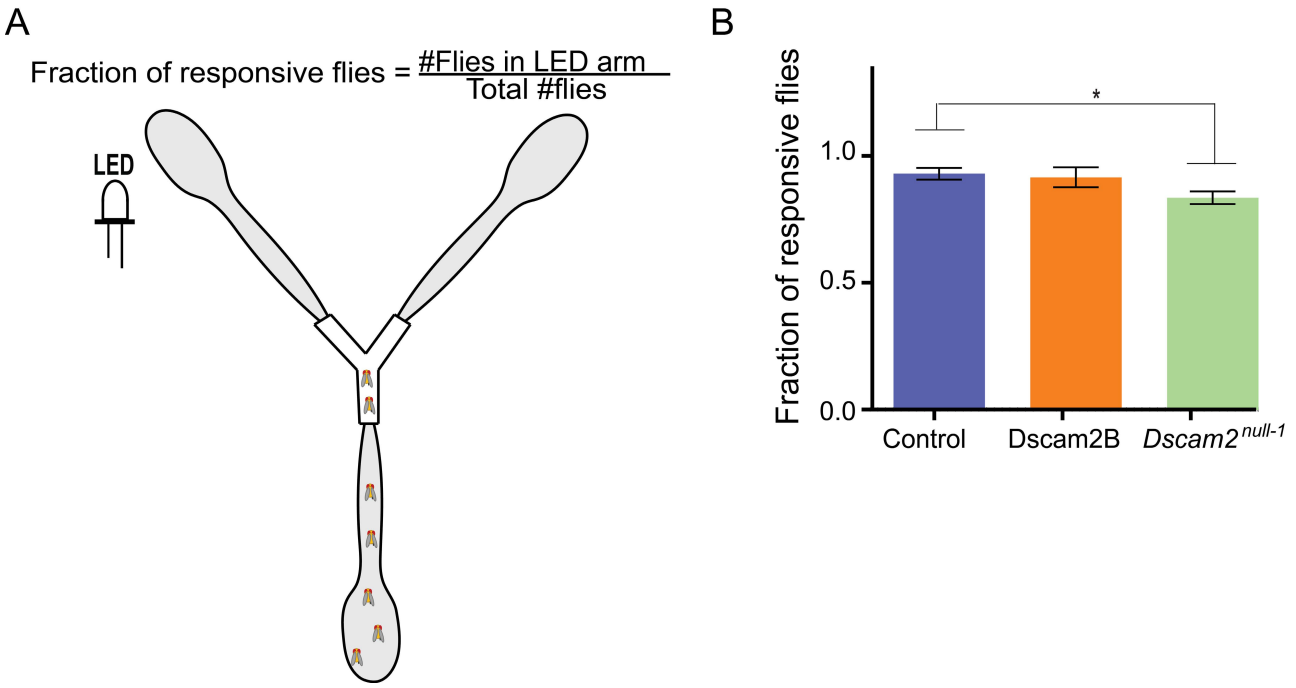

Figure 6.1. Dscam2B single isoform flies have a normal phototaxis response.
Phototaxis assay. **(A)** Flies (~15) enter the Y-maze and end up in one of the two end tubes. The fraction of responsive flies was calculated by dividing the amount of flies in the arm with the LED by the total amount of flies. **(B)** Phototaxis of control (blue), Dscam2B single isoform (orange), and *Dscam2*$^{null-1}$ flies (green) to white light. The response of *Dscam2*$^{null-1}$ flies is impaired compared to control. A student's *t*-test was performed for normal distributed data and a Mann-Whitney test for non-normal distributed data, * $p < 0.05$. For all groups at least seven Y-mazes of approximately 15 flies each were run for every condition. Error bars indicate SEM.

6.2.1.2 *Dscam2* single isoform flies have a change in acuity

To assess motion detection in the *Dscam2* single isoform flies, the tethered single fly assay described in chapter 2 was used. Single isoform data in this section is compared to *Dscam2*^{null} flies from section 4.3.3.1.

In a preliminary investigation, the visual system of Dscam2B single isoform flies was challenged by altering the spatial frequency, temporal frequency and luminance levels of the moving grating. In order to differentiate between the visual parameters more clearly, a description of the bar width in degrees (measured from the front of the fly; bar width from the rear arena to the fly is shorter, thus increasing the perceived bar width) and speed at which the bars were rotated in degrees/second is

given in Table 6.1. These stimuli included gratings that evoked normal responses, inverted responses and a complete lack of a response in control and/or *Dscam2*^{null} flies (section 4.3.3.1, figure 4.8).

Table 6.1. Visual stimuli used to access visual responses.
Overview of the used visual stimuli to access visual responses. All gratings consisted of black and green stripes with a contrast level of 1. The bar width is measured from the front of the fly.

Bar width (degree)	Velocity (degrees/sec)	Spatial frequency (cycles/degree)	Temporal frequency (Hz)	Luminance (Lux)
19.6	58.8	0.051	3	93.5
19.6	14.7	0.051	0.75	93.5
9.8	14.7	0.102	1.5	93.5
9.8	104.4	0.102	10.65	93.5
23.6	14.7	0.042	0.624	93.5
19.6	58.8	0.051	3	12.5
19.6	58.8	0.051	3	2.4

Dscam2B single isoform flies followed a grating with a bar width of 19.6 degrees and velocity of 58.8 degrees/second similar to control (figure 6.2A) and *Dscam2*^{null} flies (figure 4.8 and 6.2A). Control, Dscam2B single isoform, and *Dscam2*^{null} flies followed rightward and leftward motion with similar magnitudes, as expected.

Challenging the visual system further by lowering the velocity of this stimulus to 14.7 degrees/ second, which did not elicit a visual response in w^+ control (figure 6.2A) and *Dscam2*^{null} flies (section 4.3.3.1, figure 4.8), did elicit a response in Dscam2B single isoform lines (figure 6.2A). It is surprising that Dscam2B single isoform flies respond better than control flies, and suggests a change in visual system sensitivity of these flies. Dscam2B flies likely have a change in visual acuity considering Dscam2B flies respond to conditions to which control flies did not respond. Interestingly, the condition, i.e. a grating of 9.8 degrees wide bars at a speed of 14.7 degrees/second, where control flies respond normally to and *Dscam2*^{null} flies respond by going in the opposite direction elicited no response from Dscam2B single isoform flies.

To investigate alterations in light sensitivity in Dscam2B single isoform flies, they were exposed to a grating with a bar width of 19.6 degrees at a velocity of 58.8 degrees/second with different luminance levels. Their response to these conditions was not significantly different from control flies (figure 6.2B).

Together these results demonstrates that the visual system of Dscam2B isoform flies is less sensitive than control flies at specific conditions but more sensitive at others. This suggests a shift in visual system sensitivity in the *Dscam2* single isoform flies that is different from the *Dscam2*^{null} flies.

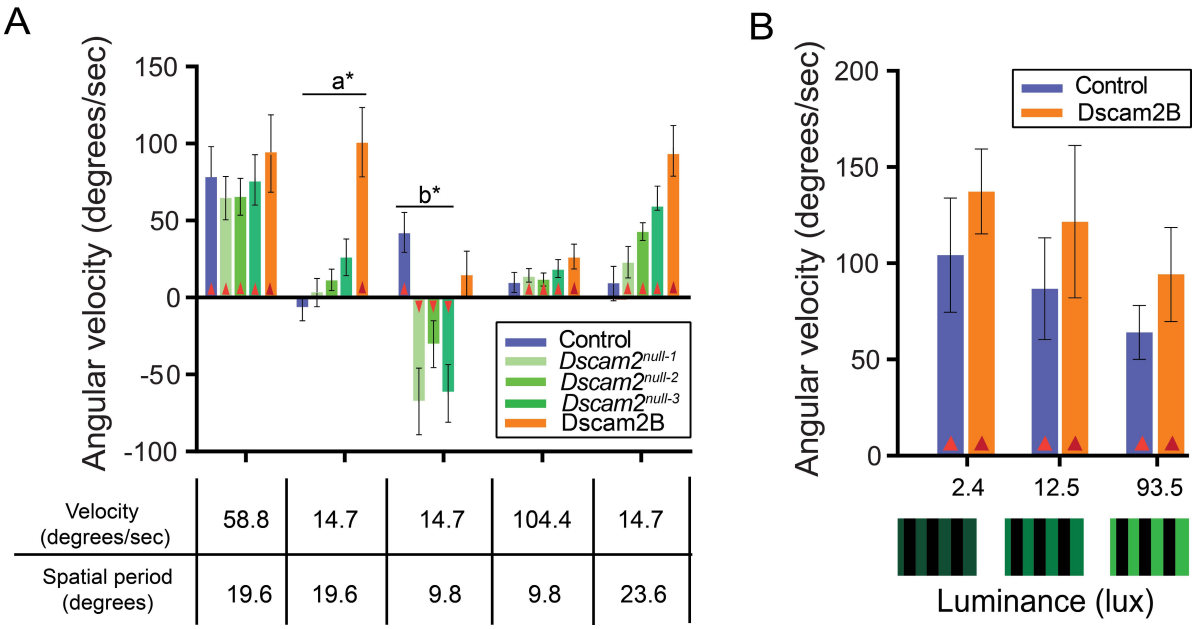

Figure 6.2. Dscam2B single isoform flies have conditional responses to motion in the single fly assay.

Visual response of Dscam2B single isoform flies to a range of visual parameters. **(A)** Visual responses of control (blue), *Dscam2*^{null} (different shades of green) and Dscam2B single isoform (orange) flies to gratings with different spatial and temporal frequencies. Data from *Dscam2*^{null} flies is reprinted from figure 4.8. **(B)** Visual response to different luminance levels at a constant grating spatial period of 19.6 degrees and velocity of 58.8 degrees/second. A Student's *t*-test was performed for normal distributed data and a Mann-Whitney test for non-normal distributed data. 'a*' indicates a significant difference between control/*Dscam2*^{null} *vs* Dscam2B single isoform flies ($p < 0.05$). 'b*' indicates a significant difference between control *vs Dscam2*^{null} ($p < 0.05$). Red triangles within bars indicate a significant difference from zero. For all groups at least seven flies were tested for every condition. Error bars indicate SEM.

6.2.1.3 *Dscam2* single isoform flies do not display object-orientation behaviour

It was demonstrated in chapter 5 that control flies fixate and *Dscam2*^{null} anti-fixate on a dark bar in the single fly virtual reality assay (figure 5.1A). Interestingly, Dscam2B single isoform flies show some preference for the bar towards the back of the arena (168°, 0° = front; figure 6.3A) with a rather high vector length of 0.43. However, a Rayleigh test *p*-value of 0.08 indicates that this response is diminished by variation in response between flies. This could potentially be improved by an increase in sample size.

The flies' response to a light bar on a dark background was also tested. This stimulus elicits anti-fixation behaviour from control and *Dscam2*^{null} flies (figure 5.1C). Dscam2B flies display some preference for the light bar towards the back of the arena (210°, 0° = front; figure 6.3C) with a rather strong vector length of 0.47 but a Rayleigh test *p*-value of 0.055 (figure 6.3D). Also here, an increase in sample size to compensate for the variation in responses between flies is required.

To conclude, although not statistically significant, it appears that Dscam2B single isoform flies behave similar to the *Dscam2*^{null} flies in terms of orientation preference.

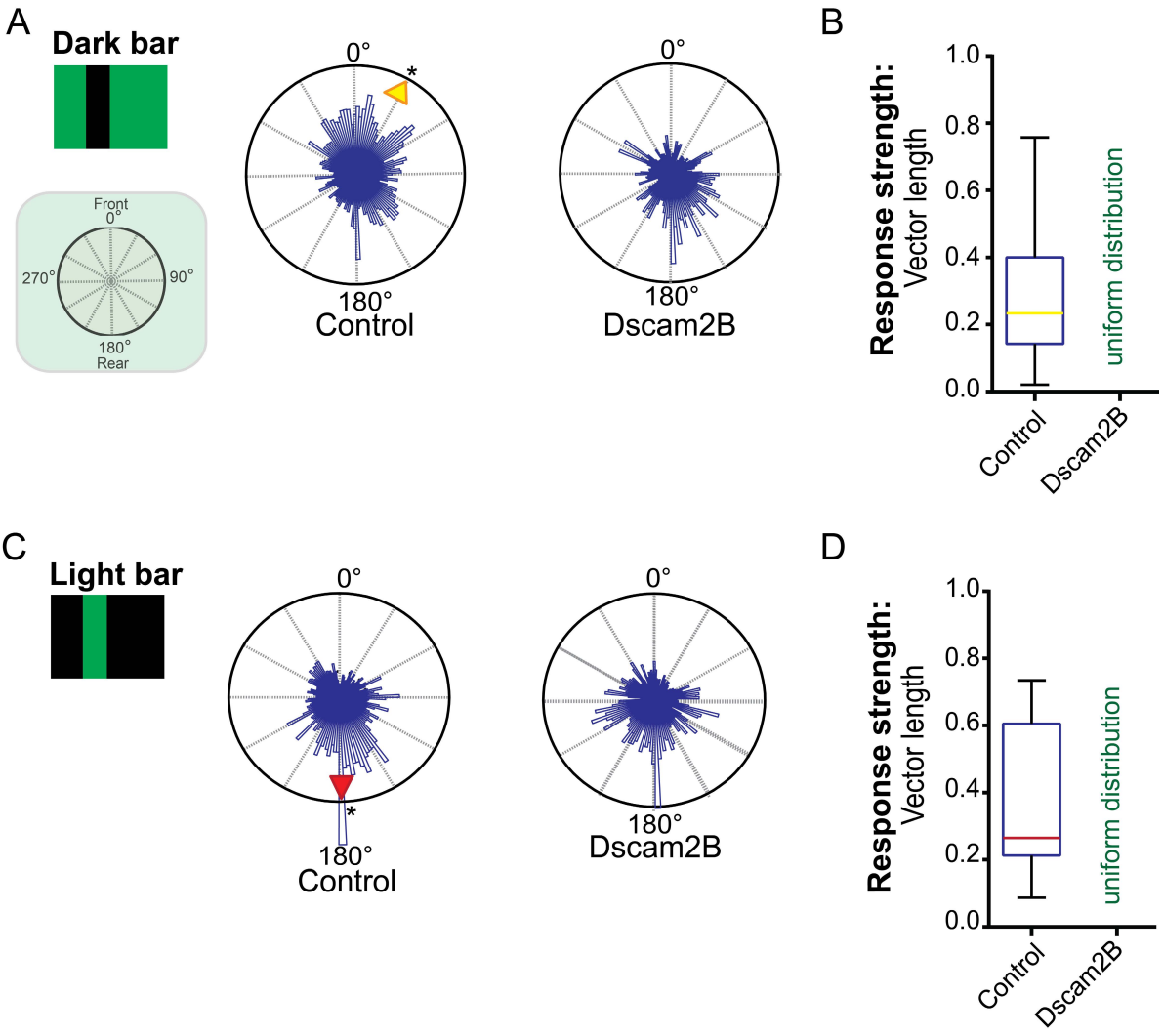

Figure 6.3. *Dscam2* single isoform flies have defects in object-orientation behaviour.
Object-orientation preference assay. Flies were presented with a bar in a closed-loop condition and their preference for the bar position was recorded. The histograms within the 360° circular plots represent a weighted value for each bar position derived from all flies of each genotype. For each fly an average bar angle was calculated, as well as a group mean direction which is graphically represented in the radial histogram as a yellow arrowhead for a bar position towards the front of the arena or red arrowhead for a bar position towards the back. A Rayleigh test confirmed the distributions were non-random * $p < 0.05$. Data of control flies reprinted from figure 5.1A/C. **(A)** Control flies show a fixation response but Dscam2B single isoform flies demonstrate a uniform response. **(B)** Control flies demonstrate variable response strengths (indicated by median vector length) and variation for the dark bar stimulus. The colour of the median line corresponds with the colour of the arrowhead (indicating direction) in A. **(C)** Control flies show an anti-fixation response but Dscam2B single isoform flies demonstrate a uniform response. **(D)** Control flies demonstrate variable response strengths (indicated with min to max whiskers in the boxplot) and variation for the light bar stimulus. As in B, the variation in strength of the response is visualized in boxplots with min to max whiskers. For all groups at least seven flies were tested for every condition.

6.3 Visual behaviour of *Dscam2* trisomic flies

As mentioned previously, *Dscam2* mediated homophilic repulsion is conserved across different species (Fuerst *et al.*, 2008, Millard *et al.*, 2007). However, studies in chick (Yamagata & Sanes, 2008) and Aplysia (Li *et al.*, 2009) demonstrate that *DSCAM* can act as an adhesive cue as well. This leads to speculation about possible adhesive roles of *Dscam2* in *Drosophila*. It is possible that *Dscam2* acts repulsively or adhesively depending on cellular context. Human *DSCAM* is found within a critical region of chromosome 21, a chromosome that is triplicated in Down syndrome. This raised the question: could three copies of *DSCAM* contribute to wiring defects in people with Down syndrome? A study by Blank *et al.* (2011) using a mouse Down syndrome model suggested mouse *DSCAM* is highly dosage sensitive. In section 4.3.2.2, it was observed that *Dscam2* is haploinsufficient to some degree as *Dscam2* heterozygotes exhibited an optomotor phenotype under specific visual conditions. One possibility is that there is a threshold for Dscam2 repulsion that is dependent on the amount of protein expressed on the cell surface. Dscam proteins are known to oligomerise and repulsion may be dictated by the ability of these oligomers to recruit the repulsive machinery. Increasing the amount of Dscam2 in the cell could therefore convert adhesive interactions into repulsive interactions by overcoming this repulsive threshold and effectively reduce the number of connections in the brain. To investigate how three copies of *Dscam2* modulate visual behaviour, flies containing a bacterial artificial chromosome (BAC) containing the *Dscam2* gene were generated in the lab. This BAC *Dscam2* line rescues morphological phenotypes observed in flies in *Dscam2* mutant flies (Joshua Li, personal communication). A control line was also generated that contained a BAC with a mutated version of *Dscam2* and this line does not rescue *Dscam2* phenotypes. Both lines were crossed into a w^+ background for behavioural experiments.

In this section, the same experiments were performed as in 6.2, but with *Dscam2* trisomic flies to investigate how three copies of *Dscam2* modulate visual behaviour.

6.3.1 *Dscam2* trisomic flies respond to light

The startle induced Y-maze phototaxis assay described in section 6.2.1 was used to assess phototactic behaviour to white light in *Dscam2* trisomic animals. Here, both BAC control and *Dscam2* trisomic flies responded strongly to the white light, resulting in over 90% of flies choosing light over dark (figure 6.4).

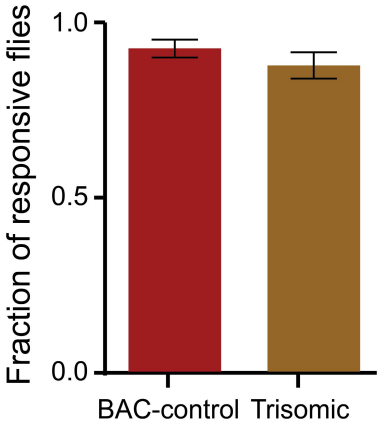

Figure 6.4. *Dscam2* trisomic flies have a normal phototaxis response.
Phototactic response of BAC control and trisomic flies. Trisomic flies respond similarly to BAC control flies. A Student's *t*-test was performed for normal distributed data and a Mann-Whitney test for non-normal distributed data. For all groups at least seven Y-mazes of approximately 10 flies each were run for every condition. Error bars indicate SEM.

6.3.2 *Dscam2* trisomy does not alter optomotor behaviour

As in section 6.2.1.2, a tethered single fly assay was used to gather preliminary data on the visual system sensitivity of trisomic flies using the same selection of visual stimuli as was used in section 6.2.1.2 (table 6.1).

Dscam2 trisomic and its control flies respond similarly to a grating with bar width of 19.6 degrees and velocity of 58.8 degrees/second (figure 6.5), demonstrating that *Dscam2* trisomic flies are able to track motion.

Challenging the visual system further by lowering the velocity of this stimulus to 14.7 degrees/second elicits a visual response of 28.14 ± 10.26 degrees/ second in control flies (figure 6.5). The response of trisomic flies at this condition is high, 90.54 ± 41.95 degrees/ second but not significantly different from zero (figure 6.5). This high variability is likely caused by the variation in responses between flies and could suggest that the visual system is affected at varying severities in this population. *Dscam2* trisomic and its control flies responded similarly at all other conditions (figure 6.5).

These data make a strong argument that the *Dscam2* trisomy itself does not affect motion detection.

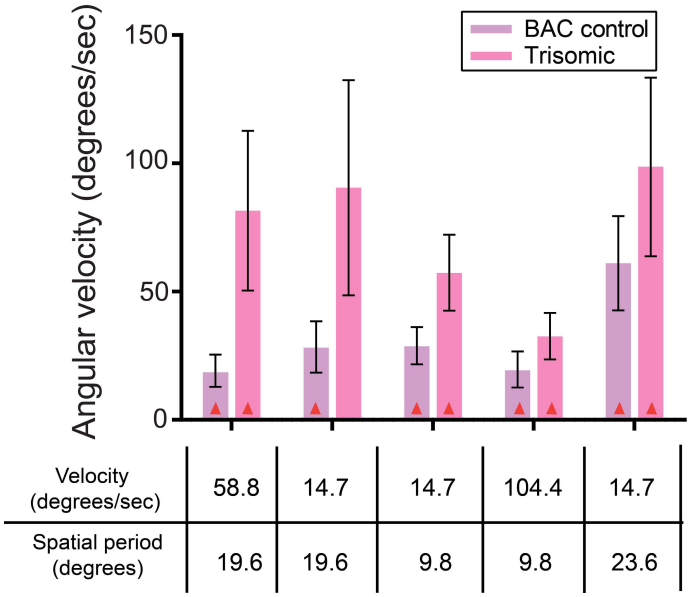

Figure 6.5. *Dscam2* trisomic flies respond to motion in the tethered single fly assay.
Visual responses of BAC control (purple) and trisomic (rose) flies to gratings with different spatial and temporal frequencies. A Student's *t*-test was performed for normal distributed data and a Mann-Whitney test for non-normal distributed data. Red triangles within bars indicate a significant difference from zero. For all groups at least seven flies were tested for every condition. Error bars indicate SEM.

6.3.3 *Dscam2* trisomic flies display only fixation behaviour

Similar to section 6.2.1.3, a tethered single fly virtual reality assay was used to gather preliminary data on orientation preferences for *Dscam2* trisomic and control flies.

BAC control flies fixate on a dark bar by placing the bar towards the front of the arena (41°, 0° = front, Rayleigh test $p < 0.05$; figure 6.6A). Trisomic flies exhibit a similar response (10°, 0° = front, Rayleigh test $p < 0.001$; figure 6.6A).

Interestingly, BAC control flies show uniform behaviour when presented with a light bar (figure 6.6B), but trisomic flies show fixation (28°, 0° = front, Rayleigh test $p < 0.05$; figure 6.6B). This is interesting considering it was previously demonstrated in section 3.3.2 that a 29.4-degree wide light bar causes anti-fixation in w^+ control flies and non-fixation at other bar widths (figure 6.6B). *Dscam2*^{null} flies anti-fixate to a 29.4-degree wide light bar but fixate to other bar widths, potentially caused by the change in visual system modularity. This result could suggest that *Dscam2* trisomic flies have visual system changes causing them to perceive the 29.4 degrees wide bar differently. These changes would be different from those in the *Dscam2*^{null} flies given that the behaviours are distinct.

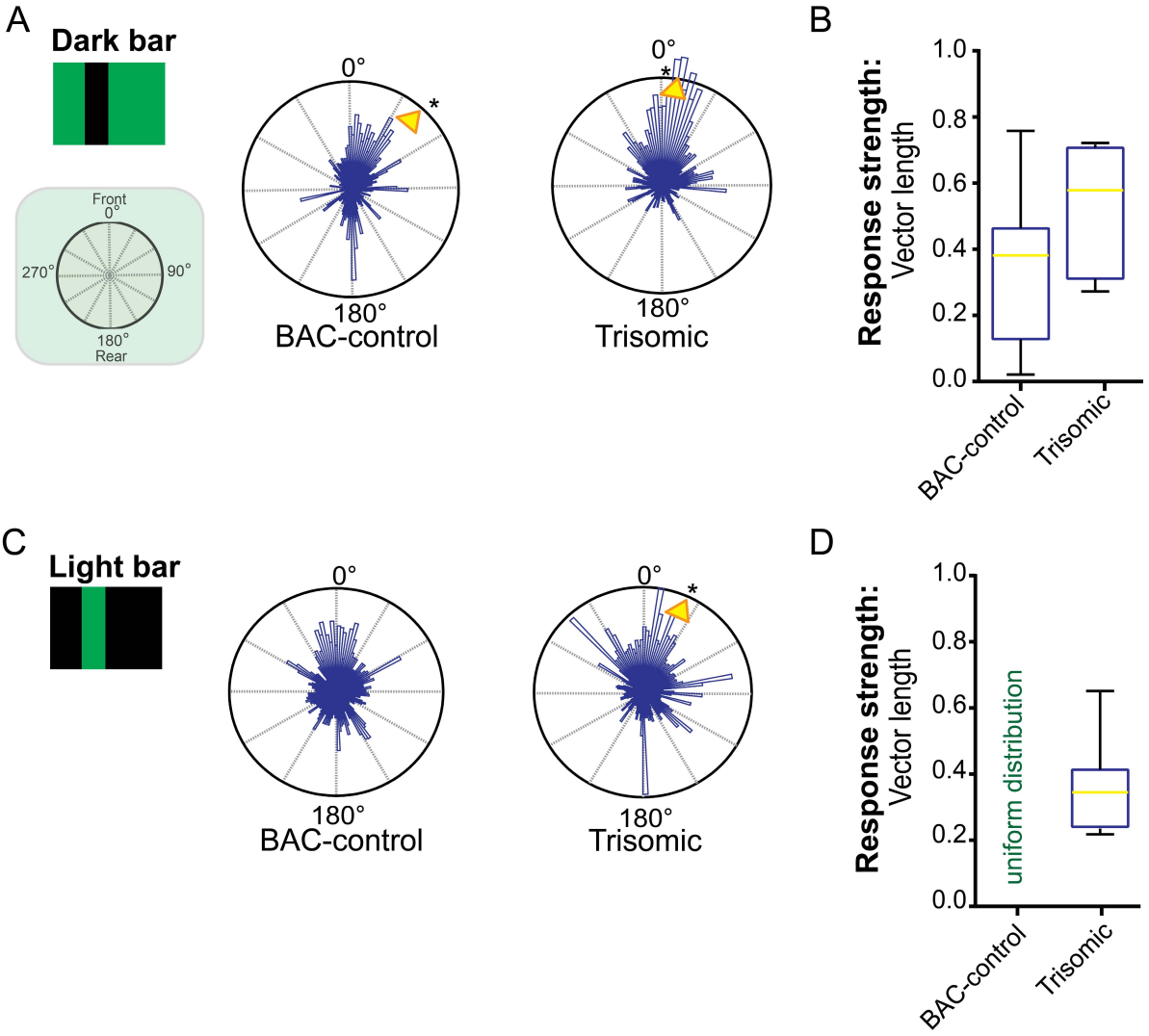

Figure 6.6. *Dscam2* trisomic flies fixate on dark and light bars.
Object-orientation preference assay. Flies were presented with a bar in a closed-loop condition and their preference for the bar position was recorded. The histograms within the 360° circular plots represent a weighted value for each bar position derived from all flies of each genotype. For each fly an average bar angle was calculated, as well as a group mean direction which is graphically represented in the radial histogram as a yellow arrowhead for a bar position. A Rayleigh test confirmed the distributions were non-uniform * $p < 0.05$ **(A)** BAC control flies and trisomic flies fixate on a dark bar. **(B)** BAC control and trisomic flies demonstrate variable response strengths (indicated with min to max whiskers in the boxplot) and variation for the dark bar stimulus. **(C)** BAC control flies demonstrate a uniform response to a light bar. Trisomic flies show a fixation response. **(D)** Trisomic flies demonstrate variation in response strengths (indicated by the min and max whiskers) and variation for the light bar stimulus. As in B, the variation in strength of the response is visualized in boxplots with min to max whiskers. For all groups at least seven flies were run for every condition. A Kruskal-Wallis test indicated no significantly difference between the vector lengths of the different fly strains.

6.4 Discussion

Chapter 4 and 5 describe how the lack of *Dscam2* results in changes in visual perception to specific motion and orientation stimuli. In this chapter, preliminary data is presented on the assessment of motion detection and orientation behaviour in *Dscam2* single isoform and *Dscam2* trisomic flies. Both *Dscam2* related manipulations lead to perturbed behavioural responses (figure 6.7).

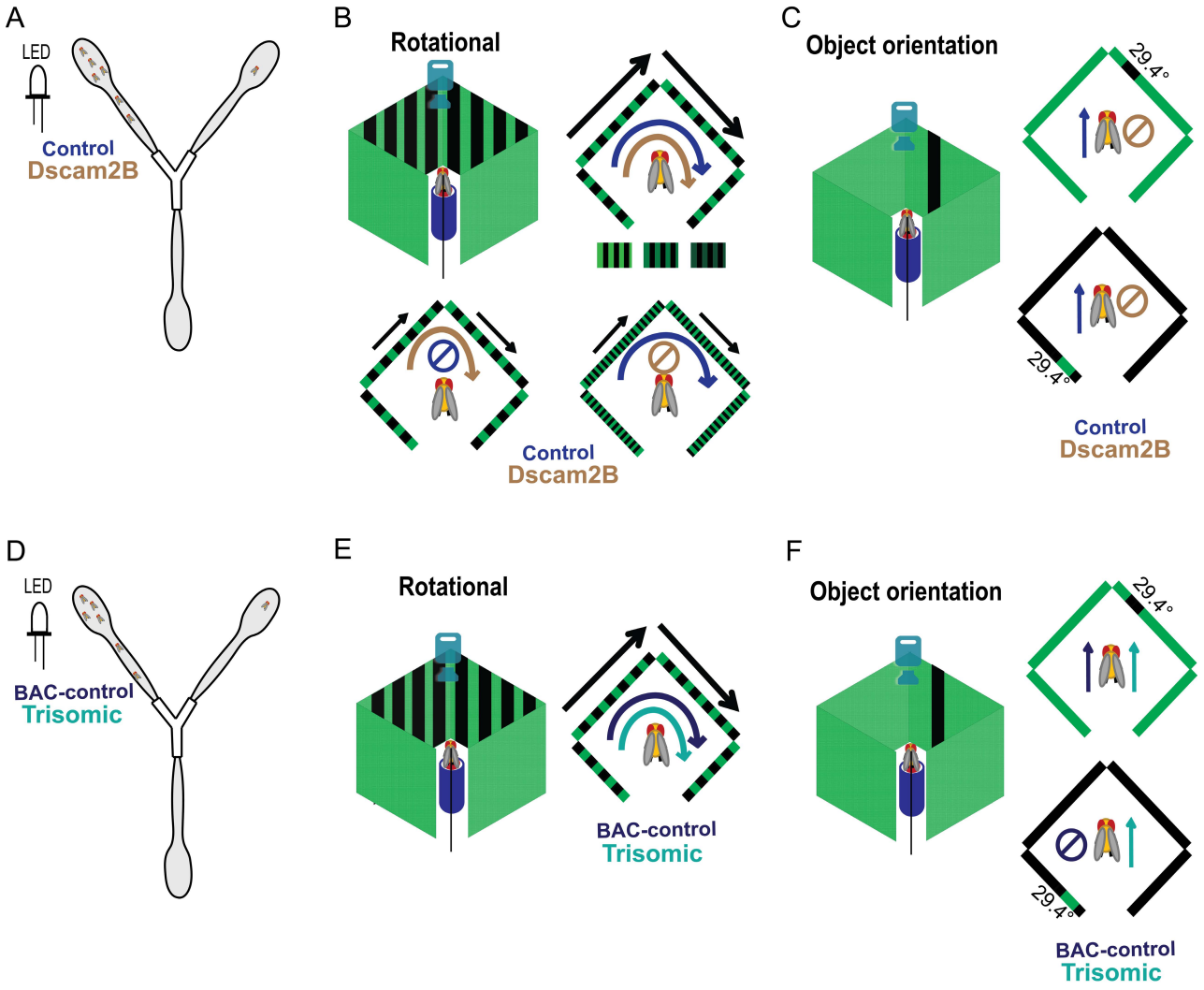

Figure 6.7. *Dscam2*-related manipulations lead to perturbed behavioural responses. Simplified schematic summarizing the average responses of Dscam2B single isoform and *Dscam2* trisomic flies compared to their control (wild-type and BAC-control respectively) flies. Details on the assays can be found in section 6.2 and 6.3. **(A)** Dscam2B single isoform flies are able to detect light. **(B)** Dscam2B single isoform flies are able to detect gratings with different luminance levels. Specific motion parameters such as slowly moving bars in a tethered single fly assay elicit no response from control but a robust optomotor response from Dscam2B flies. Slow moving narrow bars did not elicit a response from the single isoform line but did from control flies. **(C)** Control flies fixate on a dark bar and anti-fixate on a light bar. Dscam2B single isoform flies responded uniformly to both stimuli. **(D)** Trisomic flies are able to detect light. **(E)** Trisomic flies are able to detect gratings with different spatial and temporal frequencies. **(F)** BAC-control flies fixate on a dark bar and respond uniformly to a light bar. Trisomic flies fixate on both bar types.

6.4.1 *Dscam2* single isoform flies demonstrate a change in motion detection sensitivity

The change in visual perception in *Dscam2*^{null} flies is likely caused by a change in their visual system modularity. Here, a preliminary exploration was initiated to determine whether isoform specificity is necessary for visual perception. Expressing a single *Dscam2* isoform in all *Dscam2* positive cells was shown to change the size of L1 and L2 axon terminals (Lah *et al.*, 2014) and the size of cartridges and the number of photoreceptor synapses in the lamina (Sarah Kerwin, personal communication).

Motion detection in Dscam2B single isoform flies was assessed with a selection of visual stimuli that challenge the visual system (figure 6.2/6.7B). These stimuli included alterations of spatial frequency, temporal frequency and luminance, which have been demonstrated previously useful to uncover motion detection phenotypes (see section 4.3.3.2). Dscam2B single isoform flies did not demonstrate the same motion detection phenotypes as the *Dscam2*^{null} flies for all visual parameters. For example, the visual parameter which causes the *Dscam2*^{null} flies to move against the direction of the motion results in no visual response in the Dscam2B single isoform flies. These results suggest that the Dscam2B single isoform flies have wiring defects but of a different type than the *Dscam2*^{null} flies. This is consistent with the manipulation of Dscam2 in these flies. Rather than lacking Dscam2, Dscam2B flies express the same isoform in all Dscam2 positive cells. This is expected to generate inappropriate interactions between neurons that normally express different isoforms. This could result in gain of function phenotypes, as observed here, or loss of function phenotypes (depending on the isoform requirement in each circuit). Thus, the differences between the null and the single isoform behavioural phenotypes are consistent with current models of how Dscam2 functions.

Orientation behaviour of Dscam2B single isoform flies was affected as well (figure 6.3/6.7C), but in this case the Dscam2B flies exhibited responses that were similar to the null mutants. Preliminary data of Dscam2B flies suggests a trend in orientation preference towards anti-fixation to both a light and a dark bar (figure 6.3/6.7C). If an increase in sample size resulted in a significant Rayleigh test, then it would be a response very similar to the *Dscam2*^{null} flies. This would suggest that the lack of Dscam2 and the expression of a single isoform create similar problems within the fixation circuitry, and may indicate that this circuitry requires Dscam2B specific functions that cannot be compensated for by Dscam2A.

6.4.2 *Dscam2* trisomy leads to visual defects

Although masking of motion detection phenotypes in the trisomic flies due to the effect of the BAC insertion cannot be excluded, preliminary results indicate that *Dscam2* trisomy itself does not have any effects on motion detection (figure 6.5/6.7E). However, *Dscam2* trisomy affects visual perception in orientation behaviour as trisomic flies fixate to a light bar, while control flies respond uniformly (figure 6.6/6.7F). In addition, the finding that *Dscam2* trisomic flies fixate to a light bar suggests that they have visual system changes that cause them to perceive the 29.4-degree wide bar differently. These results together with the specific optomotor phenotypes of *Dscam2* heterozygous flies (section 4.3.2.2) suggest that any alteration in *Dscam2* dosage affects visual behaviour and therefore wiring of the visual system. This provides a platform to study the effects of gene dosage on neurodevelopment and behaviour. It has the potential to gain a better understanding how gene dosage imbalance such as in the aetiology of Down syndrome (Antonarakis *et al.*, 2004) can lead to alterations in neurodevelopment and results in behavioural defects.

Chapter 7

General Discussion

The brain utilizes an organized network of billions of neurons, which relay sensory information into actions. The accuracy of the wiring process is fundamental for brain function, and abnormal connectivity is suggested to be the underlying cause of numerous developmental disorders including Down syndrome, autism and fragile X syndrome (Becker *et al.*, 1991, Lightbody & Reiss, 2009, Mitchell, 2011), though exact relationships are still unclear. Understanding how miswiring during brain development leads to unique behaviours will allow for a better understanding of neurodevelopmental disorders. In this thesis, how changes in neural circuitry affect visual system behaviours is explored using assays that measure the optomotor response, object-orientation preference, and attention-like mechanisms in control and *Dscam2* mutant flies. Flies lacking *Dscam2* have a disorganized visual system, lack boundaries between neighbouring modules in the optic lobe and exhibit changes in the postsynaptic composition of photoreceptor synapses (Lah *et al.*, 2014, Millard *et al.*, 2007, Millard *et al.*, 2010). In this thesis, behavioural consequences of these wiring defects have been studied to gain a better understanding how miswiring during brain development leads to unique visual behaviours.

7.1 Behavioural readout of motion detection

The optomotor response is involved in course stabilization (Mccann & Macginitie, 1965) and can be studied by using rotating gratings of light and dark bars. Most animals respond very strongly to this stimulus likely because visual systems are particularly sensitive to vertical and horizontal orientations (Coppola *et al.*, 1998a); at least in humans (Proverbio *et al.*, 2002) and ferrets (Coppola *et al.*, 1998b). Similarly, flies are sensitive to rotating gratings (Mccann & Macginitie, 1965) and therefore provide a tool to study motion detection in *Drosophila*. Classically, optomotor assays consisted of striped paper or plastic drums but over time, these have been replaced by digital displays such as CRT monitors and LED panels. These technological advances have resulted in the generation of more diverse visual stimulus characteristics and further questions in relation to motion detection. That perception of visual stimuli is context dependent is illustrated in the assays presented in this thesis. It is demonstrated how a population and single fly visual response assay can be used to study motion detection in two different visual contexts in wild-type flies (chapter 2). Both assays explore a different

range of spatial frequencies so they can be used as complementary tools for an in-depth assessment of the acuity of the visual system. In the single tethered-fly assay, the response to gratings with narrow bars can be investigated while the population assay is well suited for assessment of the response to gratings with wide bars. Interestingly, the response in the population assay is more complex as some bar widths elicit a response from wild-type flies in the single fly assay but not in the population assay. These bar widths are larger than the flies' detection limit, suggesting that the grating in the population assay is perceived differently compared to the single fly assay. The reason for this difference can either be contributed to that flies are starved in the population assay or the visual context of the assay. Longden *et al.* (2014) observed in a tethered walking blowfly setup that a 3-day food deprivation period reduces the optomotor response to gratings with a temporal frequency of 1 Hz and higher. However, in the population visual response assay, flies are starved because previous studies showed that this increased responsiveness to visual stimuli. So although starvation affects *Drosophila* visual behaviour, it is unlikely to be the explanation for the observed differences between the two assays. Another explanation could be that the response in the population assay has a more complex visual context compared to the single fly assay. This perception of the visual stimulus depends on the flies' orientation and attention. Each fly's decision to turn left or right might be influenced by other flies, as well as reflections in the population assay. The behavioural readout in the population assay is a distribution along the exit points, which for wild-type flies is in the direction of the moving stimulus. Interestingly, an attention mutant *Dunce* has been shown to respond better than wild-type in this assay, where more of the mutant flies reach the exit point closest to the direction of the moving stimulus (Evans *et al.*, 2011). This demonstrates that flies in the population assay are exposed to attention-like processes that influence their visual response. This causes the wild-type flies to respond with a lower visual response than the *Dunce* mutant flies. It has not yet been determined whether the fly makes a decision between following the motion and not following the motion or whether it is responding to competition between the two visual stimuli, e.g. the one presented on the LED panels or its reflection. Control of visual context is a limitation in this assay and therefore a single fly assay has been setup.

In the single fly assay, one fly can be exposed to different visual stimuli. Due to the fly being unable to change its position in relation to the visual stimulus, the fly is exposed to these stimuli in a more controlled visual context. Interestingly, wild-type flies followed the direction of the motion at spatial frequencies, which did not elicit a visual response in the population assay. In conclusion, although the population assay is well suited for screening large quantities of flies for motion detection problems, it is possibly limited in its ability to identify flies with severe acuity problems as the minimum spatial period eliciting a response is far beyond the flies detection limit. This suggests that

the tethered single fly assay complements the population assay for an in-depth assessment of visual system acuity of flies to identify different severities of acuity impairments.

7.2 Behavioural readout of object orientation

The finding that flies detect and fixate on a dark bar in a tethered flying paradigm (Reichardt & Wenking, 1969) provided the foundation for theoretical models of this orientation process (Poggio & Reichardt, 1973, Poggio & Reichardt, 1976, Reichardt & Poggio, 1976). Wild-type flies were found to exhibit fixation behaviour to a dark bar and anti-fixation to a light bar in the single tethered-fly virtual reality assay, presented in this thesis. The observation that flies anti-fixate to a 29.4 degree wide light bar is interesting as it has not been observed by all groups, possibly due to a number of assay- or visual stimulus-related differences. Some groups report fixation behaviour to this stimulus (Maimon *et al.*, 2008, Reiser & Dickinson, 2008), whereas other report anti-fixation (Heisenberg & Wolf, 1979, Maimon *et al.*, 2008). Thus, this assay is well suited to study the differences between these two behavioural responses and the underlying neuronal requirements.

To have a closer look at what it is in these stimuli that evoke these responses, the correction responses to bar perturbation itself were analysed. It was found that for fixation and anti-fixation left perturbations were corrected more to the middle of the arena while right perturbations were not always corrected. This made it unclear whether flies fixate and anti-fixate to the object itself or to its edges. Literature provided evidence that flies fixate on the edges of the bars when the bars are 180 degrees in width but fixate on the centre when bars are smaller (Wehner, 1972, Zhou *et al.*, 2012) in Buridan's paradigm. This behaviour is similar to that is found in other insects such as the mealworm beetle (*Tenebrio molitor*) (Varjú, 1976) and the blowfly (Osorio *et al.*, 1990) when tested in a free- and tethered-walking paradigm. In Drosophila, edge fixation has been found to be bar height dependent, where bars shorter than 40 degrees elicit fixation to the centre of the bar (Wehner, 1972). The bars tested in this thesis were narrower than 180 degrees and approximately 60 degrees long and therefore it was expected that flies would fixate and anti-fixate to the centre of the bar in the assay presented in this thesis. When bar widths were increased, it was found that wild-type flies displayed fixation and anti-fixation orientated towards the centre of the bar rather than to the bars edges, suggesting that it is the object itself that is inducing the fixation and anti-fixation behaviour. In addition, anti-fixation was only observed at one specific light bar condition.

The data presented here raised the question of why a light bar causes flies to anti-fixate. The complexity arises from the observation that it is not only whether the bar is dark or light that dictates the response, but also the width of the bar. The preference for dark regions, scototaxis, has been observed in other studies and organisms (Varjú, 1976). Similarly, the preference for light regions has been observed in a startle-induced phototaxis assay (Benzer, 1967) and this behaviour is classically seen as a reflex mechanism as part of the escape response. After startling, the fly becomes excited, has an increased photopositive and geo-negative response (Dobzhansky & Spassky, 1969, Markow & Merriam, 1977). Gorostiza *et al.* (2015) suggests that flies in tethered single fly paradigms show negative phototaxis in response to an awareness that it is not able to move its wings. In the assay presented in this thesis, flies are unable to move their wings but show fixation to light and dark bars of specific widths, suggesting that the inability to move the wings is not an explanation for this behaviour. The fixation and anti-fixation behaviour at one specific bar width, with the only difference of the bar being light or dark suggests that there is likely to be something specific about this visual parameter that induces a behaviour opposite from fixation behaviour. Further research is required to understand why this behaviour only happens with one specific condition.

7.3 *Dscam2* is required for visual behaviours

Dscam2^{null} flies have impaired reflexive behaviours. It has been shown that geotactic behaviour is partly compromised, however walking problems in other assays have not been identified. It is possible that walking up is more challenging than walking forward caused by unidentified wiring defects in motor pathways. Dscam2 is expressed in motor neurons (Grace Lah, personal communication) so subtle defects which are only elicited during walking vertically might be present. However, also unidentified wiring defects in other geotaxis related structures might cause the impairment in this behaviour. Geotaxis relies heavily upon brain structures such as the central complex (Strauss, 2002) and components of this structure have been shown to express Dscam2 (Sarah Kerwin, personal communication). A detailed investigation of this structure in *Dscam2*^{null} flies might reveal wiring defects that could be responsible for the geotaxis phenotype. Phototactic behaviour is also impaired in *Dscam2*^{null} flies, which could be attributed to the disorganization of R7 and R8 axons. However, potential wiring defects downstream of these neurons cannot be excluded. Interestingly, this is a mild impairment and *Dscam2*^{null} flies are still able to detect UV/blue and green light, indicating that these pathways are at least partially functional.

What was unexpected was that *Dscam2*^{null} flies responded to motion in an opposite manner compared to controls. Moving gratings of alternating dark and light bars have classically been used to elicit an optomotor response from flies. The response varies depending on the particular assays. In assays where the fly is tethered, individuals turn or walk in the direction of the motion, a response that is thought to stabilize their visual world(Götz, 1964, Götz, 1968). In other assays, flies respond to a moving grating by turning against the direction of motion (Lee 2001; Zhu 2009). What regulates this behavioural switch between following and moving against motion is not known. The data presented in this thesis suggest that *Dscam2* plays a crucial role in the perception of these motion stimuli. In two different motion-tracking assays, *Dscam2*^{null} flies moved against the direction of motion, in contrast to control flies. This response was conditional in the set-up, suggesting that the circuitry that controls this behaviour is not completely dysfunctional in the mutant. Rather, *Dscam2* is necessary for the perception of visual cues that have distinct psychophysical characteristics. Presumably, these behavioural phenotypes are due to defects in visual system modularity that also compromise visual system acuity. In the *Dscam2* mutant, about 29% of the lamina cartridges are fused (Millard *et al.*, 2010), reducing the number of sampling points from 750 to 532. Each fused cartridge contains double the number of neurons found in a single cartridge and synapses form between photoreceptors from one cartridge and postsynaptic cells from the other (Millard *et al.*, 2010). For motion detection, this could lead to three different scenarios: (1) a comparison between two single sampling points, (2) a comparison between a single and fused sampling point and (3) a comparison between two fused sampling points. It is possible that motion tracking may be reversed because sampling units are no longer receiving the correct temporal information and this result in an inversion in the sign of the response.

Another possibility is that the direction of motion is misperceived due to aliasing. Aliasing is the misperception of the direction of motion due to physical constraints within the compound eye. When a grating has a spatial period shorter than two times the interommatidial angle, the fly perceives motion in the opposite direction (Buchner, 1976, Götz, 1964, Götz, 1965). Although it cannot be ruled out, it is unlikely that aliasing is the explanation for the *Dscam2*^{null} flies' inverted optomotor response, particularly in the maze. In the maze experiments, 25 degrees was the minimum spatial period attainable and a spatial period of 9.6 degrees would have been required to induce aliasing in wild-type flies. In addition, reflections in the maze will appear as bigger bars compared to the LED panel because of the distance between the fly and to the visual presentation. In mutants that have 29% of their lamina cartridges fused, it is difficult to estimate what the "average" interommatidial distance because not every sampling point is affected. However, if for simplicity, it was assumed that every cartridge was fused then the interommatidial distance would double and a spatial period of 19.2

degrees would induce aliasing in the mutants. Since this is an overestimation of the interommatidial distance in the mutant and this spatial period is less than what was produced in the maze, aliasing is a highly unlikely explanation. In the tethered-walking assay, there is less evidence against aliasing. The mutant flies responded negatively to a spatial period of around 10 degrees, which is close to the wild-type interommatidial angle. However, this stimulus did not induce aliasing in control flies. This could be due to the diamond shape of the LED arena, which results in different distances from the front and back LED panels to the fly (resulting in a spatial period of 9.8 degrees and 16.7 degrees respectively) and therefore does not elicit aliasing in wild-type but would in the mutant flies considering this spatial period is below the interommatidial distance in mutant flies. It is therefore possible that the inversed behaviour of the mutants on the ball is due to aliasing, but this would be inconsistent with the results from the maze.

To further investigate how wiring defects related to L2 in *Dscam2*^{null} flies change their visual behaviour, the response of *Dscam2*^{null} flies has been assessed to high contrast front-to-back as well as back-to-front stimuli. It has been suggested that L2 plays a role in front-to-back motion (Rister *et al.*, 2007, Tuthill *et al.*, 2013). When a grating was presented to only one eye, control flies responded to front-to-back stimuli presented at the left or right eye. They responded to back-to-front motion presented on the right eye but not left eye, a bias that was not observed with other visual stimuli. Interestingly, for the *Dscam2*^{null} flies it was found that clockwise stimuli elicit an optomotor response but counter-clockwise stimuli do not. Clockwise and counter-clockwise biases, or locomotor handedness, have been observed in humans (Souman *et al.*, 2009) and *Drosophila* (Buchanan *et al.*, 2015) but only in the absence of visual information. In addition, these biases are also suggested to be normal variation within a population without a genetic or environmental aetiology as mating two right turning biased flies does not necessarily result in right turning biased offspring (Buchanan *et al.*, 2015). Therefore, the clockwise response is unlikely to be due to variation but more likely due to a change in neuronal wiring in *Dscam2*^{null} flies which results in an inability to respond to counter-clockwise translational motion, something that has not been observed before.

A change in visual perception was not only observed with moving gratings but also with orientation behaviours. In the single fly virtual reality assay, *Dscam2*^{null} flies display anti-fixation to a 29.4-degree wide dark bar, a stimulus that elicits fixation in wild-type flies. They also display anti-fixation to a 29.4-degree wide light bar, similar to control flies. *Dscam2*^{null} flies are able to fixate and one of the mutants, *Dscam2*$^{null-1}$, does so at two dark bar conditions while wild-type flies fixate on all dark bar conditions. Although only one of the two *Dscam2*^{null} flies fixates on two dark bar conditions, both *Dscam2*^{null} flies fixate on almost all light bar conditions, except the 29.4 degree wide light bar. Wild-type flies display uniform responses to all light bar conditions, except the 29.4-degree wide light bar.

So the question arises: do the *Dscam2*^{null} flies perceive a light and dark 29.4-degree wide bar similarly? They were found to respond similar to control flies when a light or dark bar was rotated around the fly in an open-loop condition. However, the mutant flies correct light bar perturbations more to the centre of the back of the arena compared to dark bar perturbations suggesting they perceive the bars differently. In addition, *Dscam2*^{null} flies are able to fixate but do so at conditions where control flies do not fixate. This shows that *Dscam2*^{null} flies perceive the bars differently from control flies, and that this perception appears to be dependent on both the luminance and the width of the bar. Thus, as with motion detection, *Dscam2* appears to be necessary for the perception of specific visual cues, but the identity of the affected neural circuits remains to be determined. Considering *Dscam2*^{null} flies are able to fixate and anti-fixate it is possible that the circuits for these behaviours are intact but that the input into these circuits, possibly in visual integration centres, is altered.

One common theme observed with the *Dscam2*^{null} flies is that their behavioural responses in several different assays were opposite to that of controls. An opposite response is more interesting than no response at all considering it suggests that the input-output wiring is functional to a degree but that the visual perception is changed. One possibility is that these simple behaviours are binary; if a response is elicited, only two outcomes are possible. In the mutant animals, this switch is biased in one direction due to defects in neural connectivity. One problem with this model, however, is that only a sub-set of stimuli elicits an inverted response. One would have to argue that a conditional binary switch would be the only way to explain the existing data. Another possibility is that the inverted response has an inverted neural correlate. For example, inverted optomotor responses have been observed in the zebrafish *belladonna (bel)* mutant when presented with a moving grating (Neuhauss *et al.*, 1999). In these larvae a portion of the optic nerve fibres misroute in the optic chiasm, resulting in projection to the wrong hemisphere (Neuhauss *et al.*, 1999). This is unlikely in *Dscam2* mutant, however, as the optic chiasms are morphologically normal and the flies are able to respond normally to certain optomotor conditions. Therefore, the *bel* mutant demonstrates the importance of correct wiring for the optomotor response, but it does not offer an explanation for the results presented in this thesis. Visual perception in *Dscam2*^{null} flies could be changed due to the processing of information. For example, the balance between inhibitory and excitatory inputs could be disrupted leading to an inversion in optomotor responses and object detection. A study by Bulthoff and Bulthoff (1987) demonstrated that injection of the GABA-antagonist picrotoxinin led to an inversion of optomotor and object detection in the blow and fruit fly. The fly was placed on a rotatable ball in front of a monitor where moving gratings of light and dark bars were displayed. Wild-type flies showed a normal optomotor response to these moving gratings but turned against the direction of motion when injected with picrotoxinin. Fixation was also tested using a set-up similar to the one

used in this study with the exception that the tethered flies were flying rather than walking. Untreated flies demonstrated fixation to a dark bar by placing it in front of them, however injection of picrotoxinin reversed their behaviour to an anti-fixation response. The effect of picrotoxinin with a light bar stimulus was unfortunately not investigated. These studies suggest that inhibitory neurons play an important role in both optomotor and fixation responses and raise the possibility that Dscam2 plays a role in establishing the balance between inhibitory and excitatory inputs. Interestingly, GABA signalling has also been linked to cognitive defects in a mouse model of Down syndrome. Ts65Dn mice are trisomic for two thirds of the human chromosome 21 homologues in the mouse, including *DSCAM*, and have cognitive defects that are consistent with Down syndrome. The Ts65Dn mice have increased inhibitory signalling in their brain (Kurt *et al.*, 2000). Chronic treatment of these mice with low doses of picrotoxin suppressed many of these cognitive phenotypes (Fernandez *et al.* (2007)). Thus, this mouse model of disease where *DSCAM* is overexpressed has too much GABA signalling and our loss of function *Dscam2*^{null} flies behave like flies with reduced inhibitory tone. This suggests that Dscam2 could play a role in establishing the appropriate excitatory/inhibitory ratio in the fly brain, but this remains to be tested.

7.4 Differences between *Dscam2*^{null} strains

The *Dscam2*^{null} strains used in this thesis were generated approximately 10 years ago by homologous recombination (Millard *et al.*, 2007) and isogenized prior to the behavioural experiments. Surprisingly, these identical mutations occasionally caused different responses in the population assay and under specific conditions in the single tethered-fly assay. In addition, differences between the *Dscam2*^{null} strains were found in a sleep study in which all three strains displayed variation in daytime sleep fragmentation (Quirk, A., Larkin, A., Millard., S., publication in preparation). This variation between the lines was not rescued after the introduction of a copy of BAC-*Dscam2* in these strains, suggesting that these differences cannot be attributed to *Dscam2*. Founder effects or population bottlenecks within a single strain such as *Canton S* have been reported to influence behaviour, though this was observed between a single fly strain from different laboratories (Colomb & Brembs, 2014). The experiments in this thesis were performed only with healthy flies from healthy populations and no differences in visual behaviour between batches of a single strain have been found. Through the years there were moments were a single fly strain was growing better than others. Several times during the years, new cultures were started from the original line. The *Dscam2* homozygous deletion results in a 22% lethality, which is likely to induce selective pressure for survival. Therefore, the encountered variation between the strains could possibly be attributed to micro-evolution that

occurred independently in each strain. Although the differences between these strains are not ideal, all three mutant lines generally exhibit similar trends allowing us to draw conclusions from them in relation to Dscam2.

7.5 Other *Dscam2* related mutants

In addition to the work done on *Dscam2*^{null} flies some preliminary work has been performed on how *Dscam2* isoform specificity and trisomy affects visual behaviour.

Expression of only one of the two *Dscam2* isoforms is sufficient for a proper organization of the visual system with no obvious changes in morphological modularity (Lah *et al.*, 2014). However, a reduction in lamina cartridge size (Sarah Kerwin, personal communication), L1 and L2 axon arborisation size (Lah *et al.*, 2014) and synapse quantity (Sarah Kerwin, pers. communication) was found. Dscam2B single isoform flies displayed changes in motion detection and object orientation suggesting a change in visual perception. The next step is to identify whether the reduction in arborisation size for L1 and L2 axons is the cause of these behavioural changes. It is possible that the amount of formed synapses within cartridges is variable, altering some of the L1/L2 neurons less functional, resulting in a reduced visual system modularity. This could be tested using calcium imaging of these neurons during the optomotor response.

Interestingly, object-orientation behaviour of Dscam2B single isoform flies was affected similar to the null mutants, suggesting similar problems with the fixation circuitry. In addition, an increase in *Dscam2* dosage affected object-orientation behaviour but not motion detection. These *Dscam2* mutants can provide a platform to study the neuronal circuitry involved in object-orientation behaviour and contribute to the understanding if *Dscam2*^{null} flies perceive a light and dark 29.4-degree wide bar similarly.

7.6 Concluding remarks

In this study, different visual behaviours were explored in *Dscam2* mutant flies. It was found that light and motion detection are impaired in these flies as would be expected for animals with defects in the organization and number of modules in the compound eye. Interestingly, *Dscam2* mutant flies elicit behavioural responses that are opposite to that of controls in three different assays. This behavioural phenotype is only observed under specific experimental conditions suggesting that

Dscam2 is necessary for the wiring of a subset of circuits in the visual system that control the perception of visual stimuli. To our knowledge, this is the first time that modularity has been linked to how visual stimuli are perceived by the brain. More work is needed to assess the contribution of the change in photoreceptor synaptic specificity, observed in the *Dscam2* mutant (Millard *et al.*, 2010), to these behaviours. This can be achieved using calcium imaging of these neurons in a single fly assay where the fly is exposed to visual stimuli while it is walking on an air-supported ball, similar to what is done by Seelig and Jayaraman (2015). This can be complimented with neuron-specific GAL4 drivers and RNA interference reporters to affect gene function at specific locations in the fly visual system such as in the lamina. With these new technological tools, it is possible to progress the understanding of relationships between miswiring in the brain and behavioural output. This will likely uncover significant revelations about how brains work.

References

Anderson, J.C. & Laughlin, S.B. (2000) Photoreceptor performance and the co-ordination of achromatic and chromatic inputs in the fly visual system. *Vision research,* **40,** 13-31.

Antonarakis, S.E., Lyle, R., Dermitzakis, E.T., Reymond, A. & Deutsch, S. (2004) Chromosome 21 and down syndrome: from genomics to pathophysiology. *Nature reviews. Genetics,* **5,** 725-738.

Aptekar, J.W., Shoemaker, P.A. & Frye, M.A. (2012) Figure tracking by flies is supported by parallel visual streams. *Current biology : CB,* **22,** 482-487.

Bahl, A., Ammer, G., Schilling, T. & Borst, A. (2013) Object tracking in motion-blind flies. *Nature neuroscience,* **16,** 730-738.

Baines, R.A., Uhler, J.P., Thompson, A., Sweeney, S.T. & Bate, M. (2001) Altered electrical properties in Drosophila neurons developing without synaptic transmission. *The Journal of neuroscience : the official journal of the Society for Neuroscience,* **21,** 1523-1531.

Bausenwein, B., Dittrich, A.P. & Fischbach, K.F. (1992) The optic lobe of Drosophila melanogaster. II. Sorting of retinotopic pathways in the medulla. *Cell and tissue research,* **267,** 17-28.

Bausenwein, B. & Fischbach, K.F. (1992) Activity labeling patterns in the medulla of Drosophila melanogaster caused by motion stimuli. *Cell and tissue research,* **270,** 25-35.

Bausenwein, B., Wolf, R. & Heisenberg, M. (1986) Genetic dissection of optomotor behavior in Drosophila melanogaster. Studies on wild-type and the mutant optomotor-blindH31. *Journal of neurogenetics,* **3,** 87-109.

Becker, L., Mito, T., Takashima, S. & Onodera, K. (1991) Growth and development of the brain in Down syndrome. *Prog Clin Biol Res,* **373,** 133-152.

Behnia, R., Clark, D.A., Carter, A.G., Clandinin, T.R. & Desplan, C. (2014) Processing properties of ON and OFF pathways for Drosophila motion detection. *Nature,* **512,** 427-430.

Benzer, S. (1967) Behavioral mutants of Drosophila isolated by coutercurrent distribution *Proceedings of the National Academy of Sciences of the United States of America,* **58,** 1112-1119.

Berens, P. (2009) CircStat: A MATLAB Toolbox for Circular Statistics. *J Stat Softw,* **31,** 1-21.

Blank, M., Fuerst, P.G., Stevens, B., Nouri, N., Kirkby, L., Warrier, D., Barres, B.A., Feller, M.B., Huberman, A.D., Burgess, R.W. & Garner, C.C. (2011) The Down Syndrome Critical Region Regulates Retinogeniculate Refinement. *The Journal of neuroscience : the official journal of the Society for Neuroscience,* **31,** 5764-5776.

Blondeau, J. & Heisenberg, M. (1982) The three-dimensional optomotor torque system of Drosophila melanogaster. *J. Comp. Physiol.,* **145,** 321-329.

Borst, A. (2014) Neural circuits for elementary motion detection. *Journal of neurogenetics,* **28,** 361-373.

Borst, A. & Haag, J. (2002) Neural networks in the cockpit of the fly. *Journal of comparative physiology. A, Neuroethology, sensory, neural, and behavioral physiology,* **188,** 419-437.

Bosch, D.S., van Swinderen, B. & Millard, S.S. (2015) Dscam2 affects visual perception in Drosophila melanogaster. *Frontiers in Behavioral Neuroscience,* **9**.

Boyle, M., Nighorn, A. & Thomas, J.B. (2006) Drosophila Eph receptor guides specific axon branches of mushroom body neurons. *Development,* **133,** 1845-1854.

Braitenberg, V. (1970) [Order and orientation of elements in the visual system of the fly]. *Kybernetik,* **7,** 235-242.

Braitenberg, V. & Hauser-Holschuh, H. (1972) Patterns of projection in the visual system of the fly. II. Quantitative aspects of second order neurons in relation to models of movement perception. *Experimental brain research,* **16,** 184-209.

Broda, H. & Wright, R. (1978) Prolonged depolarising afterpotentials in red-eyed Drosophila. *Journal of Insect Physiology,* **24,** 681-684.

Buchanan, S.M., Kain, J.S. & de Bivort, B.L. (2015) Neuronal control of locomotor handedness in Drosophila. *Proceedings of the National Academy of Sciences of the United States of America,* **112,** 6700-6705.

Buchner, E. (1976) Elementary Movement Detectors in an Insect Visual-System. *Biol. Cybernetics,* **24,** 85-101.

Buchner, E., Buchner, S. & Bulthoff, H. (1984) Identification of [3H]deoxyglucose-labelled interneurons in the fly from serial autoradiographs. *Brain research,* **305,** 384-388.

Bülthoff, H. (1980) Orientation Behavior of Drosophila melanogaster. Department Human Perception, Cognition and Action, Max Planck Institute for Biological Cybernetics, Max Planck Society.

Bulthoff, H. & Bulthoff, I. (1987) GABA-antagonist inverts movement and object detection in flies. *Brain research,* **407,** 152-158.

Bülthoff, H., Götz, K. & Herre, M. (1982) Recurrent inversion of visual orientation in the walking fly,Drosophila melanogaster. *J. Comp. Physiol.,* **148,** 471-481.

Buschbeck, E.K. & Strausfeld, N.J. (1996) Visual motion-detection circuits in flies: small-field retinotopic elements responding to motion are evolutionarily conserved across taxa. *The Journal of neuroscience : the official journal of the Society for Neuroscience,* **16,** 4563-4578.

Calcagno, B., Eyles, D., van Alphen, B. & van Swinderen, B. (2013) Transient activation of dopaminergic neurons during development modulates visual responsiveness, locomotion and brain activity in a dopamine ontogeny model of schizophrenia. *Translational psychiatry,* **3,** e206.

Chou, W.H., Hall, K.J., Wilson, D.B., Wideman, C.L., Townson, S.M., Chadwell, L.V. & Britt, S.G. (1996) Identification of a novel Drosophila opsin reveals specific patterning of the R7 and R8 photoreceptor cells. *Neuron,* **17,** 1101-1115.

Chou, W.H., Huber, A., Bentrop, J., Schulz, S., Schwab, K., Chadwell, L.V., Paulsen, R. & Britt, S.G. (1999) Patterning of the R7 and R8 photoreceptor cells of Drosophila: evidence for induced and default cell-fate specification. *Development,* **126,** 607-616.

Clandinin, T.R. & Zipursky, S.L. (2002) Making connections in the fly visual system. *Neuron,* **35,** 827-841.

Clark, D.A., Bursztyn, L., Horowitz, M.A., Schnitzer, M.J. & Clandinin, T.R. (2011) Defining the computational structure of the motion detector in Drosophila. *Neuron,* **70,** 1165-1177.

Collett, T.S. & Land, M.F. (1975) Visual control of flight behaviour in the hoverfly Syritta pipiens L. *Journal of Comparative Physiology A: Neuroethology, Sensory, Neural, and Behavioral Physiology,* **99,** 1-66.

Colomb, J. & Brembs, B. (2014) Sub-strains of Drosophila Canton-S differ markedly in their locomotor behavior. *F1000Res,* **3,** 176.

Coombe, P.E. (1984) The Role of Retinula Cell-Types in Fixation Behavior of Walking Drosophila-Melanogaster. *J. Comp. Physiol.,* **155,** 661-672.

Coombe, P.E. & Heisenberg, M. (1986) The structural brain mutant Vacuolar medulla of Drosophila melanogaster with specific behavioral defects and cell degeneration in the adult. *Journal of neurogenetics,* **3,** 135-158.

Coombe, P.E., Srinivasan, M.V. & Guy, R.G. (1989) Are the large monopolar cells of the insect lamina on the optomotor pathway? *Journal of Comparative Physiology A,* **166,** 23-35.

Coppola, D.M., Purves, H.R., McCoy, A.N. & Purves, D. (1998a) The distribution of oriented contours in the real world. *Proceedings of the National Academy of Sciences of the United States of America,* **95,** 4002-4006.

Coppola, D.M., White, L.E., Fitzpatrick, D. & Purves, D. (1998b) Unequal representation of cardinal and oblique contours in ferret visual cortex. *Proceedings of the National Academy of Sciences of the United States of America,* **95,** 2621-2623.

Davenport, C.B. & Perkins, H. (1897) A Contribution to the Study of Geotaxis in the Higher Animals. *J Physiol,* **22,** 99-110.

Desroches, C.E., Busto, M., Riedl, C.A., Mackay, T.F. & Sokolowski, M.B. (2010) Quantitative trait locus mapping of gravitaxis behaviour in Drosophila melanogaster. *Genetics research,* **92,** 167-174.

Dobzhansky, T. & Spassky, B. (1969) Artificial and natural selection for two behavioral traits in Drosophila pseudoobscura. *Proceedings of the National Academy of Sciences of the United States of America,* **62,** 75-80.

Douglass, J.K. & Strausfeld, N.J. (1995) Visual motion detection circuits in flies: peripheral motion computation by identified small-field retinotopic neurons. *The Journal of neuroscience : the official journal of the Society for Neuroscience,* **15,** 5596-5611.

Douglass, J.K. & Strausfeld, N.J. (1996) Visual motion-detection circuits in flies: parallel direction- and non-direction-sensitive pathways between the medulla and lobula plate. *The Journal of neuroscience : the official journal of the Society for Neuroscience,* **16,** 4551-4562.

Duistermars, B.J., Care, R.A. & Frye, M.A. (2012) Binocular interactions underlying the classic optomotor responses of flying flies. *Front Behav Neurosci,* **6,** 6.

Duistermars, B.J., Chow, D.M., Condro, M. & Frye, M.A. (2007) The spatial, temporal and contrast properties of expansion and rotation flight optomotor responses in Drosophila. *The Journal of experimental biology,* **210,** 3218-3227.

Eichner, H., Joesch, M., Schnell, B., Reiff, D.F. & Borst, A. (2011) Internal structure of the fly elementary motion detector. *Neuron,* **70,** 1155-1164.

Evans, O., Paulk, A.C. & van Swinderen, B. (2011) An automated paradigm for Drosophila visual psychophysics. *PloS one,* **6,** e21619.

Fernandez, F., Morishita, W., Zuniga, E., Nguyen, J., Blank, M., Malenka, R.C. & Garner, C.C. (2007) Pharmacotherapy for cognitive impairment in a mouse model of Down syndrome. *Nature neuroscience,* **10,** 411-413.

Fox, J.L., Aptekar, J.W., Zolotova, N.M., Shoemaker, P.A. & Frye, M.A. (2014) Figure–ground discrimination behavior in Drosophila. I. Spatial organization of wing-steering responses. *Journal of Experimental Biology,* **217,** 558-569.

Fuerst, P.G., Koizumi, A., Masland, R.H. & Burgess, R.W. (2008) Neurite arborization and mosaic spacing in the mouse retina require DSCAM. *Nature,* **451,** 470-474.

Gao, S., Takemura, S.Y., Ting, C.Y., Huang, S., Lu, Z., Luan, H., Rister, J., Thum, A.S., Yang, M., Hong, S.T., Wang, J.W., Odenwald, W.F., White, B.H., Meinertzhagen, I.A. & Lee, C.H. (2008) The neural substrate of spectral preference in Drosophila. *Neuron,* **60,** 328-342.

Gao, X.J., Potter, C.J., Gohl, D.M., Silies, M., Katsov, A.Y., Clandinin, T.R. & Luo, L. (2013) Specific kinematics and motor-related neurons for aversive chemotaxis in Drosophila. *Current biology : CB,* **23,** 1163-1172.

Giurfa, M. & Menzel, R. (1997) Insect visual perception: complex abilities of simple nervous systems. *Curr Opin Neurobiol,* **7,** 505-513.

Gorostiza, E.A., Colomb, J. & Brembs, B. (2015) *A value-based behavioural choice underlies phototaxis in Drosophila*.

Gotz, K.G. (1980) Visual guidance in Drosophila. *Basic Life Sci,* **16,** 391-407.

Götz, K.G. (1964) [Optomoter studies of the visual system of several eye mutants of the fruit fly Drosophila]. *Kybernetik,* **2,** 77-92.

Götz, K.G. (1965) Die optischen Übertragungseigenschaften der Komplexaugen von Drosophila. *Kybernetik,* **2,** 215-221.

Götz, K.G. (1968) Flight control in Drosophila by visual perception of motion. *Kybernetik,* **4,** 199-208.

Götz, K.G. (1972) Principles of optomotor reactions in insects. *Bibliotheca ophthalmologica : supplementa ad ophthalmologica,* **82,** 251-259.

Götz, K.G. (1987) Course-control, metabolism and wing interference during ultralong tethered flight in Drosophila melanogaster. *Journal of experimental biology,* **128,** 35-46.

Götz, K.G. & Wenking, H. (1973) Visual control of locomotion in the walking fruitflyDrosophila. *J. Comp. Physiol.,* **85,** 235-266.

Grenningloh, G., Rehm, E.J. & Goodman, C.S. (1991) Genetic analysis of growth cone guidance in Drosophila: fasciclin II functions as a neuronal recognition molecule. *Cell,* **67,** 45-57.
Hadjieconomou, D., Timofeev, K. & Salecker, I. (2011) A step-by-step guide to visual circuit assembly in Drosophila. *Current opinion in neurobiology,* **21,** 76-84.
Hamada, F.N., Rosenzweig, M., Kang, K., Pulver, S.R., Ghezzi, A., Jegla, T.J. & Garrity, P.A. (2008) An internal thermal sensor controlling temperature preference in Drosophila. *Nature,* **454,** 217-220.
Hardie, R. (1979) Electrophysiological analysis of fly retina. I: Comparative properties of R1-6 and R 7 and 8. *J. Comp. Physiol.,* **129,** 19-33.
Harrison, R.G. (1910) The outgrowth of the nerve fiber as a mode of protoplasmic movement. *J Exp Zool,* **9,** 787-848.
Hassenstein, B. & Reichardt, W. (1956a) Systemtheoretische Analyse Der Zeit, Reihenfolgen Und Vorzeichenauswertung Bei Der Bewegungsperzeption Des Russelkafers Chlorophanus. *Z Naturforsch Pt B,* **11,** 513-524.
Hassenstein, B. & Reichardt, W.E. (1956b) Functional structure of a mechanism of perception of optical movement. *Proceedings of the First International Congress on Cybernetics, Namur***,** 797-801.
Hausen, K. (1982) Motion sensitive interneurons in the optomotor system of the fly. *Biol. Cybernetics,* **45,** 143-156.
Hausen, K. (1984) The Lobula-Complex of the Fly: Structure, Function and Significance in Visual Behaviour. In Ali, M.A. (ed), *Photoreception and Vision in Invertebrates.* Springer US, pp. 523-559.
Heisenberg, M. (1984) *Vision in Drosophila : genetics of microbehavior / M. Heisenberg, R. Wolf,* Springer-Verlag, Berlin ; New York.
Heisenberg, M. (2003) Mushroom body memoir: from maps to models. *Nat Rev Neurosci,* **4,** 266-275.
Heisenberg, M. & Bohl, K. (1979) Isolation of anatomical brain mutants of Drosophila by histological means. *Zeitschrift fur Naturforschung,* **34,** 143-147.
Heisenberg, M. & Wolf, R. (1979) On the fine structure of yaw torque in visual flight orientation of Drosophila melanogaster. *J. Comp. Physiol.,* **130,** 113-130.
Heisenberg, M., Wonneberger, R. & Wolf, R. (1978) Optomotor-blind H31—a Drosophila mutant of the lobula plate giant neurons. *J. Comp. Physiol.,* **124,** 287-296.
Hodge, J.J.L. (2009) Ion Channels to Inactivate Neurons in Drosophila. *Frontiers in Molecular Neuroscience,* **2,** 13.
Horn, E. & Wehner, R. (1975) The mechanism of visual pattern fixation in the walking fly,Drosophila melanogaster. *J. Comp. Physiol.,* **101,** 39-56.
Huberman, A.D., Clandinin, T.R. & Baier, H. (2010) Molecular and cellular mechanisms of lamina-specific axon targeting. *Cold Spring Harb Perspect Biol,* **2,** a001743.
Inagaki, H.K., Kamikouchi, A. & Ito, K. (2010) Methods for quantifying simple gravity sensing in Drosophila melanogaster. *Nature protocols,* **5,** 20-25.
Joesch, M., Schnell, B., Raghu, S.V., Reiff, D.F. & Borst, A. (2010) ON and OFF pathways in Drosophila motion vision. *Nature,* **468,** 300-304.
Joesch, M., Weber, F., Eichner, H. & Borst, A. (2013) Functional specialization of parallel motion detection circuits in the fly. *The Journal of neuroscience : the official journal of the Society for Neuroscience,* **33,** 902-905.
Kain, J., Stokes, C., Gaudry, Q., Song, X., Foley, J., Wilson, R. & de Bivort, B. (2013) Leg-tracking and automated behavioural classification in Drosophila. *Nature communications,* **4,** 1910.
Kamikouchi, A., Inagaki, H.K., Effertz, T., Hendrich, O., Fiala, A., Göpfert, M.C. & Ito, K. (2009) The neural basis of Drosophila gravity-sensing and hearing. *Nature,* **458,** 165-171.
Kirschfeld, K. (1967) [The projection of the optical environment on the screen of the rhabdomere in the compound eye of the Musca]. *Experimental brain research,* **3,** 248-270.

Kitamoto, T. (2001) Conditional modification of behavior in Drosophila by targeted expression of a temperature-sensitive shibire allele in defined neurons. *Journal of Neurobiology,* **47,** 81-92.
Kretschmer, F., Kretschmer, V., Kunze, V.P. & Kretzberg, J. (2013) OMR-arena: automated measurement and stimulation system to determine mouse visual thresholds based on optomotor responses. *PloS one,* **8,** e78058.
Kurt, M.A., Davies, D.C., Kidd, M., Dierssen, M. & Florez, J. (2000) Synaptic deficit in the temporal cortex of partial trisomy 16 (Ts65Dn) mice. *Brain research,* **858,** 191-197.
Lah, G.J., Li, J.S. & Millard, S.S. (2014) Cell-specific alternative splicing of Drosophila Dscam2 is crucial for proper neuronal wiring. *Neuron,* **83,** 1376-1388.
Lee, C.H., Herman, T., Clandinin, T.R., Lee, R. & Zipursky, S.L. (2001) N-cadherin regulates target specificity in the Drosophila visual system. *Neuron,* **30,** 437-450.
Lefranc, A., Jeune, B., Thomas-Orillard, M. & Danchin, E. (2001) Non-independence of individuals in a population of Drosophila melanogaster: effects on spatial distribution and dispersal. *Comptes rendus de l'Academie des sciences. Serie III, Sciences de la vie,* **324,** 219-227.
Li, H.-L., Huang, B.S., Vishwasrao, H., Sutedja, N., Chen, W., Jin, I., Hawkins, R.D., Bailey, C.H. & Kandel, E.R. (2009) Dscam Mediates Trans-Synaptic Interactions for Remodeling of Glutamate Receptors in Aplysia During De Novo and Learning-Related Synapse Formation. *Neuron,* **61,** 527.
Li, Z. & Sheng, M. (2003) Some assembly required: the development of neuronal synapses. *Nat Rev Mol Cell Biol,* **4,** 833-841.
Lightbody, A.A. & Reiss, A.L. (2009) Gene, Brain, and Behavior Relationships in Fragile X Syndrome: Evidence from Neuroimaging Studies. *Developmental disabilities research reviews,* **15,** 343-352.
Lilliefors, H.W. (1967) On the Kolmogorov-Smirnov Test for Normality with Mean and Variance Unknown. *Journal of the American Statistical Association,* **62,** 399-402.
Lin, D.M., Lin, D.M., Fetter, R.D., Kopczynski, C. & Grenningloh, G. (1994) Genetic analysis of Fasciclin II in drosophila: Defasciculation, refasciculation, and altered fasciculation. *Neuron (Cambridge, Mass.),* **13,** 1055-1069.
Longden, K.D., Muzzu, T., Cook, D.J., Schultz, S.R. & Krapp, H.G. (2014) Nutritional state modulates the neural processing of visual motion. *Current biology : CB,* **24,** 890-895.
Maimon, G., Straw, A.D. & Dickinson, M.H. (2008) A simple vision-based algorithm for decision making in flying Drosophila. *Current biology : CB,* **18,** 464-470.
Maisak, M.S., Haag, J., Ammer, G., Serbe, E., Meier, M., Leonhardt, A., Schilling, T., Bahl, A., Rubin, G.M., Nern, A., Dickson, B.J., Reiff, D.F., Hopp, E. & Borst, A. (2013) A directional tuning map of Drosophila elementary motion detectors. *Nature,* **500,** 212-216.
Markow, T.A. & Merriam, J. (1977) Phototactic and geotactic behavior of countercurrent defective mutants of Drosophila melanogaster. *Behavior genetics,* **7,** 447-455.
McCann, G.D. (1965) Optomotor response studies of insect vision. *Proceedings - Royal Society. Biological sciences,* **163,** 369.
McCann, G.D. & MacGinitie, G.F. (1965) Optomotor response studies of insect vision. *Proceedings of the Royal Society of London. Series B, Biological sciences,* **163,** 369-401.
Meinertzhagen, I. & Hanson Thomas, E. (1993) *The Development of Drosophila melanogaster,* Cold Spring Harbor Laboratory Press, New York.
Meinertzhagen, I.A. & Hanson, T.E. (1993) The development of the optic lobe. In Bate, M. & Martinez-Arias, A. (eds), *The Development of Drosophila melanogaster.* Cold Spring Harbor, NY: Cold Spring Harbor Press, pp. 1363-1491.
Meinertzhagen, I.A. & O'Neil, S.D. (1991) Synaptic organization of columnar elements in the lamina of the wild type in Drosophila melanogaster. *Journal of comparative neurology (1911),* **305,** 232-263.
Meinertzhagen, I.A. & Sorra, K.E. (2001) Synaptic organization in the fly's optic lamina: few cells, many synapses and divergent microcircuits. *Progress in brain research,* **131,** 53-69.

Millard, S.S., Flanagan, J.J., Pappu, K.S., Wu, W. & Zipursky, S.L. (2007) Dscam2 mediates axonal tiling in the Drosophila visual system. *Nature,* **447,** 720-724.

Millard, S.S., Lu, Z., Zipursky, S.L. & Meinertzhagen, I.A. (2010) Drosophila dscam proteins regulate postsynaptic specificity at multiple-contact synapses. *Neuron,* **67,** 761-768.

Mitchell, K. (2011) The miswired brain: making connections from neurodevelopment to psychopathology. *BMC Biology,* **9,** 23.

Moore, R.J., Taylor, G.J., Paulk, A.C., Pearson, T., van Swinderen, B. & Srinivasan, M.V. (2014) FicTrac: a visual method for tracking spherical motion and generating fictive animal paths. *Journal of neuroscience methods,* **225,** 106-119.

Morton, P.D. & Cosens, D. (1978) Vision in Drosophila: evidence for the involvement of retinula cells 1–6 in the orientation behaviour of Drosophila melanogaster. *Physiological Entomology,* **3,** 323-334.

Navarro, J. & del Solar, E. (1975) Pattern of spatial distribution in Drosophila melanogaster. *Behavior genetics,* **5,** 9-16.

Neuhauss, S.C. (2003) Behavioral genetic approaches to visual system development and function in zebrafish. *Journal of neurobiology,* **54,** 148-160.

Neuhauss, S.C., Biehlmaier, O., Seeliger, M.W., Das, T., Kohler, K., Harris, W.A. & Baier, H. (1999) Genetic disorders of vision revealed by a behavioral screen of 400 essential loci in zebrafish. *The Journal of neuroscience : the official journal of the Society for Neuroscience,* **19,** 8603-8615.

Osorio, D., Srinivasan, M.V. & Pinter, R.B. (1990) What causes edge fixation in walking flies? *The Journal of experimental biology,* **149,** 281-292.

Papatsenko, D., Sheng, G. & Desplan, C. (1997) A new rhodopsin in R8 photoreceptors of Drosophila: evidence for coordinate expression with Rh3 in R7 cells. *Development,* **124,** 1665-1673.

Paulk, A.C., Kirszenblat, L., Zhou, Y. & van Swinderen, B. (2015) Closed-Loop Behavioral Control Increases Coherence in the Fly Brain. *The Journal of neuroscience : the official journal of the Society for Neuroscience,* **35,** 10304-10315.

Paulk, A.C., Stacey, J.A., Pearson, T.W., Taylor, G.J., Moore, R.J., Srinivasan, M.V. & van Swinderen, B. (2014) Selective attention in the honeybee optic lobes precedes behavioral choices. *Proceedings of the National Academy of Sciences of the United States of America,* **111,** 5006-5011.

Perttunen, V. (1963) Effect of Desiccation on the Light Reactions of some Terrestrial Arthropods. In Autrum, H., Bünning, E., v. Frisch, K., Hadorn, E., Kühn, A., Mayr, E., Pirson, A., Straub, J., Stubbe, H. & Weidel, W. (eds), *Orientierung der Tiere / Animal Orientation.* Springer Berlin Heidelberg, pp. 90-97.

Poggio, T. & Reichardt, W. (1973) A theory of the pattern induced flight orientation of the fly Musca domestica. *Kybernetik,* **12,** 185-203.

Poggio, T. & Reichardt, W. (1976) Visual control of orientation behaviour in the fly. Part II. Towards the underlying neural interactions. *Q Rev Biophys,* **9,** 377-438.

Posner, M.I. (1980) Orienting of attention. *The Quarterly journal of experimental psychology,* **32,** 3-25.

Proverbio, A.M., Esposito, P. & Zani, A. (2002) Early involvement of the temporal area in attentional selection of grating orientation: an ERP study. *Brain Res Cogn Brain Res,* **13,** 139-151.

Pulver, S.R., Pashkovski, S.L., Hornstein, N.J., Garrity, P.A. & Griffith, L.C. (2009) Temporal dynamics of neuronal activation by Channelrhodopsin-2 and TRPA1 determine behavioral output in Drosophila larvae. *Journal of neurophysiology,* **101,** 3075-3088.

Ramón y Cajal, S. (1890) *A quelle époque apparaissent les expansions des cellules nerveuses de la moelle épinière du poulet?,* Gustav Fischer.

Ramón y Cajal, S. (1913) *Estudios sobre la degeneración y regeneración del sistema nerviosa,* Imprenta de Hijos de Nicolás Moya.

Reichardt, W. & Poggio, T. (1976) Visual control of orientation behaviour in the fly. Part I. A quantitative analysis. *Q Rev Biophys,* **9,** 311-375, 428-338.

Reichardt, W. & Rosenblith, W. (1961) Autocorrelation, a principle for evaluation of sensory information by the central nervous system. *Symposium on Principles of Sensory Communication 1959.* MIT Press, pp. 303-317.

Reichardt, W. & Wenking, H. (1969) Optical detection and fixation of objects by fixed flying flies. *Die Naturwissenschaften,* **56,** 424-425.

Reiff, D.F., Plett, J., Mank, M., Griesbeck, O. & Borst, A. (2010) Visualizing retinotopic half-wave rectified input to the motion detection circuitry of Drosophila. *Nature neuroscience,* **13,** 973-978.

Reiser, M.B. & Dickinson, M.H. (2008) A modular display system for insect behavioral neuroscience. *Journal of neuroscience methods,* **167,** 127-139.

Rister, J., Pauls, D., Schnell, B., Ting, C.Y., Lee, C.H., Sinakevitch, I., Morante, J., Strausfeld, N.J., Ito, K. & Heisenberg, M. (2007) Dissection of the peripheral motion channel in the visual system of Drosophila melanogaster. *Neuron,* **56,** 155-170.

Salcedo, E., Huber, A., Henrich, S., Chadwell, L.V., Chou, W.H., Paulsen, R. & Britt, S.G. (1999) Blue- and green-absorbing visual pigments of Drosophila: ectopic expression and physiological characterization of the R8 photoreceptor cell-specific Rh5 and Rh6 rhodopsins. *The Journal of neuroscience : the official journal of the Society for Neuroscience,* **19,** 10716-10726.

Sato, M., Suzuki, T. & Nakai, Y. (2013) Waves of differentiation in the fly visual system. *Developmental biology,* **380,** 1-11.

Schnell, B., Raghu, S.V., Nern, A. & Borst, A. (2012) Columnar cells necessary for motion responses of wide-field visual interneurons in Drosophila. *Journal of comparative physiology. A, Neuroethology, sensory, neural, and behavioral physiology,* **198,** 389-395.

Seelig, J.D., Chiappe, M.E., Lott, G.K., Dutta, A., Osborne, J.E., Reiser, M.B. & Jayaraman, V. (2010) Two-photon calcium imaging from head-fixed Drosophila during optomotor walking behavior. *Nat Methods,* **7,** 535-540.

Seelig, J.D. & Jayaraman, V. (2015) Neural dynamics for landmark orientation and angular path integration. *Nature,* **521,** 186-191.

Sen, A., Grimm, S., Hofmeyer, K. & Pflugfelder, G.O. (2014) Optomotor-blind in the development of the Drosophila HS and VS lobula plate tangential cells. *Journal of neurogenetics,* **28,** 250-263.

Shinomiya, K., Karuppudurai, T., Lin, T.Y., Lu, Z., Lee, C.H. & Meinertzhagen, I.A. (2014) Candidate neural substrates for off-edge motion detection in Drosophila. *Current biology : CB,* **24,** 1062-1070.

Silies, M., Gohl, D.M., Fisher, Y.E., Freifeld, L., Clark, D.A. & Clandinin, T.R. (2013) Modular use of peripheral input channels tunes motion-detecting circuitry. *Neuron,* **79,** 111-127.

Souman, J.L., Frissen, I., Sreenivasa, M.N. & Ernst, M.O. (2009) Walking straight into circles. *Current biology : CB,* **19,** 1538-1542.

Sperry, R.W. (1963) Chemoaffinity in the Orderly Growth of Nerve Fiber Patterns and Connections. *Proceedings of the National Academy of Sciences of the United States of America,* **50,** 703-710.

Stark, W.S. & Carlson, S.D. (1983) Ultrastructure of the compound eye and first optic neuropile of the photoreceptor mutant oraJK84 of Drosophila. *Cell and tissue research,* **233,** 305-317.

Strausfeld, N.J. (1984) Functional Neuroanatomy of the Blowfly's Visual System. In Ali, M.A. (ed), *Photoreception and Vision in Invertebrates.* Springer US, pp. 483-522.

Strausfeld, N.J. & Bassemir, U.K. (1985) Lobula plate and ocellar interneurons converge onto a cluster of descending neurons leading to neck and leg motor neuropil in Calliphora erythrocephala. *Cell and tissue research,* **240,** 617-640.

Strausfeld, N.J. & Campos-Ortega, J.A. (1973) The L4 monopolar neurone: a substrate for lateral interaction in the visual system of the fly Musca domestica (L.). *Brain research,* **59,** 97-117.

Strausfeld, N.J. & Campos-Ortega, J.A. (1977) Vision in insects: pathways possibly underlying neural adaptation and lateral inhibition. *Science,* **195,** 894-897.
Strausfeld, N.J. & Lee, J.K. (1991) Neuronal basis for parallel visual processing in the fly. *Visual neuroscience,* **7,** 13-33.
Strauss, R. (2002) The central complex and the genetic dissection of locomotor behaviour. *Current opinion in neurobiology,* **12,** 633-638.
Strauss, R., Renner, M. & Gotz, K. (2001) Task-specific association of photoreceptor systems and steering parameters in Drosophila. *Journal of comparative physiology. A, Sensory, neural, and behavioral physiology,* **187,** 617-632.
Straw, A.D. (2008) Vision egg: an open-source library for realtime visual stimulus generation. *Front Neuroinformatics,* **2,** 4.
Sun, Y., Liu, L., Ben-Shahar, Y., Jacobs, J.S., Eberl, D.F. & Welsh, M.J. (2009) TRPA channels distinguish gravity sensing from hearing in Johnston's organ. *Proceedings of the National Academy of Sciences of the United States of America,* **106,** 13606-13611.
Takemura, S.Y., Bharioke, A., Lu, Z., Nern, A., Vitaladevuni, S., Rivlin, P.K., Katz, W.T., Olbris, D.J., Plaza, S.M., Winston, P., Zhao, T., Horne, J.A., Fetter, R.D., Takemura, S., Blazek, K., Chang, L.A., Ogundeyi, O., Saunders, M.A., Shapiro, V., Sigmund, C., Rubin, G.M., Scheffer, L.K., Meinertzhagen, I.A. & Chklovskii, D.B. (2013) A visual motion detection circuit suggested by Drosophila connectomics. *Nature,* **500,** 175-181.
Takemura, S.Y., Karuppudurai, T., Ting, C.Y., Lu, Z., Lee, C.H. & Meinertzhagen, I.A. (2011) Cholinergic circuits integrate neighboring visual signals in a Drosophila motion detection pathway. *Current biology : CB,* **21,** 2077-2084.
Tammero, L.F., Frye, M.A. & Dickinson, M.H. (2004) Spatial organization of visuomotor reflexes in Drosophila. *The Journal of experimental biology,* **207,** 113-122.
Tayler, T.D. & Garrity, P.A. (2003) Axon targeting in the Drosophila visual system. *Current opinion in neurobiology,* **13,** 90-95.
Tessier-Lavigne, M. & Goodman, C.S. (1996) The molecular biology of axon guidance. *Science,* **274,** 1123-1133.
Tuthill, J.C., Nern, A., Holtz, S.L., Rubin, G.M. & Reiser, M.B. (2013) Contributions of the 12 neuron classes in the fly lamina to motion vision. *Neuron,* **79,** 128-140.
van Swinderen, B. & Brembs, B. (2010) Attention-like deficit and hyperactivity in a Drosophila memory mutant. *The Journal of neuroscience : the official journal of the Society for Neuroscience,* **30,** 1003-1014.
van Swinderen, B. & Flores, K.A. (2007) Attention-like processes underlying optomotor performance in a Drosophila choice maze. *Developmental neurobiology,* **67,** 129-145.
Varjú, D. (1976) Visual edge fixation and negative phototaxis in the mealworm beetle Tenebrio molitor. *Biol. Cybernetics,* **25,** 17-26.
Vogt, N. & Desplan, C. (2007) The first steps in Drosophila motion detection. *Neuron,* **56,** 5-7.
Wang, J., Zugates, C.T., Liang, I.H., Lee, C.H. & Lee, T. (2002) Drosophila Dscam is required for divergent segregation of sister branches and suppresses ectopic bifurcation of axons. *Neuron,* **33,** 559-571.
Wardill, T.J., List, O., Li, X., Dongre, S., McCulloch, M., Ting, C.Y., O'Kane, C.J., Tang, S., Lee, C.H., Hardie, R.C. & Juusola, M. (2012) Multiple spectral inputs improve motion discrimination in the Drosophila visual system. *Science,* **336,** 925-931.
Wehner, R. (1972) Spontaneous pattern preferences of Drosophila melanogaster to black areas in various parts of the visual field. *Journal of Insect Physiology,* **18,** 1531-1543.
Wolf, R. & Heisenberg, M. (1980) On the fine structure of yaw torque in visual flight orientation of Drosophila melanogaster. *J. Comp. Physiol.,* **140,** 69-80.
Woodard, C., Huang, T., Sun, H., Helfand, S.L. & Carlson, J. (1989) Genetic analysis of olfactory behavior in Drosophila: a new screen yields the ota mutants. *Genetics,* **123,** 315-326.
Yamagata, M. & Sanes, J.R. (2008) Dscam and Sidekick proteins direct lamina-specific synaptic connections in vertebrate retina. *Nature,* **451,** 465-469.

Yamaguchi, S., Wolf, R., Desplan, C. & Heisenberg, M. (2008) Motion vision is independent of color in Drosophila. *Proceedings of the National Academy of Sciences,* **105,** 4910-4915.

Zhan, X.L., Clemens, J.C., Neves, G., Hattori, D., Flanagan, J.J., Hummel, T., Vasconcelos, M.L., Chess, A. & Zipursky, S.L. (2004) Analysis of Dscam diversity in regulating axon guidance in Drosophila mushroom bodies. *Neuron,* **43,** 673-686.

Zhou, Y., Ji, X., Gong, H., Gong, Z. & Liu, L. (2012) Edge detection depends on achromatic channel in Drosophila melanogaster. *The Journal of experimental biology,* **215,** 3478-3487.

Zhu, Y. (2013) The Drosophila visual system: From neural circuits to behavior. *Cell adhesion & migration,* **7,** 333-344.

Zhu, Y. & Frye, M. (2009) Neurogenetics and the "fly-stampede": dissecting neural circuits involved in visual behaviors. *Fly (Austin),* **3,** 207-209.